UNIVERSITY OF TURIN

DEPARTMENT OF LIFE SCIENCES AND SYSTEMS BIOLOGY

PhD PROGRAMME IN EXPERIMENTAL MEDICINE AND THERAPY

CYCLE XXXIII

Cardiovascular effects of trimethylamine N-oxide (TMAO)

STUDENT: **Giulia Querio**

TUTOR: **Prof.ssa Maria Pia Gallo**

COORDINATOR: **Prof. Pasquale Pagliaro**

ACADEMIC YEARS: **2017-2021**

SCIENTIFIC DISCIPLINARY SECTOR OF AFFERENCE: **BIO/09**

GLOSSARY

ITALIAN	**ENGLISH**
Dipartimento di Scienze della Vita e Biologia dei Sistemi	Department of Life Sciences and Systems Biology
Dottorato di ricerca in Medicina e Terapia Sperimentale	PhD Programme in Experimental Medicine and Therapy
Ciclo XXXIII	Cycle XXXIII
Effetti cardiovascolari della trimetilammina N-ossido (TMAO)	Cardiovascular effects of trimethylamine N-oxide (TMAO)
Tesi presentata da Giulia Querio	Thesis' author Giulia Querio
Tutor Prof.ssa Maria Pia Gallo	Supervisor Prof.ssa Maria Pia Gallo
Coordinatore del Dottorato Prof. Pasquale Pagliaro	PhD Programme Co-ordinator Prof. Pasquale Pagliaro
Anni Accademici 2017-2021	Academic years of enrolment 2017-2021
Settore Scientifico Disciplinare di afferenza BIO/09	Code of scientific discipline BIO/09

TABLE OF CONTENTS

SUMMARY

Cardiovascular diseases (CVD) are multifactorial conditions related to both intrinsic and extrinsic factors. CVD are the leading cause of mortality worldwide, and, due to their multifactorial nature, different aspects of their development have to be considered in clinical interventions.

Diet and wrong nutritional habits have been grouped among extrinsic CVD risk factors, and they can directly influence the development of cardiac and vascular damage. In particular, it has been underlined that Western Diet, rich in animal-derived and poor in vegetables and fibre-rich foods, can improve the development of atherosclerosis and its associated cardiovascular outcomes. Moreover, diet can modulate microbial populations that reside in the human gut, and it has been outlined that Western Diet promotes a reduction in microbial diversity favoring dysbiosis and its associated patho-physiological manifestations. It is now widely accepted that the gut microbiota composition is modulated by the host, and microbiota-released molecules can modulate the physiology of the host in a symbiotic relationship.

Recent studies underline a connection between the gut microbiota and the cardiovascular system showing that several gut-derived molecules are regulators of cardiovascular patho-physiology. In this tangled network connecting diet, gut microbiota and cardiovascular health, the discovery of new diet- and gut-derived markers of disease could be of primary importance for a timely intervention to reduce severe or even fatal outcomes.

Among diet- and gut-derived metabolites, trimethylamine N-oxide (TMAO), has been recently studied for its implication in CVD development. Animal studies have outlined different physiological functions of TMAO, in particular, it acts as an osmolyte, a protein stabilizer and an electron acceptor able to balance hydrostatic and osmotic pressures in deep sea fishes. So, due to their high content, fish products represent for human a direct dietary source of TMAO. Other dietary precursors, such as choline, L-carnitine, and ergothioneine, can be metabolized by the gut microbiota to form trimethylamine, that is then N-oxidized to TMAO by hepatic flavin containing monooxygenases 3.

Laboratory tests and clinical studies define different human plasma TMAO concentrations, ranging from 1.74 to 103.81 µmol/L. Even if, specific defined plasma TMAO values for pathology are still lacking, all physicians agree with the evidence that higher levels of circulating TMAO occur in CVD.

Aim of this study was to evaluate in two different *in vitro* models the direct role of TMAO in the development of cardiac and vascular damage, both in basal treatment and in presence of stressors. For all treatments with TMAO the concentration of 100 µM was chosen and considered the pathological threshold, according to scientific literature.

As already outlined different factors can contribute to cardiac and vascular damage, and in this study only a few of them were considered to evaluate the effect of TMAO in a pathological development.

The first part of the project was centered on cardiac tissue and used primary isolated adult rat cardiomyocytes for *in vitro* experiments. The choice of primary cardiac cells was motivated by their similarity with the cellular characteristics that can be found in *in vivo* models. So, different parameters of cellular physiology were monitored starting from cells viability. Ischemia reperfusion injury (IRI) figures as the most relevant CVD, and it is characterized by consistent death of cardiac cells at the time of reperfusion and consequent loss of functionality of the cardiac tissue. First experiments evaluated TMAO effects on cardiomyocytes viability both in basal condition and in a simulated IRI protocol in order to assess if the molecule could modulate or accelerate the damaging effect of the simulated stress system.

Anthracyclines, largely used in chemotherapeutic treatments, have shown cardiotoxic effects as the most relevant side effect. Now it is widely accepted that Doxorubicin (DOXO), a widely used anthracycline in clinical practice, has cardiotoxic effects and it could be utilized as a stressor to simulate the pro-oxidant environment that characterizes the cardiac tissue of anthracycline treated patients.

So, further experiments using cardiomyocytes monitored structural variations in a prolonged treatment with DOXO or H_2O_2, alone or in a simultaneous treatment with TMAO in order to evaluate if the diet-derived compound could have any effect in modulating cardiomyocytes sarcomeric structure during the treatment with different stressors.

Moreover, given that several cardiac pathologies develop from an oxidative environment, last experiments using cardiomyocytes were addressed to the evaluation of TMAO effect in modulating oxidative stress indicators, such as reactive oxygen species and mitochondrial membrane potential. Experiments were performed in basal treatment with TMAO or using both H_2O_2, to simulate acute stress, and DOXO, to simulate prolonged stress, in presence of TMAO. Aim of these different treatments was to evaluate if TMAO could influence oxidative stress indicators and thus cellular response to different stressors.

The second part of the project was centered on endothelial effect of TMAO on bovine aortic endothelial cells (BAE-1) largely used to study *in vitro* endothelial function and dysfunction. Also for these set of experiments first evaluations were focused on cells viability and, due to cellular characteristics, TMAO treatment was tested for longer times than primary cardiomyocytes, allowing to perform a chronic stimulation of endothelium.

As endothelial dysfunction is related to oxidative stress and mitochondrial impairment, also for BAE-1 reactive oxygen species and mitochondrial membrane potential were monitored both in basal treatment with TMAO and in a simultaneous treatment with a vitamin K3 precursor, Menadione, largely used to simulate *in vitro* endothelial dysfunction.

Even if endothelial dysfunction is characterized by an oxidative stress environment the most important manifestation of this pathological condition is related to impaired nitric oxide (NO) release. NO is an important endothelial gasotransmitter that regulates vascular smooth muscle cells contraction, favouring the vasodilatory mechanism. Physiological NO synthesis by endothelial cells could be driven by different stimulations and, among them, paracrine ATP release due to shear stress has been widely studied. Subsequent activation of endothelial purinergic response to ATP induces intracellular calcium increase that causes the activation of endothelial nitric oxide synthase (eNOS) through its phosphorylation and NO synthesis from L-Arginine. Impairment in purinergic response to ATP and NO synthesis causes improper function of the vasodilatory mechanism, thus favoring endothelial dysfunction.

Last experiments using BAE-1 evaluated if TMAO could have any role in modulating ATP-stimulated NO synthesis. As upstream regulator of the pathway, the rise of intracellular calcium was monitored with a specific fluorescent probe, after ATP stimulation in TMAO pretreated BAE-1. To support obtained results, NO synthesis was detected through a specific fluorescent probe in time course imaging and expression of eNOS and its phosphorylated active form ($eNOS^{Ser1179}$) were quantified with Western Blot analyses in the same experimental conditions.

In conclusion, this study shows that TMAO has no impact on primary cardiomyocytes viability in basal treatment and in a IRI model, and it does not alter sarcomeric structure and oxidative stress indicators both in basal treatment and in presence of the cardiac stressors H_2O_2 and DOXO. Furthermore, TMAO is not able to reduce endothelial cells viability, and to enhance oxidative stress status in basal treatment or in presence of Menadione. Interestingly, TMAO interferes with NO synthesis impairing the rise of intracellular calcium, and eNOS activation, in purinergic response to ATP, thus suggesting its involvement in the vasodilatory mechanism.

1. INTRODUCTION

1.1 CHAPTER 1

1.1.1 Cardiovascular diseases

Cardiovascular diseases (CVD) are a group of disorders that involve the heart and blood vessels. Among most revelant CVD there are: ischemic heart disease, coronary artery disease, cerebrovascular disease, peripheral arterial disease, rheumatic heart disease, congenital heart disease, deep vein thrombosis and pulmonary embolism. Epidemiological data suggest that CVD are the primary cause of death worldwide, and low- and middle-income countries are mainly affected because of the population's poorer clinical support. In particular, data from the Global Burden Disease estimate that 17.8 million deaths were caused by CVD worldwide in 2017 and 50% were caused by ischemic heart disease (IHD) while 35% were caused by stroke (Townsend et al., 2021). Likewise, data restricted to the European country show that in the same period 44% of total deaths were caused by CVD and, in particular, 44% were caused by IHD and 25% by stroke (Townsend et al., 2021). Cardiovascular mortality has some differences between women and men. Although in european countries it is the first cause of mortality for both, the rate of deaths due to CVD has been observed to be higer in women (46%) than in men (39%) (Figure 1) (Townsend et al., 2021).

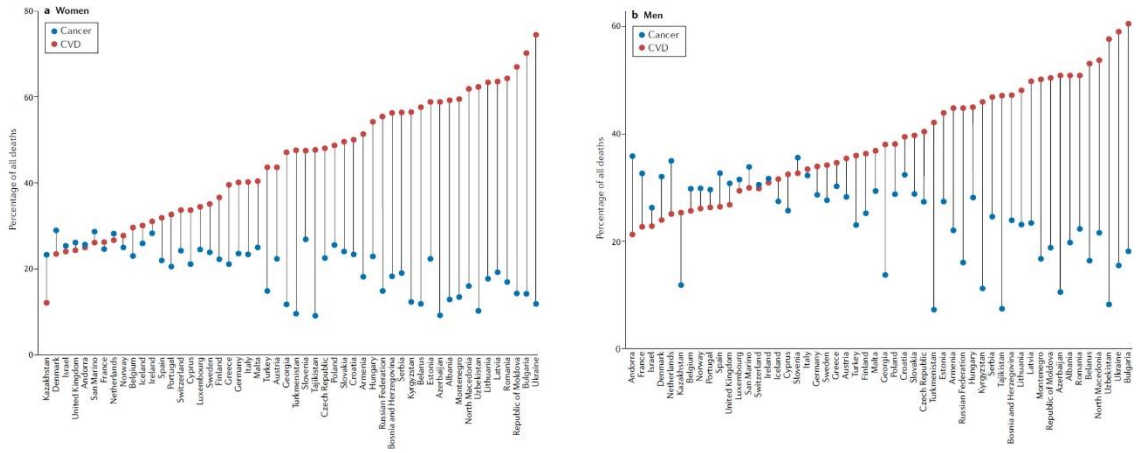

Figure 1. *Percentage of CVD and cancer deaths in Europe in the period from 2007 and 2016. Data present latest registration available for each country in women* ***(a)*** *and men* ***(b)****. Figure from Townsend et al., 2021.*

Furthermore, median age-standardized incidence and prevalence for CVD was higher in men than women, and also disability-adjusted life years (DALYs) was higher for men, even though its trend decreased from 1990 to 2017 (Townsend et al., 2021). CVD could be

classified as chronic diseases that are asymptomatic for a long time before the first appereance of symptoms which could even have a fatal outcome. As it takes a long time for CVD to develop, they are classified as multifactorial pathological conditions and several risk factors can appear in different life stages, influencing and powering each other. In particular, CVD risk factors can be classified as non-modifiable and modifiable. Age, sex, genetic factors belong to the first group and cannot be changed and represent starting points to control modifiable risk factors. This second group is strictly related to life-style habits and, in particular, smoke, diet-derived conditions, such as obesity, diabetes, hyperlipidemia, hypertension, and physical inactivity are the most relevant, especially for elderly patients (Francula-Zaninovic & Nola, 2018). Among these controllable risk factors tobacco smoke, both active and passive, augment the incidence of CVD, indeed, different constituents of cigarettes, as nicotine, tar and carbon monoxide contribute to the exacerbation of CVD (Kondo et al., 2019). To discourage the use of cigarettes some European countries have already adopted informational campaigns and settled some smoke-free zones, such as schools and public transports (Francula-Zaninovic & Nola, 2018). Dietary habits and physical inactivity are other two relevant factors that contribute to the development of CVD. In particular, it has been outlined that the Mediterranean Diet figures as the best nutritional approach to limit saturated lipid and simple carbohydrates uptake, favouring the introduction of vegetables, balance animal- and plat-derived proteins, supporting fish uptake and unsaturated fat-containing foods that are stricly recommended for patients with CVD (Francula-Zaninovic & Nola, 2018; Martínez-González et al., 2019; Temple et al., 2019). Furthermore, it has been outlined that regular physical activity can improve cardiac and vascular physiology thus contrasting CVD development (Francula-Zaninovic & Nola, 2018; Lavie et al., 2019). Recent publications point out that also chemotherapeutic agents used for cancer treatment can be involved in the development of CVD, and in particular anthracyclines show the most deleterius cardiotoxic effects (Noutsias & Maisch, 2011).

In line with what already described, prevention of CVD is of primary importance to preserve health condition and to reduce economic expenses caused both by health care interventions and production loss due to CVD-derived disability. In general, three lines of intervention have been delineated to prevent CVD: life-style habits changes, physical activity improvement and limiting smoke for general population; reduction of risk factors for patients at high risk; worse outcome development control for patients with diagnosed CVD (Francula-Zaninovic & Nola, 2018).

1.1.2 Myocardial ischemia reperfusion injury

As already outlined, ischemic heart disease (IHD) is the leading cause of death worldwide. Epidemiological data support sex-dependent differences in IHD outcome, showing women at higher risk during menopause due to loss in estrogenic-mediated cardiovascular protection (Querio, Antoniotti, et al., 2021; Querio, Geddo, et al., 2021). Sexual dimorphism has also been outlined in symptoms development, and women are characterized by no obstructive coronary artery disease (INOCA), microvascular dysfunction and plaque erosion, while men have a higher chance to develop plaque rupture as cause of myocardial infarction. Prevalence of INOCA in women is 65%, while in men is 32%, and these divergencies are underlined by higher mortality rate in women due to improper diagnosis in clinical practices (Querio, Antoniotti, et al., 2021). Ischemic heart disease is a pathological condition characterized by reduced or absent blood flow in coronary arteries due to atherosclerotic plaque or blood cloth formation that cause a partial or total occlusion of these vessels (Heusch, 2020). Consequences of this condition are related to insufficient nutrients and oxygen supply to the cardiac tissue that needs these substrates for its mechanical and physiological functions. When prolonged ischemia occurs, myocardial infaction can develop causing loss of cardiac cells and heart functionality. To prevent prolonged ischemia and its related heart damage, restoration of blood flow is essential.

Starting from first studies on canine hearts and then in clinical practice on patients, it was obvious that blood flow restoration, called reperfusion, prevents futher damage in the cardiac tissue, but it causes detrimental effects too, exacerbating those started by ischemia, and determining the so called ischemia reperfusion injury (IRI) (Figure 2) (Heusch, 2020; Kalogeris et al., 2012).

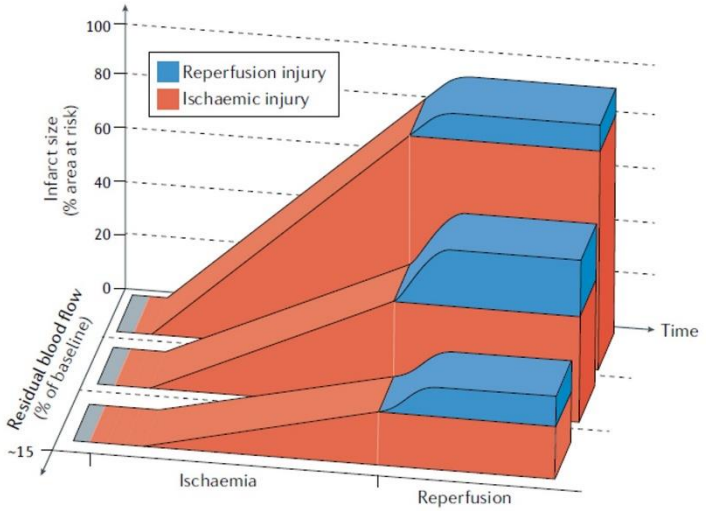

Figure 2. *Infarct size after ischemia reperfusion injury. Both ischemia and reperfusion participate to infarct size of the myocardium. Figure from Heusch, 2020.*

Strategies aimed to prevent the deleterious effects of IRI focus on conditioning approaches, based on brief periods of ischemia and reperfusion that are induced in a period before (preconditioning) or after (postconditioning) the index ischemic event (Penna et al., 2015). Early and late preconditioning have outlined protective effects in animal models, but the translation of this approach in clinical practice is difficult, because of the unpredictability of the index ischemia. Postconditioning is more feasible in patients because it is based on alternation of brief occlusion and reperfusion cycles suddenly after the index ischemia. Recent evidences suggest remote conditioning as a possible line of intervention because it is a non-invasive approach based on arm cuff inflation-deflation cycles during (perconditioning) or after (postconditioning) the index ischemia. Also pharmacological cardioprotection has been proposed through drugs administration as metoprolol, cyclosporine A, adenosine or nitrite before reperfusion (Figure 3) (Heusch, 2020; Penna et al., 2015).

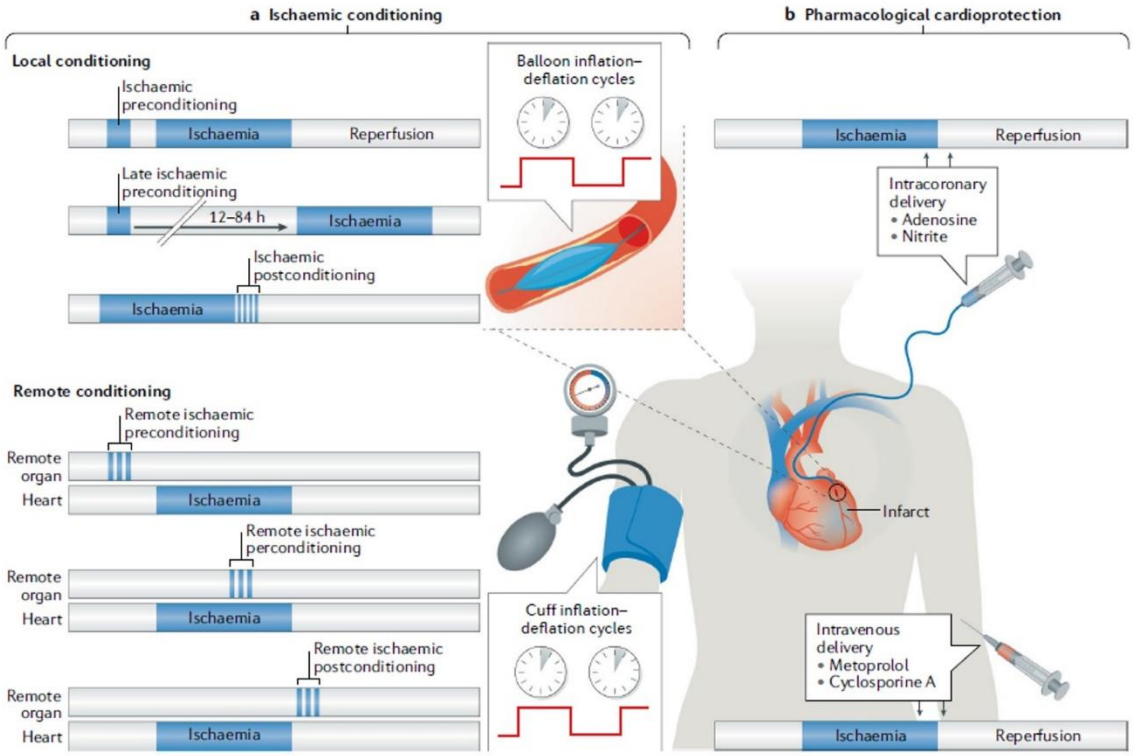

Figure 3. *Cardioprotective interventions to reduce ischemia reperfusion injury.* ***a)*** *Ischemic conditioning is based on brief cycles of ischemia and reperfusion before (preconditioning,*

remote conditioning) of after (postconditioning) the index ischemia. Remote conditioning is based on arm cuff inflation-deflation cycles before (preconditioning), during (perconditioning) or after (postconditioning) the index ischemia. Among all conditioning techniques postconditioning and remote conditioning are the most feasible for clinical use. ***b)*** *Cardiac protection can also be induced by pharmacological intervention administering drugs such as metoprolol, cyclosporine A, adenosine or nitrite before reperfusion. Figure from Heusch, 2020.*

1.1.2.1 Pathophysiology of myocardial ischemic injury

Reduced nutrients and oxygen supply that occurs during ischemia activates a series of metabolic changes. Oxidative phosphorylation interruption, thus causing intracellular H^+ accumulation due to augmented anaerobic glycolysis, and insufficient ATP availability cause impaired cardiac contractility (Frank et al., 2012). In this scenario, alterations of ion exchangers occur: both reduced activity of Na^+/K^+ pumps and enhanced activity of Na^+/H^+ exchangers increase intracellular Na^+ concentration; decreased and reversed activity of $2Na^+/Ca^{2+}$ exchanger (Frank et al., 2012) mediates Na^+ extrusion from the intracellular compartments and Ca^{2+} entry from the extracellular environment, thus augmenting intracellular Ca^{2+} concentration. Moreover, the $2Na^+/Ca^{2+}$ exchanger has shown reduced activity due to high $[Na^+]_i$ (Despa & Bers, 2013), and to low pH, which occurs during anaerobic glycolysis (S. Chen & Li, 2012). Activation of L-type voltage-gated calcium channels and opening of the Ryanodine Receptors in sarcoplasmic reticulum further enhance the rise of intracellular Ca^{2+}. Destabilization of mitochondrial membrane potential is prevented by reverse activation of the ATPase hydrolysis of ATP, which contributes to the reduction of ATP availability and the increase of inorganic phosphate concentration in mitochondria (Figure 4) (Hausenloy & Yellon, 2013).

1.1.2.2 Pathophysiology of myocardial reperfusion injury

Clinical and laboratory data show that restoration of blood flow during reperfusion induces further damage in cardiac cells. Indeed, reactivation of electron transport chain causes the rise of reactive oxygen species (ROS) that induces opening of the mitochondrial permeability transition pore (mPTP), mediates sarcoplasmic reticulum impairment and activates the oxidative damage of cell structures, as membrane lipids, proteins and DNA. Furthermore, during reperfusion, the Na^+/H^+ exchanger restores physiological pH, with a resultant rising in intracellular Na^+ concentration that activates the $2Na^+/Ca^{2+}$ exchanger which mediates extracellular transport of Na^+ and intracellular overload of Ca^{2+}. Calcium accumulation in intracellular compartments further enhances mPTP opening.

Physiological pH restoration, ROS and calcium overload are all involved in mPTP opening that figures as an important actor in the induction of the reperfusion injury. Indeed, the mPTP is a nonselective channel of the inner mithochondrial membrane that regulates the permeabilization of this otherwise impermeable structure. Mitochondrial permeabilization regulated by mPTP opening defines the severity of IRI, that can be minimal or can cause programmed cell death or even necrosis in more serious outcomes. All intracellular changes that occur during both ischemia and reperfusion, such as H^+ accumulation, calcium overload and opening of the mPTP induce ROS overproduction enhancing a feedback loop that exacerbates the exhisting oxidative stress. ROS increase activates pro-inflammatory pathways that induce the release of pro-inflammatory cytokines that act as chemoattractant for neutrophils that accumulate in the infarcted area and exacerbate contractile dysfunction, hypertrophy, fibrosis and derived cells death that occur in IRI (Figure 4) (Frank et al., 2012; Hausenloy & Yellon, 2013).

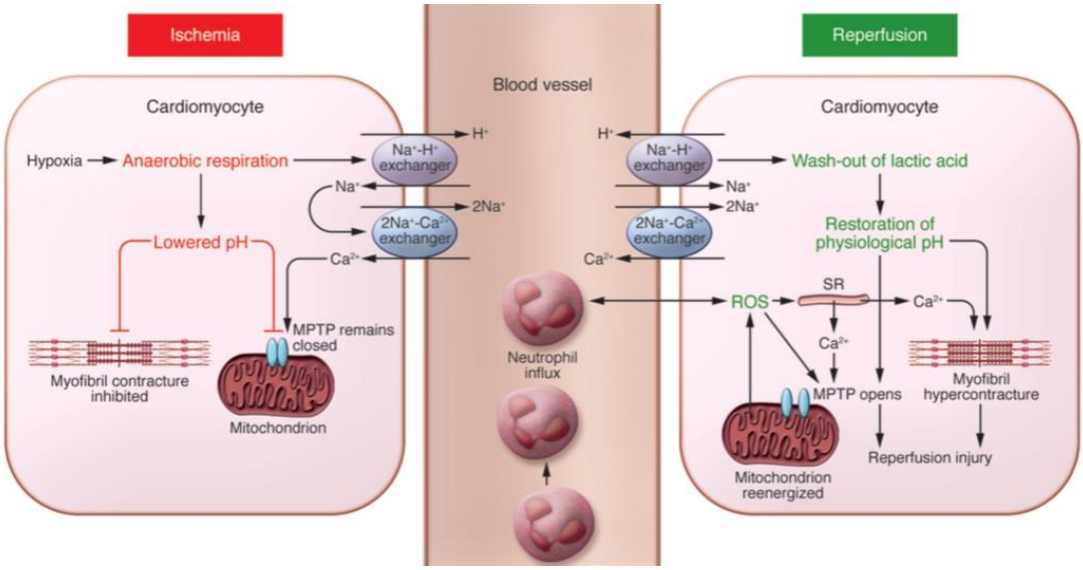

Figure 4. *Ischemia reperfusioin injury activated pathways. Ischemia reduces oxygen and nutrients supply to the cardiac tissue and activates the anaerobic respiration as principal source of energy. This contributes to decrease intracellular pH. Unavailability of ATP reduces the activity of Na^+/K^+ pumps and enhances the activity of Na^+/H^+ exchangers with the derived increase in intracellular Na^+ concentration. Furthermore, decreased or reversed activity of $2Na^+/Ca^{2+}$ exchangers augment intracellular Ca^{2+} concentration. During reperfusion the rise of ROS induces opening of the mitochondrial permeability transition pore (MPTP), mediates sarcoplasmic reticulum impairment and activates the oxidative damage of cell membranes and DNA. Reactivation of the Na^+/H^+ exchangers restores physiological pH, and further enhances the opening of MPTP. ROS also act as chemoattractant for neutrophils that accumulate in the infarcted area, thus contributing to reperfusion injury exacerbation. Figure from Hausenloy and Yellon, 2013.*

1.1.3 Anthracycline cardiotoxicity

Anthracyclines are a group of antibiotics synthesized by different species of *Streptomyces* bacteria. Anthracyclines are a wide group of molecules and, among them, doxorubicin, daunorubicin and epirubicin are the most known. They are broadly used as chemotherapeutic agents against different types of tumors. In particular, breast cancer, lymphomas, soft tissue sarcomas, osteogenic sarcomas, urinary bladder carcinoma, esophageal carcinoma, stomach carcinoma, hepatocellular carcinoma and variuos leukemia are treated with anthracyclines (Saleh et al., 2021). Their widespread use in chemotherapeutic interventions is due to their effectiveness in fighting tumor development. Indeed, the use of anthracyclines has reduced by 20-30% breast cancer mortality (Saleh et al., 2021). Two main effects mediated by anthracyclines in cancer cells have been delineated: DNA damage through intercalation with DNA base pairs and stabilization of topoisomerase IIα (TOP2α); and prevention of DNA and RNA synthesis (Al-Malky et al., 2020). Even if anthracycline treatment on tumor progression has concrete successful evidences, recent clinical outcomes have delineated an anthracycline-induced cardiomyopathy. A high number of patients develop cardiotoxicity after the treatment, and this condition is dose and age dependent: higher doses and younger ages are at higher risk in developing adverse effects (Murabito et al., 2020; Saleh et al., 2021).

It has been outlined that cardiotoxic effects of anthracyclines can be different in patients and they have been classified according to their time of onset: *acute toxicity,* characterized by supraventricular arrhytmia, transient left ventricular dysfunction, electrocardiographic changes that occur up to 2 weeks after anthracycline infusion in 1% of the patients and is often reversible; *early-onset chronic toxicity,* with left ventricular dysfunction that develops in heart failure and occurs in the first year of the treatment in 98% of the patients; *late-onset chronic toxicity,* characterized by dilated cardiomyopathy and restrictive cardiomyopathy that occur years later the chemiotherapeutic treatment (Saleh et al., 2021; Songbo et al., 2019).

Intracellular mechanisms of anthracycline-induced cardotoxicity are still under investigation, aiming to develop primary prevention strategies to avoid cardiac outcome during drug treatment, and secondary prevention startegies to reduce cardiac failure progression (Murabito et al., 2020).

1.1.3.1 Doxorubicin-induced cardiac toxicity

Doxorubicin (DOXO) is an antibiotic anthracycline synthesized by *Streptomyces peucetius var. Caesius*. Its molecular structure consists of four anthraquinone rings with an amino

sugar residue (Figure 5) (Al-Malky et al., 2020). Doxorubocin is the most effective anti-cancer drug and it is used in the preparation of chemotherapeutic regimens or sometimes it is administered with other interventions such as radiotherapy. Whilst its therapeutic effectiveness in cancer has been widely recognized, DOXO, as other anthracyclines, can induce several manageable side effects, like gastrointestinal disturbances, loss of hair or stomatitis and other more serious side effects, as cardiotoxicity. Two main mechanisms induced by DOXO have been highlighted in cancer cells: oxidative stress-mediated cell damage and inhibition of DNA repair through TOP2α. The first mechanism is based on DOXO convertion into a semiquinone form and the subsequent reversion in its original form, that induces ROS formation. Increased ROS cause cellular apoptosis through the oxidation of membrane lipids and proteins and DNA damage. The second mechanism activated by DOXO is mediated by its intercalation between DNA bases and inhibition of TOP2α, involved in DNA repair. These mechanisms induce p53 and FOXO3 activation, thus starting the apoptotic cascade. Other proposed mechanisms for DOXO-activated apoptosis concern the suppression of DNA and RNA synthesis and the stimulation of mithocondrial ROS rising (Al-Malky et al., 2020; Songbo et al., 2019).

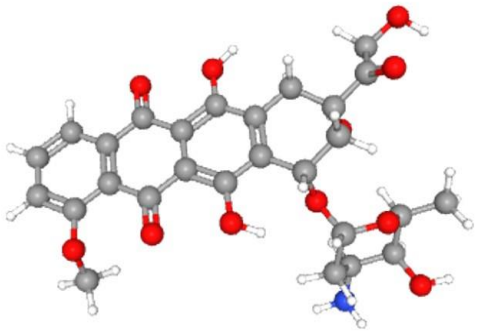

Figure 5. *Doxorubicin ball and stick molecular structure. Doxorubicin is formed by four anthraquinone rings with an amino sugar residue. Image from PubChem (https://pubchem.ncbi.nlm.nih.gov/compound/Doxorubicin). Ball color legend: blue: nitrogen; grey: carbon; white: hydrogen, red: oxygen.*

Like cancer cells, also cardiac tissue is highly susceptible to DOXO-mediated effects and, in particular, oxidative stress-induced damage is the first proposed mechanism involved in DOXO cardiotoxicity. Different lines of investigations have underlined several actors participating in DOXO-activated oxidative stress (Figure 6) (Henninger & Fritz, 2017): mitochondria, endothelial nitric oxide synthase (eNOS) and NADPH oxidases (NOX).

Due to their high energy demand, cardiomyocytes are equipped with a large number of mitochondria. During DOXO treatment, the drug accumulates in the inner mitochondrial membrane and irreversibly binds with cardiolipin, which is a fundamental element of electron transport chain. Thus, electron transport chain impairement occurs and a high amount of superoxide (O_2•) is released, enhancing hydrogen peroxide (H_2O_2) formation and exacerbating the rise of ROS (Al-Malky et al., 2020; Songbo et al., 2019).

Endothelial nitric oxide synthase and NADPH oxidases are both expressed in cardiomyocytes and several studies have underlined that both enzymes are involved in DOXO conversion into its semiquinone form, that induces O_2• release and H_2O_2 and peroxynitrite formation (Al-Malky et al., 2020, pag.; Songbo et al., 2019).

Furthermore, DOXO induces oxidative damage in cardiac cells through its interaction with free iron. Formation of Fe-doxorubicin complexes can react with O_2 and favour the conversion of H_2O_2 to hydroxyl radical (•OH) thus exacerbating reactive oxygen species damaging effects (Al-Malky et al., 2020, pag.; Songbo et al., 2019). Generation of Fe-doxorubicin complexes is also favoured by doxorubicinol, a doxorubicin-derived metabolite, that inhibits iron regulatory protein (IRP-1) and enhances free iron availability (Al-Malky et al., 2020; Songbo et al., 2019).

Other proposed cardiotoxic mechanisms mediated by doxorubicin are not dependent on oxidative stress. First mechanism concerns apoptosis stimulation through two different pathways: heat shock ptoteins-mediated Bax and p53 activation and toll-like receptors activation of nuclear factor kappa-light-chain-enhancer of activated B cells (NF-kB) pathway, both inducing cardiac cells loss (Al-Malky et al., 2020; Songbo et al., 2019).

Doxorubicin cardiac damage could also be induced by the rise of intracellular calcium due to the inhibition of $2Na^+/Ca^{2+}$ exchangers and activation of L-type calcium channels and this last mechanism could be both directly mediated by doxorubicin or by doxorubicin-induced ROS increase (Al-Malky et al., 2020; Songbo et al., 2019).

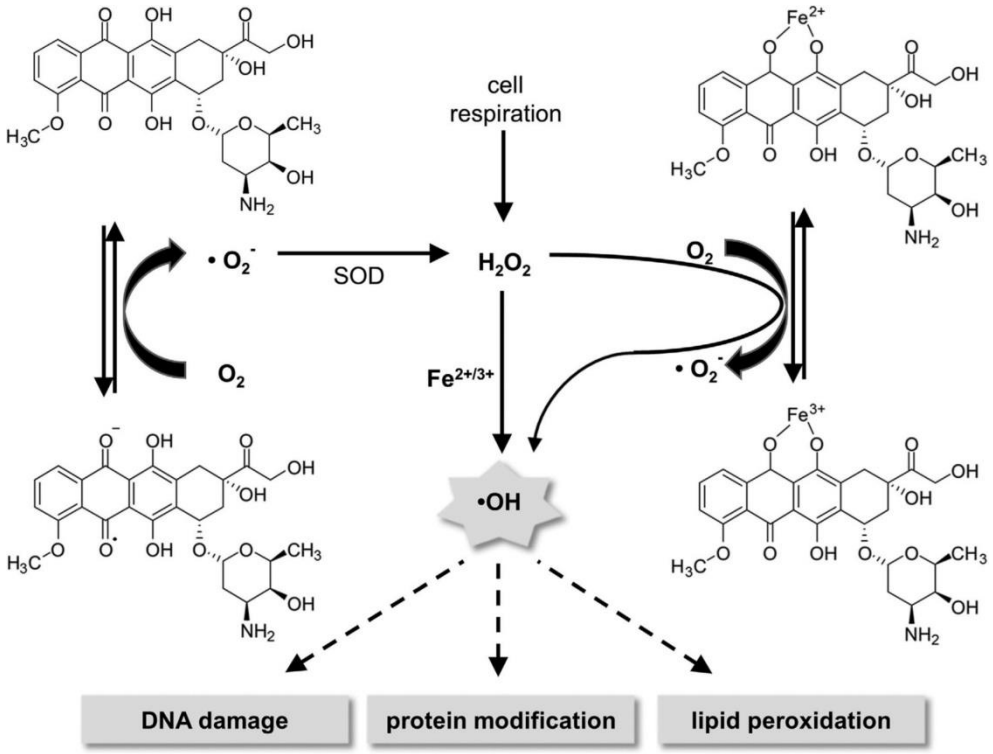

Figure 6. *Molecular mechanism of doxorubicin induced oxidative stress. Doxorubicin generates O_2• through the alternative conversion from its semiquinonic form to its more stable quinonic form. O_2• is converted by superoxide dismutase (SOD) to H_2O_2 that can generate OH• through Fenton reactions. Also iron-doxorubicin complexes can contribute to the formation of OH• from H_2O_2. Rise of ROS can induce DNA damage, protein modification and lipid peroxidation. Figure from Henninger and Fritz, 2017.*

1.1.4 Endothelial dysfunction

Blood vessels wall is made up of three different layers: *tunica intima*, *tunica media* and *tunica adventitia*. Vessels lumen is lined by a single layer of endothelial cells (EC), that form the *tunica intima* involved in several functions regulating vascular physiology; *tunica media* consists of smooth muscle cells, that directly respond to vasodilator and vasoconstrictor mediators released by EC; *tunica adventitia* is formed by perivascular adipose tissue cells, fibroblasts, nerve endings and collagen fibers, that favour adherence to the surrounding tissues (Figure 7) (Zhao et al., 2015). In particular, EC do not only have a barrier function, they also have an autocrine, paracrine and endocrine role that modulate vascular homeostasis, vascular tone, inflammatory and immune response, blood fluidity and neovascularization (Deanfield et al., 2007; Godo & Shimokawa, 2017). Endothelium impairment drives towards endothelial dysfunction, a pathological condition characterized

by increased oxidative stress and inflammation, and consequent activation and improper function of endothelial cells (Hadi et al., 2005; Incalza et al., 2018).

EC activation entails cell adhesion molecules (CAMs) expression. In particular, the selectin family, the integrin family and the immunoglobulin superfamily, are the most expressed CAMs that recruit and facilitate inflammatory cells transmigration in response to pro-inflammatory cytokines (Incalza et al., 2018).

Improper function of EC is indeed characterized by imbalanced synthesis of vasoconstrictor and vasodilator mediators that predispose to a pro-thrombotic and pro-atherosclerotic environment (Hadi et al., 2005; Incalza et al., 2018). Leading actor of endothelial function and dysfunction is nitric oxide (NO): a decreased synthesis or augmented degradation of this gasotransmitter lead to impaired vasodilation, thus representing the earliest event of endothelial dysfunction (Deanfield et al., 2007; Hadi et al., 2005; Incalza et al., 2018). Recently, endothelial dysfunction has gained clinical relevance because it precedes and develops with different CVD, so, proper and timely diagnosis could contribute to prevent serious and sometimes fatal outcomes. Several risk factors have been outlined to favor endothelial dysfunction; they could be grouped in traditional and novel risk factors, and all of them are strictly associated with CVD development. In particular, aging, smoking, metabolic disorders, such as hyperglicemia, hyperinsulinemia, insulin resistance, hyperlipidemia, and hypertension are the most relevant risk factors (Godo & Shimokawa, 2017; Hadi et al., 2005; Incalza et al., 2018). High blood pressure and associated altered shear stress have been highlighted as key factors in endothelial dysfunction and other CVD (Strassheim et al., 2020).

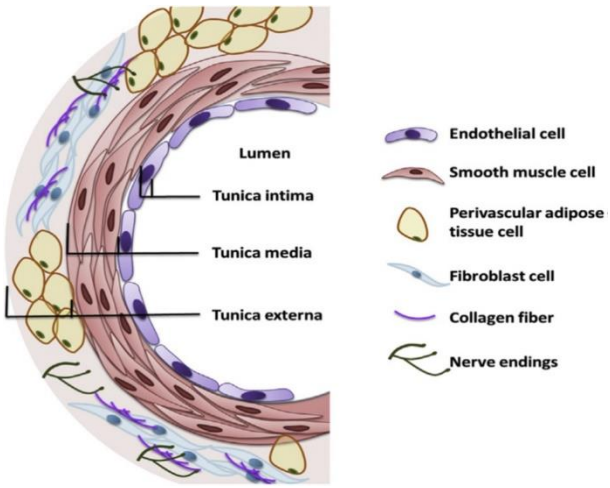

Figure 7. *Blood vessel cross section. Vascular wall is formed by different layers, starting from the lumen they are: tunica intima, lined by a single layer of endothelial cells, tunica media formed by smooth muscle cells directly involved in the response to vasodilator/vasoconstrictor mediators secreted by endothelial cells, and tunica externa (or adventitia), in which perivascular adipose tissue cells, fibroblasts, collagen fibers and nerve endings favour adherence to the surrounding tissues. Figure from Zhao et al., 2015.*

1.1.4.1 Oxidative stress in endothelial dysfunction

As already outlined, one of the most relevant factors involved in endothelial dysfunction development is oxidative stress and, in particular, O_2• increase, caused by cell's endogenous and exogenous antioxidant systems reduced ability to turn off this free radical. Furthermore, oxidative stress can be exacerbated by O_2•-derived radicals, H_2O_2, OH• and peroxynitrite (ONOO-).

Interestingly ONOO-, product of O_2• and NO reaction, is a free radical that contributes to oxidative stress deleterious effects and subtracts NO from its vasodilatory role, thus favouring a negative loop that worsens the development of endothelial dysfunction (Incalza et al., 2018). Different molecular factors are involved in the rise of O_2• and, among all, can be mentioned Complex I and Complex III in mitochondrial respiratory chain, xanthine oxidase, NADPH oxidases and uncoupled endothelial nitric oxide synthase (eNOS) (Förstermann & Sessa, 2012; Incalza et al., 2018) (Figure 8).

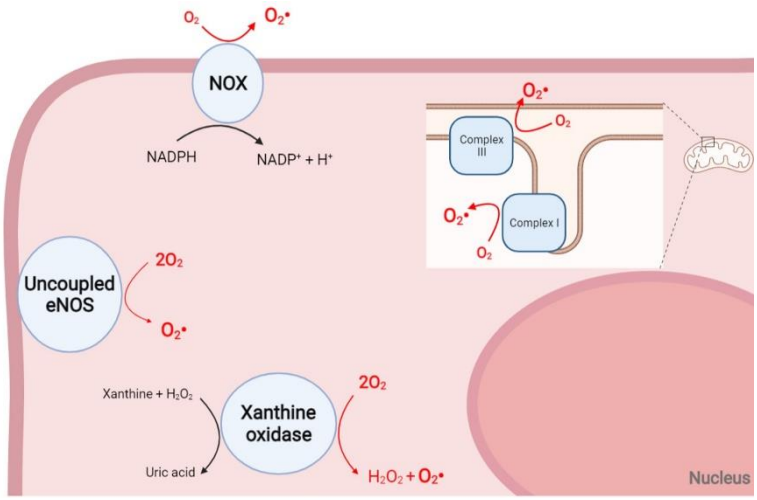

Figure 8*. Different cellular sources of superoxide anion (O_2•) in endothelial cells. Principal endothelial sources of O_2• are: mitochondrial Complex I and III during electron transport chain, xanthine oxidase in the conversion of xanthine to uric acid, NADPH oxidase (NOX) and uncoupled eNOS. Figure created with BioRender.com.*

1.1.4.1.1 Menadione induced endothelial dysfunction through oxidative stress

Several studies point out the involvement of menadione (MEN) in the induction of oxidative stress and endothelial dysfunction in *in vitro* models (Bik et al., 2021; Lee et al., 1999, 2001). Menadione is a quinone, precursor of vitamin K3, and thanks to its molecular characteristics it is able to freely cross cell membranes (May et al., 2003). It is involved in a redox cycle that contributes to O_2• increase. In particular, an electron from nicotinamide-adenine-dinucleotide phosphate (NADPH) can be transferred by NADPH cytochrome P-450 reductase or NADH-ubiquinone oxidoreductase to menadione with the consequent formation of its semiquinone form and the release of O_2• (Bik et al., 2021; Burdette et al., 2002; N. O. Thomas et al., 2016)(Figure 9).

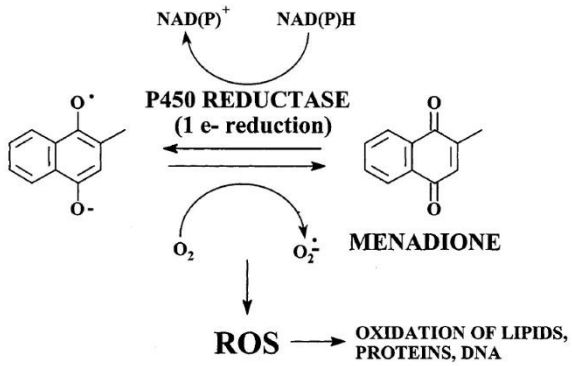

Figure 9. *Menadione redox cycle. Reciprocal conversion from the quinonic to the semiquinonic forms of menadione causes the release of O_2•. Increased intracellular ROS can activate lipids, proteins and DNA oxidation. Figure from Burdette et al. 2002.*

MEN-dependent O_2• increase, as already described, induces endothelial dysfunction associated with reduced cells viability (Kossenjans et al., 1996; Lee et al., 2001; May et al., 2003), endothelial inflammation (Bik et al., 2021) and impairment of the vasodilatory response (Lee et al., 1999, 2001; May et al., 2003). Another mechanism proposed for MEN-induced oxidative stress is related to glutathione (GSH) depletion. In particular, two different pathways have been described: the first outlines that the O_2• released by MEN is converted by superoxide dismutase (SOD) to H_2O_2, that is then reduced by glutathione peroxidase at expense of GSH; the second mechanism outlines a direct action of MEN on GSH oxidation. Both proposed processess occur in presence of D-glucose and concur in endogenous antioxidant defenses lowering (May et al., 2003). Furthermore, MEN has been described to induce mitochondrial membrane potential ($\Delta\Psi m$) depolarization (Halilovic et al., 2016; Lovatt et al., 2018), thus exacerbating ROS production and enhancing endothelial

dysfunction. Even if MEN effects are primarily related to oxidative stress, new evidences support its possible involvement in inducing endothelial dysfunction also by inhibiting endothelial nitric oxide synthase enzymatic activity, thus interfering with the vasodilatory mechanism of blood vessels (Lee et al., 2001; May et al., 2003). This last described effect of MEN has not been proved in clinical experiments yet.

According to presented data, MEN is the best candidate to study pathophysiological oxidative stress activation in endothelial cells.

1.1.4.2 Nitric oxide

Nitric oxide is the most important gasotransmitter involved in the regulation of the vascular tone and it could be synthesized by both an enzymatic and a non-enzymatic pathway (Figure 10) (Lundberg et al., 2008).

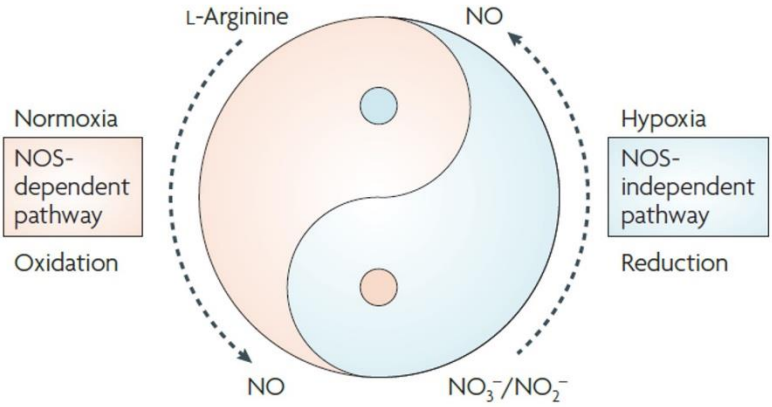

Figure 10. *Nitric oxide (NO) can be synthesized by both enzymatic and non-enzymatic pathways. During normoxia NO synthesis is primarily regulated by nitric oxide synthase enzymes through L-Arginine conversion to L-citrulline. In hypoxic condition that can occur durning ischemia or prolonged exercise the non-enzymatic nitrate-nitrite-NO pathway prevails to maintain physiological levels of NO. Figure from Lundberg et al., 2008.*

NO is synthesized primarily by nitric oxide synthase (NOS) enzymes in normoxic conditions. Three different isoforms of nitric oxide synthase are expressed in mammalian cells: *neuronal NOS* (n-NOS or NOS-1), involved in the regulation of neurotransmitters release, neuronal excitability, synaptic plasticity, memory and learning processes; *inducible NOS* (iNOS; NOS-2), which expression is induced only during infections, chronic inflammation or in tumors; *endothelial NOS* (eNOS; NOS-3), which is primarily expressed in EC, but it is also found in cardiac myocytes, platelets, mast cells, erythrocytes, leukocytes and renal epitelium (Dudzinski & Michel, 2007). Endothelial NOS is mainly involved in the

vasodilatoy mechanism in response to different agonists/antagonists (Förstermann & Sessa, 2012; Kolluru et al., 2010; Zhao et al., 2015).

NO pool can also be fueled by NOS-independent mechanisms, among them, S-nitrosothiols are involved in NO transfer from a donor S-nitrosylated protein to a S-nitrosylated substrate. S-nitrosothiols can release NO in presence of transition metal ions, like Cu^{2+} and Fe^{2+}, and the reaction can be also mediated by flash photolysis (Zhao et al., 2015).

Furthermore, as already underlined, non-enzymatic NO synthesis can also be regulated by the nitrate-nitrite-NO pathway. In particular, dietary nitrate (NO_3^-), abundant in green leafy vegetables, is reduced to nitrite (NO_2^-) by salivary bacteria that express nitrate reductase, absent in mammalian cells. Once NO_2^- reaches the stomach, it can be directly absorbed and released in the systemic circulation, or it can be protonated to nitrous acid (HNO_2) by acidic gastric environment. HNO_2 then decomposes to NO and other nitrogen oxides that can diffuse to the systemic circulation. Circulating NO_2^- can be further reduced to NO by other mammalian enzymes, among them haemoglobin, myoglobin, xanthine oxidoreductase are the most studied (Figure 11) (DeMartino et al., 2019; Lundberg et al., 2008; Schiffer et al., 2020).

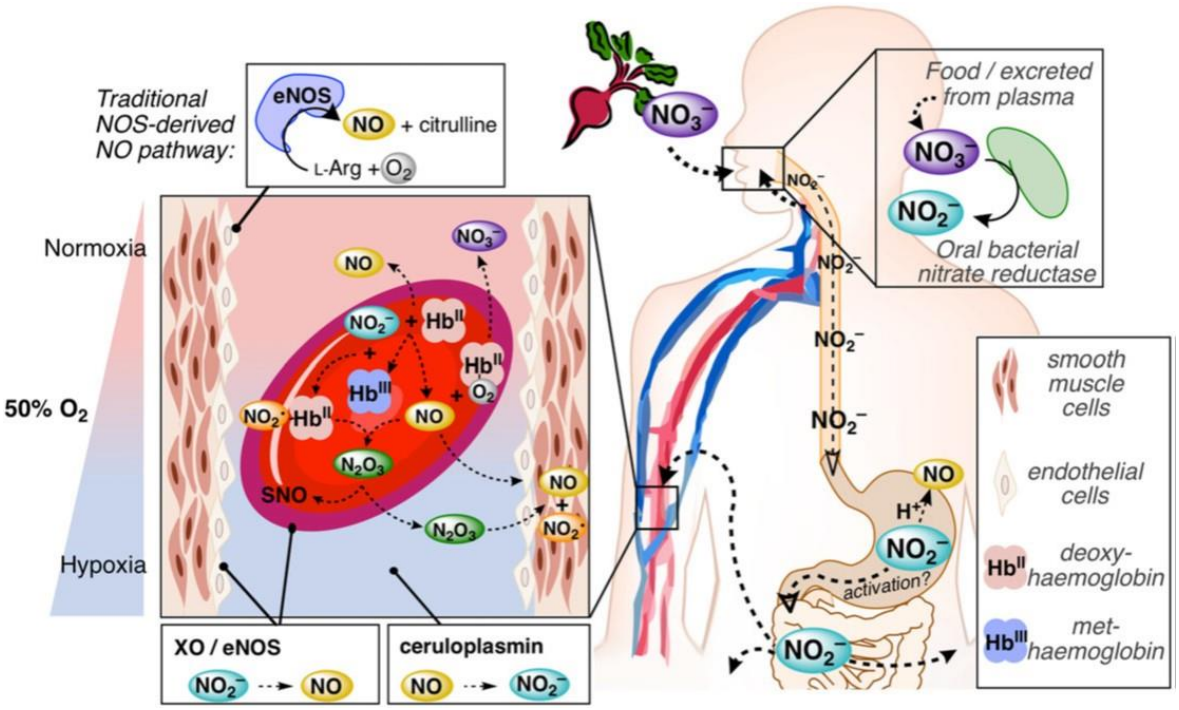

Figure 11. *Enzymatic and non-enzymatic synthesis of nitric oxide. Both enzymatic and non-enzymatic pathways contribute to NO synthesis and their activation is related to oxygen supply, that has a crucial role in the enzymatic reactions mediated by nitric oxide synthases (NOS) (upper left panel). NO can be also synthesized from dietary precursors, as* NO_3^-*,*

abundant in green leafy vegetables (upper right part of the figure). Salivary bacterial nitrate reductase reduces NO_3^- to NO_2^- that moves to the stomach where it is in part reduced to NO by gastric acidic environment or it is directly absorbed in the systemic circulation. NO_2^- can be reduced to NO by haemoglobin in red blood cells (central left panel) or it can be transformed to dinitrogen trioxide (N_2O_3) which moves from red blood cells to smooth muscle cells that mediate NO synthesis. Heamoglobin-mediated reaction can also synthesize NO_3^- which can start a new cycle for NO synthesis. Xantine oxidases (lower left panel) are also involved in NO generation from NO_2^-, while ceruloplasmin (lower central panel) mediates the formation of NO_2^- from NO. Figure from DeMartino et al., 2019.

Primary NO function is related to the modulation of the vascular tone, but several other endothelial roles of the molecule has been underlined. Indeed, NO also regulates cells migration and proliferation, extracellular matrix degradation, platelet function, and reduces leukocytes interaction with vessel walls, exhibiting an anti-inflammatory effect (Kolluru et al., 2010). As a regulator of the vascular tone, NO activates different vasodilatory pathways in smooth muscle cells of the tunica media, with the resulting decrease of intracellular Ca^{2+} concentrations and the subsequent vasodilatory effect (Figure 12) (Zhao et al., 2015). In particular, NO diffuses from endothelial cells to smooth muscle cells where it activates soluble guanilate cyclase (sGC) which generates cGMP from GTP. Subsequent activation of Ca^{2+} uptake in the sarcoplasmic reticulum, Ca^{2+} extrusion in the extracellular environment, opening of calcium-activated potassium channels contribute to intracellular calcium decrease. Reduced intracellular calcium inactivates myosin light chain kinase, thus inducing muscle relaxation and vasodilation.

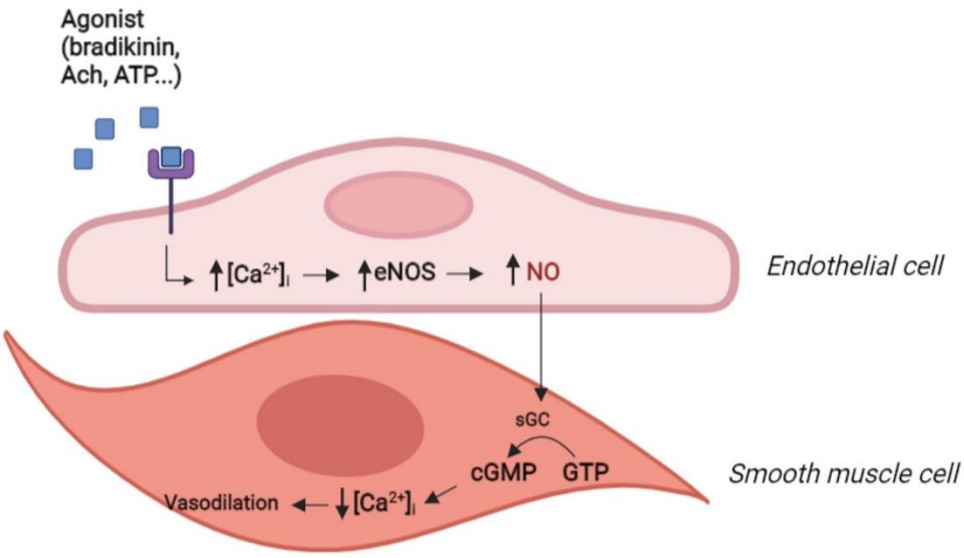

Figure 12. *Schematic overview of nitric oxide (NO) activated vasodilation. Receptor-agonists binding increases intracellular Ca^{2+} levels which activates eNOS and NO synthesis in endothelial cells. NO diffuses in smooth muscle cells of the tunica media and activates sGC that forms cGMP from GTP.Subsequent activated pathways enhance intracellular Ca^{2+} decrease and the vasodilatory process. Abbreviations: Ach (Acetylcholine); eNOS (endothelial nitric oxide synthase); NO (nitric oxide), sGC (soluble guanylate cyclase), GTP (Guanosine triphosphate); cGMP (cyclic guanosine monophosphate). Figure created with BioRender.com.*

1.1.4.2.1 Endothelial Nitric Oxide Synthase (eNOS)

As already mentioned, eNOS enzymes are primarily involved in NO synthesis in endothelial cells. Expression and function of eNOS can be regulated at different levels, such as transcriptional, post-transcriptional and post-translational. The enzyme is formed by a C-terminal reductase domain that transfers electrons from NADPH to the N-terminal oxygenase domain, which is directly involved in NO synthesis from L-Arginine and O_2. The reaction catalyzed by eNOS is strictly related to its dimerization and to the presence of several cofactors, in particular, tetrahydrobiopterin (BH_4), iron (Fe), flavin-mononucleotide (FMN), flavin-adenine-dinucleotide (FAD) and NADPH (Förstermann & Sessa, 2012; Kolluru et al., 2010). Activation of eNOS could be Ca^{2+}-dependent or Ca^{2+}-independent. Ca^{2+}-dependent eNOS activation is mediated by the rise of intracellular Ca^{2+} in response to several stimuli, such as bradikinin, acetylcholine, ATP or glutamate (Negri et al., 2020). Intracellular Ca^{2+} increase can be mediated by its entry from the extracellular environment, due to the opening of calcium permeable channels in the plasmatic membrane, and by its release from intracellular organelles, in particular, the endoplasmic reticulum. When Calmodulin (CaM) binds to Ca^{2+}, it moves to the catalytic site of eNOS and favors electron passage from the reductase domain containing NADPH, FAD and FMN, in one of the enzyme's monomers to the oxygenase domain of the other monomer. Consequent electron transfer form ferrous-dioxy species of ferric haem, in presence of BH_4 and L-Arginine results in the formation of L-Citrulline, NO and the radical BH_3•. Finally, BH_3• is reduced by eNOS flavins or ascorbic acid to reconstitute BH_4 (Förstermann & Sessa, 2012)(Figure 13).

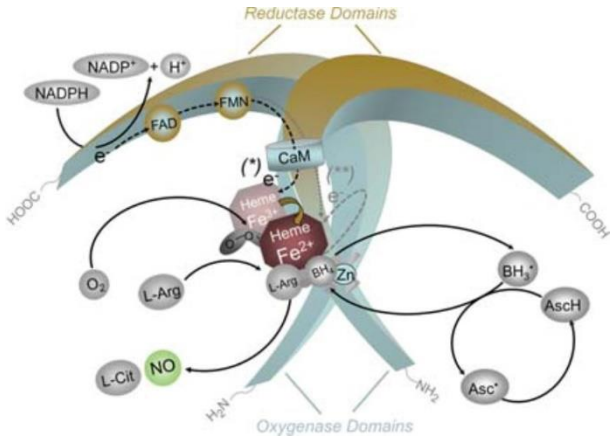

Figure 13. *Endothelial nitric oxide synthase (eNOS) calcium-dependent catalytic mechanism. Once calcium binds to calmodulin (CaM), it favours the passage of electrons from NADPH, FAD, FMN chain to Heme group that, when reduced, forms L-Citrulline and NO from L-Arginine and* BH_4*. Figure from Förstermann & Sessa, 2012.*

Calcium-independent activation of eNOS is related to post-translational modifications of the enzyme, that occur for example as a result of increased shear stress, and is mediated by different regulatory proteins, as heat shock protein 90 (hsp90) and Caveolin-1 (Cav-1) (Dudzinski & Michel, 2007; Förstermann & Sessa, 2012; Kolluru et al., 2010). Among eNOS post-translational modifications, irreversible myristoylation provides membrane association and caveolar compartmentalization of the enzyme, and reversible palmytoylation allows the enzyme to move across different membrane microdomains. Caveolar eNOS compartmentalization is fundamental to allow eNOS interaction with regulatory proteins, facilitating the communication with upstream and downstream pathways (Dudzinski & Michel, 2007; Förstermann & Sessa, 2012; Kolluru et al., 2010). In particular, in caveolae Cav-1 binding to eNOS can occur, and this mechanism represses the enzyme's activity. Indeed, caveolar Cav-1 binds eNOS through a protein-protein interaction blocking eNOS-stimulatory signals and calmodulin binding site of the enzyme (Dudzinski & Michel, 2007). Conversely, hsp90 activates eNOS enhancing calmodulin binding and NO synthesis (Dudzinski & Michel, 2007).

Post-translational modifications of eNOS can also be mediated by kinases or phosphatases and NO synthesis is often regulated by a phosphorylation/dephosphorylation mechanism in response to different extracellular stimuli (Figure 14). In particular, phosphorylation of different residues activates the enzyme: Ser1177/Ser1179 (human /bovine) is the most studied eNOS post-translational modification that inhibits calmodulin dissociation from the enzyme and is mediated by different kinases, as kinase Akt (protein kinase B), cyclic AMP-

dependent protein kinase (PKA), AMP-activated protein kinase (AMPK), PKG and CaM kinase II (Dudzinski & Michel, 2007; Förstermann & Sessa, 2012; Kolluru et al., 2010). Also, phosphorylation at Ser615/Ser617 (human/bovine) by Akt and PKA inhibits calmodulin dissociation and probably enhances other sites phosphorylation (Dudzinski & Michel, 2007; Förstermann & Sessa, 2012; Kolluru et al., 2010). Activation of the enzyme also occurs when Ser633/Ser635 (human/bovine) is phosphorylated by PKA (Dudzinski & Michel, 2007; Förstermann & Sessa, 2012; Kolluru et al., 2010). Inactivation of the enzyme occur when Ser116 and Thr495/Thr497 (human/bovine) are phosphorylated by protein kinase C and AMPK, with the resulting weakening of calmodulin eNOS binding (Figure 14). Also Tyr81 and Tyr657 can be phosphorylated but their role in eNOS activation has to be fully elucidated (Dudzinski & Michel, 2007; Förstermann & Sessa, 2012; Kolluru et al., 2010). Dephosphorylation of these residues is mediated by phosphatases and, according to the involved site, these modifications can activate or inhibit eNOS. For example, serine-threonine protein phasphatase 1 (PP1) activates eNOS through Thr495 dephosphorylation and the same effect is mediated by calcineurin that acts both on Ser116 and Thr495. Furthermore, serine-threonine protein phosphatase 2A (PP2A) dephosphorylates eNOS on Ser1177 thus acting as a negative regulator of the enzyme (Dudzinski & Michel, 2007).

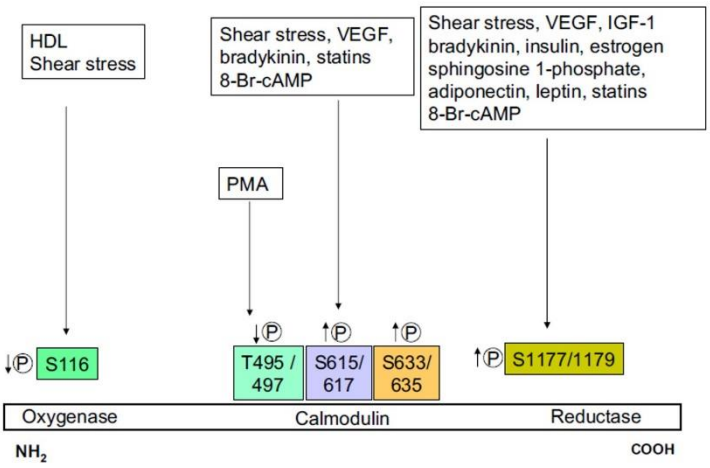

Figure 14. *Different phosphorylation sites of eNOS. Shear stress, vascular endothelial growth factor, bradikinin enhance eNOS activity activating phosphorylation at Ser615(human)/617(bovine); Ser633(human)/635(bovine) and Ser1177(human)/1179(bovine) and reducing phosphorylation at Ser116 and Thr495(human)/497(bovine). Figure from Kolluru et al., 2010.*

Another proposed post-translational modification of eNOS is its S-nitrosylation at Cys94 and Cys99 residues that inhibits the enzyme's activity. Some evidences suggest that S-

nitrosylation of eNOS is dependent on its cellular localization: membrane proximity seems to facilitate the reaction causing the enzyme's inhibition, while cytosolic reducing environment seems to facilitate eNOS denitrosylation and its activation (Dudzinski & Michel, 2007).

According to all described regulations of eNOS activity, Dudzinski and Michel proposed a model for eNOS post-translational modifications and NO synthesis (Figure 15) (Dudzinski & Michel, 2007). The authors show that in an inactive state eNOS is anchored in caveolar membrane sites through myristoylation and palmitoylation, it is bound to Cav-1, phosphorylated at Ser116 and S-nitrosylated, therefore, the calmodulin (CaM) interaction in the active site of the enzyme is inhibited (Figure 15 panel 1). Agonist stimulation, mediated for example by bradykinin, vascular endothelial growth factor (VEGF) or ATP (Fulton et al., 2008; Jl et al., 2013), induces intracellular Ca^{2+} increase and its binding to CaM. Ca^{2+}-CaM complex interacts with eNOS, contributing to its detachment from Cav-1 (Figure 15 panel2). Further activation of the enzyme is accompanied by dephosphorylation at Ser116, denitrosylation and phosphorylation at Ser1179 (Figure 15 panel 3). Prolonged stimulation by the agonist causes the detachment of the enzyme from the plasma membrane through depalmytoylation and its translocation to intracellular compartments. Furthermore, Ser116 phosphorylation and calmodulin dissociation occour, thus favouring the binding of eNOS to Cav-1 which restores its inactive form (Figure 15 panel 4-1) (Dudzinski & Michel, 2007).

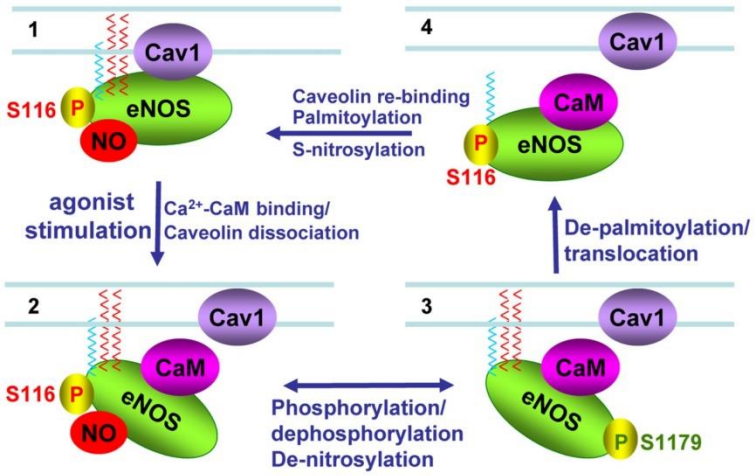

Figure 15. *Endothelial nitric oxide post-translational modifications. 1) eNOS is inactive and located near the plasma membrane through mirystoylation and palmitoylation. Its inactive state is favoured by Cav-1 binding, phosphorylation at Ser116 and S-nitrosylation. 2) Intracellular calcium increase due to agonist stimulation dissociates Cav-1 binding and enhances Calmodulin (CaM) binding to the active site of eNOS. 3)Further activation of the enzyme favours Ser116 dephosphorylation, denitrosylation and Ser1179 phosphorylation. 4)Internalization of eNOS is favoured by depalmitoylation that is followed by dephosphorylation at Ser1179. Subsequent phosphorylation at Ser116 inactivates the enzyme and drives it again to its quiescent state. Figure from Dudzinski & Michel, 2007.*

Among the large amount of agonists involved in eNOS activation and thus in the modulation of vascular tone, extracellular nucleotides have been extensively investigated (da Silva et al., 2009; Strassheim et al., 2020). Nucleotides can be released in extracellular compartments from the intracellular environment by exocytosis and membrane transport systems in response to cellular activation or cell death. In particular, nucleotides bind to specific receptors (P2), that are classified in P2X, ligand-gated ion channels, and P2Y, G-protein coupled receptors. Different P2 receptors subtypes are expressed in humans, in particular there have been characterized seven P2X subtypes (P2X1-P2X7) and eight P2Y subtypes (P2Y1, P2Y2, P2Y4, P2Y6, P2Y11-P2Y14). P2X receptors exclusively binds ATP and their activation favours direct extracellular Ca^{2+} entry; while P2Y binds ATP, ADP, UTP and UDP and activates Ca^{2+} release from intracellular stores (da Silva et al., 2009). Recent studies underline that exogenous ATP stimulation of endothelial cells activates P2 receptor-mediated intracellular calcium increase that facilitate CaM binding to eNOS and Ser1177 phosphorylation, thus stimulating NO synthesis and vasodilatory response (Cale & Bird, 2006; da Silva et al., 2009). Moreover, it is now widely accepted that shear stress caused by blood flow can induce endothelial ATP release which acts in a paracrine and autocrine way inducing intracellular calcium increase, due both to its entry from the extracellular environment through opening of calcium permeable channels in the plasma membrane and to its release from intracellular organelles, and activating endothelial NO release (Figure 16) (Andrews et al., 2014; Yamamoto et al., 2018).

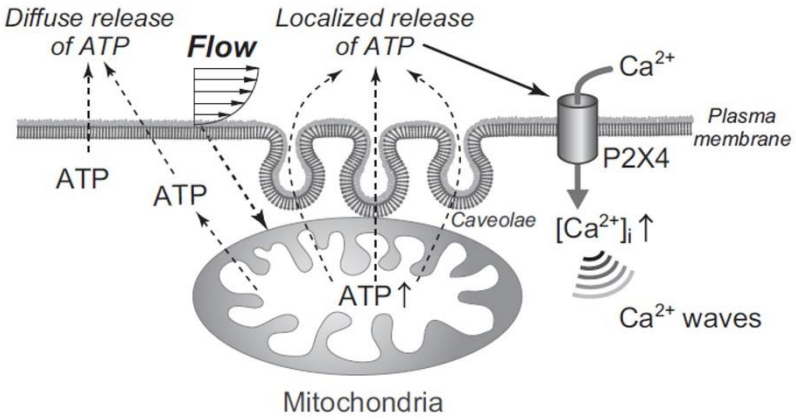

Figure 16. *Shear stress induces augmented ATP release by endothelial cells. Blood flow causes an increased release of ATP from mitochondria. ATP can diffuse to the extracellular compartments from the entire cell surface or from caveolae rich regions. Extracellular ATP binds to purinergic receptors thus inducing the rise of intracellular* Ca^{2+} *and activation of calcium-dependent pathways. Shear stress-induced ATP release has a paracrine effect on the regulation of the vasodilatory mechanism. Figure from Yamamoto et al., 2018.*

Da Silva and other groups propose the possible pathway activated by exogenous ATP and other nucleotides through P2Y receptors, that are G-protein coupled receptors and activate Ca^{2+} release from intracellular stores, as already underlined. ATP binding to its receptor activates Gαq subunit that starts phospholipase C (PLC)-mediated response with the induction of the rise of intracellular Ca^{2+} through inositol triphosphate (IP3). Calcium increase enhances CaM binding to eNOS and phospho kinase C δ (PKCδ) activation, that directly phosphorylates eNOS (Figure 17) (Andrews et al., 2014; da Silva et al., 2009).

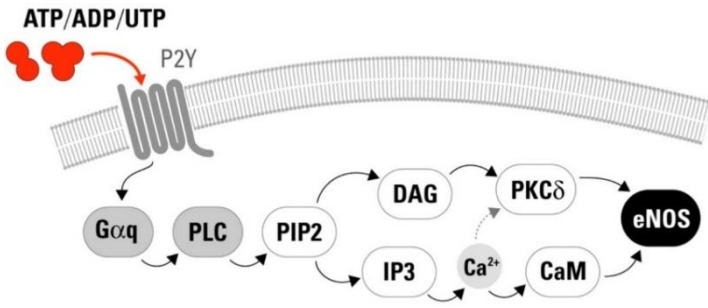

Figure 17. *Extracellular nucleotides activation of eNOS. ATP binds to its receptor P2Y and activates the intracellular pathways involving phospholipase C (PLC) that through IP3 induces the rise of intracellular calcium that activates Calmodulin (CaM) binding to eNOS and phospho kinase C δ (PKCδ) eNOS phosphorylation at Ser1177. Figure from da Silva et al., 2009.*

1.2 CHAPTER 2

1.2.1 Trimethylamine (TMA)

Trimethylamine (TMA; N,N-dimethylmethanamine) is a tertiary amine which is both derived from the environment and synthesized by the human body from dietary precursors. TMA is a colorless volatile compound with a characteristic fishy odour. The presence of the amine nitrogen in its molecular structure allows the molecule to form hydrogen bonds with the surrounding water (Figure 18) (Chhibber-Goel et al., 2016; Rozenberg et al., 2012).

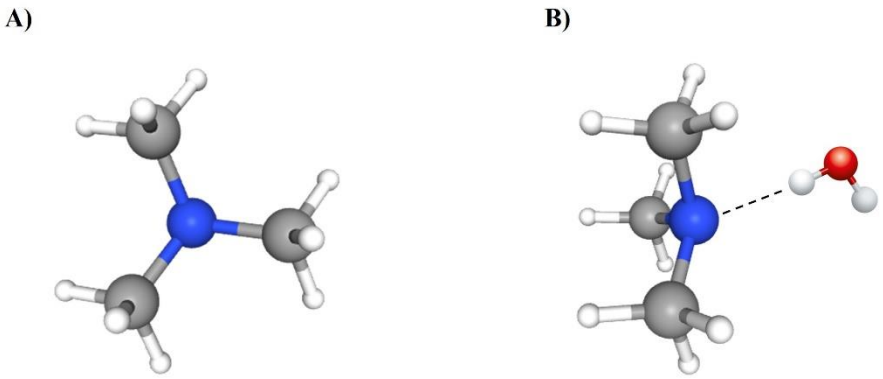

Figure 18. *Molecular structure of trimethylamine (TMA) and its interaction with water. A) Ball and stick structrural model of TMA. Image from PubChem (https://pubchem.ncbi.nlm.nih.gov/compound/Trimethylamine). B) The amine nitrogen allows the molecule to form hydrogen bonds with water. Image adapted from Rozenberg et al., 2012. Ball color legend: blue: nitrogen; grey: carbon; white: hydrogen; red: oxygen.*

TMA is an air pollutant that generates from vehicular exhaust, anaerobic fermentation of foods waste and husbandry industry, like fish-meal plants and swine waste storage pits (Chhibber-Goel et al., 2016). Workers employed in these production processess are continuously exposed to this pollutant, which, due to its physical properties, can enter the human body through breath or skin causing different systemic pathologies (Chhibber-Goel et al., 2016; Kiouptsi et al., 2018; Schmidt & Leroux, 2020; Ufnal, 2020).

TMA can also be synthesized by the human gut microbiota from several dietary precursors, in particular trimethylamine N-oxide (TMAO), choline, L-carnitine and ergothioneine. Next paragraphs will discuss dietary origin and metabolic pathways that drive to TMA synthesis from its precursors (Figure 19).

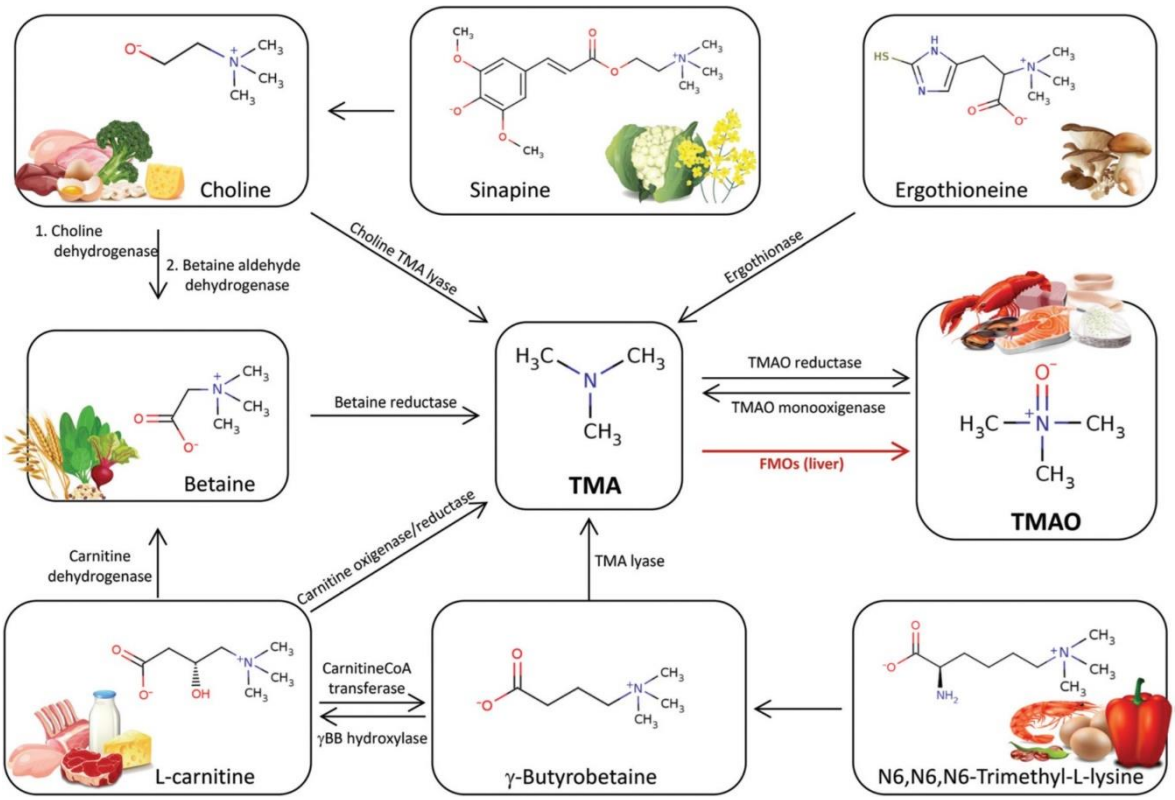

Figure 19. *Dietary precursors of trimethylamine (TMA). Trimethylamine N-oxide from seafood products is converted to TMA by TMAO monooxygenase; Choline, and its derived metabolites sinapine and betaine, from animal-derived foods are transformed to TMA by Choline TMA lyases (encoded by CutC/CutD genes); L-Carnitine and γ-Butyrobetaine from meat and dairy products are converted to TMA by Carnitine oxigenase/reductase (encoded by CntA/CntB genes) and TMA lyase; Ergothioneine derived from mushrooms forms TMA by Ergothionase mediated reactions. Figure from Simó C. & García-Cañas V., 2020.*

1.2.2 TMA precursors

1.2.2.1 Trimethylamine N-oxide (TMAO)

TMAO, which is the N-oxygenated form of TMA (see below), is present in high concentrations in marine fishes and shell fish products (Treberg, 2006). In particular, concentrations of TMAO can vary among species and different concentration ranges can be registered in the same species, for example ray-finned fishes can contain from 8 mg to 789 mg / 100 g and cartilaginous fishes from 262 mg to 789 mg /100 g of TMAO (Simó & García-Cañas, 2020). Once introduced through diet, TMAO can be converted to TMA by TMAO monooxygenase encoded from gut bacterial *torA*-like gene (Figure 19) (Hoyles et al., 2018; Janeiro et al., 2018; Méjean et al., 1994; Simó & García-Cañas, 2020).

1.2.2.2 Choline

Choline is the most studied precursor of TMA. Choline has several biological functions in human body being involved in cell membrane structure, lipid metabolism and acetylcholine synthesis (Tang et al., 2013). In this scenario, choline figures as a semi-essential nutrient and its dietary intake is important to sustain endogenous synthesis to face with metabolic demands. Indeed, the European Food Safety Authority (EFSA) assesses at 400 mg the proper daily intake of the nutrient for both men and women (Simó & García-Cañas, 2020). Choline can be introduced in its free form, but also through other different forms: phosphocholine, glycerophosphocholine, phosphatidylcholine, betaine and sphingomyelin. Choline and its different forms are highly present in eggs, liver, and other animal-derived foods such as meat, fish or dairy products (Figure 19). Choline is also present in lower amounts in whole grains, fruits and vegetables, in particular a phenolic choline ester, sinapine, has been found in members of the *Brassicaceae* family (Simó & García-Cañas, 2020). It has been untlined that high intake of choline and its derived metabolites, as occurs in Western Diet rich in animal-derived foods, can favour the proliferation of choline metabolizing bacteria in the gut microbiota, thus favoring the formation of TMA.

The enzymes implicated in choline-TMA formation are expressed by the choline utilization gene cluster *CutC* and *CutD*, that encode respectively for the choline TMA-lyase and its S-adenosyl-L-methionine activating protein (Falony et al., 2015; Simó & García-Cañas, 2020). *CutC*/*CutD* are expressed prevalently by bacteria belonging to Firmicutes, Proteobacteria and Actinobacteria phyla (Falony et al., 2015; Jameson et al., 2018; Rath et al., 2017; Simó & García-Cañas, 2020). Furthermore, some Proteobacteria species have been shown to express the oxygenase/reductase system *YeaW*/*YeaX*, which catalizes the conversion of choline to TMA (Figure 20) (Falony et al., 2015; Simó & García-Cañas, 2020).

1.2.2.3 L-Carnitine

L-Carnitine, and its derived metabolite γ-Butyrobetaine, represent further TMA precursors (Rajakovich et al., 2021). L-Carnitine mediates the transfer of long-chain fatty acids through the mitochondrial membrane for β-oxidation. Because of its essential physiological role, L-Carnitine is endogenously synthesized from methionine and lysine, and when no sufficient supply is provided by the endogenous pool, an exogenous source has to be provided. Usually, dietary intake thruogh animal-derived foods is sufficient to ensure necessary missing quantities (Figure 19). In particular, L-Carnitine content in meat ranges from 45 to 66 mg /100 g while dairy products can contain from 3 to 42 mg / 100 g of the compound (Simó & García-Cañas, 2020). Sometimes in vegetarian and vegan diets L-Carnitine deficit occurs

and it is necessary to integrate the nutrient with dietary supplements. Excessive uptake of L-Carnitine-rich foods causes the metabolic conversion of the molecule to TMA by gut bacteria expressing the oxygenase/reductase system (*Cnt*A/*Cnt*B). Particularly *Proteobacteria* species have been outlined to express *Cnt*A/*Cnt*B (Falony et al., 2015; Jameson et al., 2018; Rath et al., 2017; Simó & García-Cañas, 2020). Moreover, recent evideneces suggest that also *YeaW*/*YeaX* can synthesize TMA from L-Carnitine (Falony et al., 2015; Simó & García-Cañas, 2020) (Figure 20).

1.2.2.4 Ergothioneine

Ergothioneine is a sulfur-derivative of histidine and it is introduced in human body by its dietary intake. In particular, ergothioneine is present in mushrooms, where its content ranges from 0.9 to 1.1 mg / 100 g. Its conversion to TMA in the gut is mediated by the enzyme ergothionase (Falony et al., 2015; Simó & García-Cañas, 2020) (Figure 19).

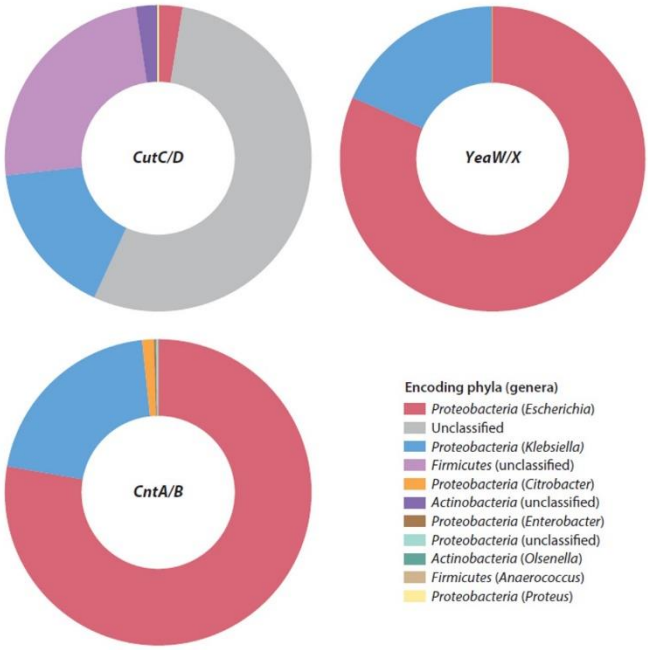

Figure 20. *Microbiota Phyla carrying the genes involved in TMA synthesis. The choline TMA-lyase and its S-adenosyl-L-methionine activating protein (CutC/D), expressed primarily by Firmicutes, Proteobacteria and Actinobacteria, catalyzes the synthesis of TMA from choline. The oxygenase/reductase systems CntA/B and YeaW/X particularly expressed by Proteobacteria are involved in TMA synthesis from L-carnitine. Figure from Falony et al., 2015.*

1.2.3 TMA in systemic circulation

Once synthesized, TMA can be directly excreted through faeces or can cross the intestinal barrier thanks to its small dimensions and volatility properties. Part of absorbed TMA enters the systemic circulation, through which it can face directly with different tissues before being excreted in urine, sweat and breath (Mitchell & Smith, 2003, 2016). Due to its volatility and to its odour of rotten fish, different studies have been addressed to the evaluation of a possible role of TMA as a chemical messenger able to be detected even at low olfactory thresholds. Human olfactory system has developed specific receptors, the trace-amine associated receptors (TAARs), and in particular TAAR5 recognizes the molecule at a detection threshold of 1 µM and a EC_{50} value of 116 µM in *in vitro* models (Catucci et al., 2019; Mitchell & Smith, 2016; Schmidt & Leroux, 2020; Wallrabenstein et al., 2013). As other olfactory receptors, also TAAR5 variants can affect the perception of TMA, influencing the subsequent responses to this volatile compound (Gisladottir et al., 2020).

A pathological condition associated with excessive circulating TMA is the 'fishy odor syndrome' or trimethylaminuria (TMAU), characterized by the malodorous-TMA excretion from sweat and breath. TMAU is caused by an impaired activity of the flavin containing monooxygenase 3 (FMO3), which catalyses the N-oxidation of TMA, reducing its levels in the systemic circulation (Catucci et al., 2019). Even if this condition is not associated with any physical disability, a disabling psychological discomfort affects TMAU patients. Indeed, due to their smell, they tend to isolate from the community and often develop severe depression (Roddy et al., 2020).

Circulating TMA has also shown toxic effects. In particular, N-nitrosodimethylamine, one of its metabolic byproducts, can be converted to methyldiazonium, which can form different adducts, such as O^6Methylguanine, that acts as a tumorigenic factor (Figure 21) (Chhibber-Goel et al., 2016).

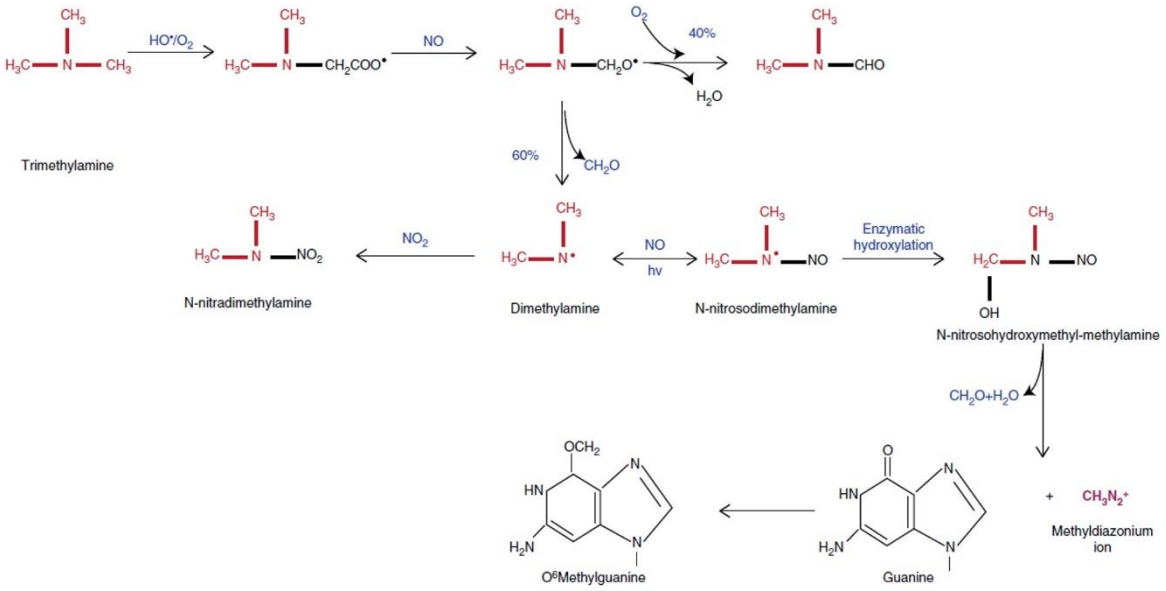

Figure 21. *TMA nitrosation. Once TMA enters the human body it can be transformed to N-nitrosodimethylamine, which is then converted to O[6]Methylguanine, a carcinogenic compound. Figure from Chhibber-Goel et al., 2016.*

1.2.4 Trimethylamine N-oxide (TMAO)

Trimethylamine N-oxide (TMAO) is the product of N-oxygenation of TMA. This reaction occours in the liver, where TMA is carried by the portal circulation. Enzymes involved in TMA oxidation are flavin containing monooxygenases (FMOs). Five functionally active FMO's isoforms are present in human body: FMO1, principally expressed in kidneys and small intestine; FMO2, expressed in kidneys and lungs; FMO3 and FMO5, expressed in the liver, and FMO4 expressed at low level in several tissues (Catucci et al., 2019; Fennema et al., 2016). FMOs participate to xenobiotics detoxification process in parallel with cytocrome P450 family enzymes, and their catalytic cycle forms S- or N-oxides easily excreted with urine. The reaction of TMA conversion to TMAO in adult human liver is specifically catalyzed by FMO3 (Catucci et al., 2019; Fennema et al., 2016; Lang et al., 1998). The reaction catalyzed by FMO3 needs TMA and O_2 as substrates and NADPH and FAD as cofactors and the resulting products are TMAO and H_2O (Figure 22) (Catucci et al., 2019). In particular, the catalytic cycle is composed by a first reductive half-reaction, in which the enzyme binds NADPH, receives two electrons on the FAD cofactor and then binds O_2. Then, a subsequent oxidative half-reaction occurs, in which TMA can access the active site and receives an atom of oxygen thus forming its N-oxide, TMAO, and H_2O. Once the reaction is completed, $NADP^+$ leaves FMO3's active site and FAD cofactor is regenerated for further

reactions (Catucci et al., 2019). It has been already underlined that genetic mutations of FMO3 cause impairment of its activity and the development of TMAU.

Figure 22. *Reaction catalyzed by flavin containing monooxygenase 3 (FMO3) which induces the N-oxygenation of TMA to TMAO. Figure from Catucci et al., 2019.*

TMAO is a colourless to yellow solid and, differently from its precursor, is odourless. It solubilizes in water thanks to the formation of hydrogen bonds between the oxygen in its hydrophilic head and hydrogen residues of H_2O molecules (Figure 23) (Ufnal et al., 2015). This physical property of TMAO favours its presence in body fluids of different organisms.

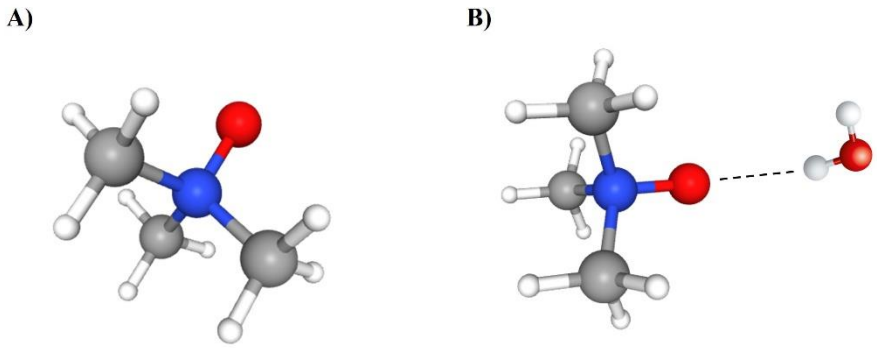

Figure 23. *Molecular structure of trimethylamine N-oxide (TMAO). Ball and stick structural model of TMAO. Image from PubChem (https://pubchem.ncbi.nlm.nih.gov/compound/Trimethylamine). B) The oxygen present in TMAO allows the molecule to form hydrogen bonds with water. Image adapted from Ufnal et al., 2015. Ball color legend: blue: nitrogen; grey: carbon; white: hydrogen; red: oxygen.*

First studies focused on TMAO and its physiological role have been targeted to marine animals, in which its concentrations are higher than other species (Catucci et al., 2019). In particular, it has been outlined that deep-sea fishes present the highest TMAO plasma concentrations. Recent evidences suggest a possible adaptative role of TMAO, that in these organisms acts as an osmolyte, able to balance hydrostatic and osmotic pressures that characterize deep-sea habitats (Ufnal et al., 2015). Furthermore, it has been shown that TMAO acts as a protein stabilizer, functioning as a chemical chaperone, able to balance other molecules deleterious effects on protein structure (Catucci et al., 2019; Ufnal et al.,

2015). Three different models have been proposed to describe TMAO-mediated protein stabilization mechanism: the first suggests that TMAO forms a protective shell that favours the maintainance of the native form of the protein. The second model proposes a direct interaction of TMAO with protein backbone, with the formation of hydrogen bonds that stabilize the structure. The third model presents TMAO as a surfactant that stabilizes protein surface. Probably, TMAO acts in all three ways depending on the solution's pH that shapes its protonated or deprotonated form (Catucci et al., 2019; Ufnal et al., 2015).

1.2.5 TMAO in systemic circulation

Once TMAO in synthesized in the liver, it is released in the systemic circulation through the involvement of different membrane transporters. Indeed, due to its solubility in hydrophilic solvents, as already underlined, cytoplasmic TMAO figures as a zwitterione unable to cross the lipophilic barrier of cell membranes. Teft and collaborators suggested the involvement of ATP Binding Cassette (ABC) transporters in the regulation of TMAO efflux from hepatocytes. In particular, they found that ABCB1, ABCG2, ABCC2 and ABCC4 are primarily involved in TMAO transport to the systemic circulation (Teft et al., 2017). In order to reduce TMAO accumulation in body fluids, it is excreted through kidneys, as many other detoxification byproducts released by the liver. So, further studies were addressed to the evaluation of renal influx-efflux systems that regulate TMAO clearance. Evidences suggest that renal cells regulate TMAO influx by the organic cation transporter 2 (OCT2) while its efflux is mediated by the same transporters involved in the hepatic extrusion of the molecule (Miyake et al., 2017; Samodelov et al., 2020; Teft et al., 2017).

A plethora of recent publications and meta-analysis prospective studies try to outline TMAO plasmatic concentrations in order to define reference ranges. Obtained results showed that human TMAO plasma concentrations range from 1.74 to 103.81 µmol/L and these differences are probably due to divergencies in studied cohorts. Furthermore, it has to be considered that different other factors can contribute to the modulation of circulating TMAO. First, dietary precursors uptake that can directly modulate TMA, and thus TMAO, synthesis. Second, expression and activation of FMO3, that can influence TMAO synthesis. Third, TMA and TMAO renal clearance capacity, that is strictly related to the expression of specific membrane transporters. Even if a fixed range of TMAO concentrations is still lacking, all physicians agree that its higher plasma concentrations are strictly related to severe cardiovascular outcomes and chronic kidney disease development (Gatarek & Kaluzna-Czaplinska, 2021; Heianza et al., 2017).

Figure 24 summarizes the already explained metabolic pathways involved in TMA synthesis and its transformation to TMAO (Zeisel & Warrier, 2017).

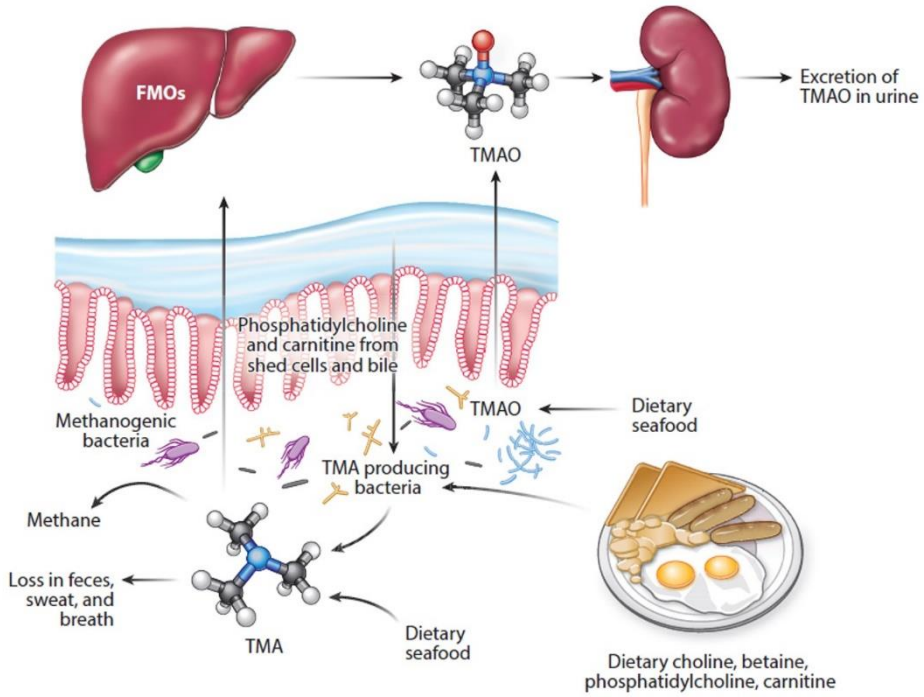

Figure 24. *Endogenous synthesis of trimethylamine (TMA) and its N-oxygenated form (TMAO). Dietary precursors, primarily choline, L-carnitine and ergothioneine are converted by the gut microbiata to TMA which enters the portal circulation and in the liver is N-oxygenated to TMAO by FMO3 enzymes. TMAO is then excreted through renal filtration. Figure from Zeisel and Warrier, 2017.*

1.3 CHAPTER 3

1.3.1 Cardiovascular diseases and the gut microbiota

The human body hosts a high number of microorganisms that play a pivotal role in mediating inner and outer environments communication. The microflore residing in human body is called microbiota, and is localized mainly in the gastrointestinal tract, in particular in the gut (Novakovic et al., 2020). Gut microbiota is composed by microorganisms that belong principally to two phyla, *Bacteroidetes* and *Firmicutes*. Members of *Actinobacteria*, *Proteobacteria*, *Cyanobacteria*, *Fusobacteria* and *Verrucomicrobia* phyla have also been isolated. Gut microbiota resides primarily in the colon and counts of approximately 1000 species (Novakovic et al., 2020).

Intra- and inter-individual differences have been outlined in microbes colonizing the gut: they are in continuous balance with the host and change throughout life. In particular, perinatal composition of the intestinal microbiota is highly influenced by the way of birth: vaginally birth is characterized by *Lactobacillus*, *Prevotella*, and *Atopobium* colonization, while caesarean section provides a major *Staphylococcus* colonization, principally derived from mother's skin. During growth, a switch towards anaerobic microbes occurs and an abundance of *Bifidobacteria* and *Clostridia* characterizes the gut microbiota of adolescents. Adulthood presents a more stable and differentiated composition in microbial phyla, that are mainly represented by *Bacteroidetes*, *Firmicutes*, *Actinobacteria*, *Cyanobacteria*, *Fusobacteria*, *Proteobacteria* and *Verrucomicrobia*. During old ages loss of microbial phyla diversity occurs, predisposing to age-related physiological dysfunctions (Figure 25) (Novakovic et al., 2020).

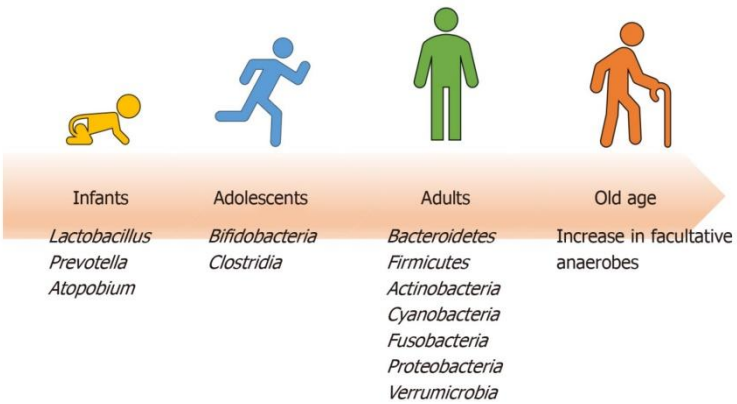

Figure 25. *Microbiota composition changes throughout life. Perinatal period is strictly influenced by the way of birth: vaginally birth induces a high number of Lactobacillus, Prevotella, and Atopobium microorganisms. During adolescence changes from the aerobic to anaerobic environment cause Bifidocteria and Clostridia prevalence. In adulthood a stable composition of the microbiota occurs with Bacteroidetes, Firmicutes, Actinobacteria, Cyanobacteria, Fusobacteria, Proteobacteria and Verrumicrobia prevalence. In elderly ages the shift in Bacteroidetes to Firmicutes ratio is caused by a complessive decline of physiological functions. Figure from Novakovic et al., 2020.*

Recent evidences point out that both intrinsic (genetic, sex) and extrinsic (environment, life style, pharmachologic therapies) factors play a pivotal role in shaping microbiota composition (Novakovic et al., 2020).

The gut microbiota has different physiological functions in human body, defining a symbiotic relationship that causes the reciprocal influence between these microorganisms and the host.

Gut microbiota is involved in the digestive process, favouring the metabolic transformation of some nutrients and their absorption by enterocytes (Rowland et al., 2018). A general classification based on microorganisms's metabolic profile in the gut recognizes a saccharolytic and a proteolytic group. The first group synthesizes short chain fatty acids (SCFA) from sugars metabolism, and the second synthesizes SCFA, amines, phenols and indoles from protein fermentation (Tang et al., 2017). Furthermore, gut microbiota is involved in essential micronutrients synthesis, in particular vitamin K and vitamin B group, making them available for intestinal absorption (Rowland et al., 2018).

The gut microbiota is also involved in the regulation of the intestinal barrier and the immunological activation against pathogens (Novakovic et al., 2020; Tang et al., 2017).

Alteration of the gut microbiota population milieu, called dysbiosis, is associated with different pathological conditions such as gastrointestinal disorders, allergies, asthma, cancers, central nervous system disorders and metabolic syndrome (Kazemian et al., 2020; Novakovic et al., 2020; Tang et al., 2017; Witkowski et al., 2020). Dysbiosis is also related to the leaky gut syndrome, indeed, tight junction loss and augmented gut permeability due to intestinal mucosal barrier impairment, favor pathogens and toxins entry from the external environment enhancing further gut damage (Novakovic et al., 2020; Witkowski et al., 2020).

Recent studies outline gut microbiota implication in cardiovascular diseases development (Kazemian et al., 2020; Novakovic et al., 2020; Tang et al., 2017; Witkowski et al., 2020).

Gut microbiota effects on the cardiovascular system are mediated by a plethora of factors, classified in two main groups, direct and indirect (Kazemian et al., 2020).

1.3.1.1 Direct microbiota-mediated effects in CVD

Different molecules synthesized by the gut microbiota have been directly involved in CVD development. The way these molecules enter the systemic circulation can be different: mediated passage through enterocytes absorption or free passage thanks to augmented gut-permeability (Figure 26).

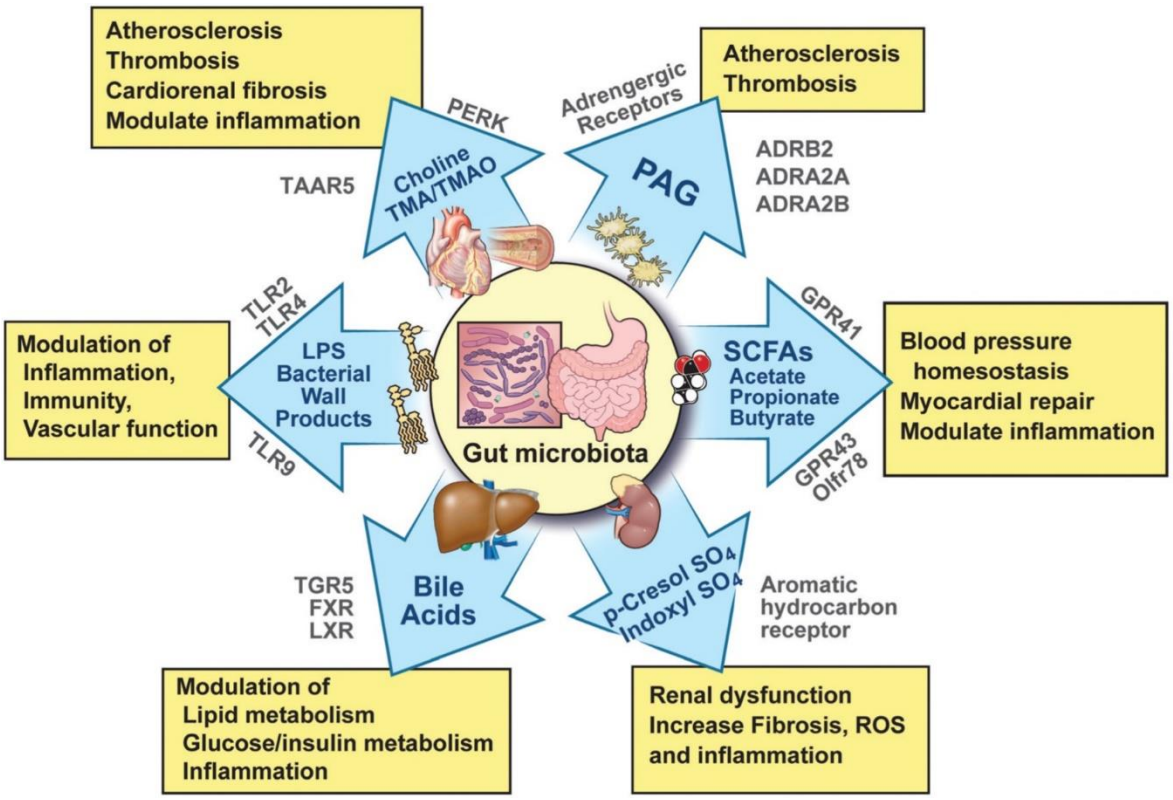

Figure 26. *Direct effects of gut microbiota in the development of cardiovascular diseases. Lipopolysaccharides, bile acids, short chain fatty acids (SCFAs) and secondary microbial metabolites such as uremic toxins (p-cresol sulfate and indoxyl sulfate), phenylacetylglutamine (PAG), trimethylamine (TMA) and trimethylamine N-oxide (TMAO) have been implicated in the development of cardiovascular diseases. Figure from Witkowski et al., 2020.*

1.3.1.1.1 Lipopolysaccharides

Lipopolysaccharides (LPS), known as endotoxins, are cell membranes components of Gram-negative bacteria, expressed also by gut microbial populations. LPS binding to toll-like receptors (TLR), expressed by immune system cells, activates pro-inflammatory cytokines

release. Higher circulating levels of LPS have been associated with CVD development, because of their contribution in activating and exacerbating the inflammatory state of higher risk patients (Novakovic et al., 2020; Witkowski et al., 2020). Furthermore, new evidences suggest a direct association between bacterial infection and CVD. In particular, gut microbiota bacterial species have been found in the atherosclerotic plaques suggesting a possible relation between microbial infection and pathological outcome (Novakovic et al., 2020) (Figure 26).

1.3.1.1.2 Short chain fatty acids

Short chain fatty acids (SCFA) are metabolic products of the gut microbiota, primarily derived from the fermentation of complex carbohydrates, like fibers. Acetate, propionate and butyrate are the principal SCFA produced in the gut and several studies have underlined their physiological function in mediating host-microbes signalling, energy utilization and pH control. New evidences show a protective role of SCFA in CVD development, playing a fundamental role in intestinal barrier integrity maintenance, lowering circulating cholesterol levels and lowering blood pressure (Kazemian et al., 2020; Witkowski et al., 2020). Furthermore, SCFA show a protective role in ischemia/reperfusion injury, myocardial infarction and impaired arterial compliance (Witkowski et al., 2020) (Figure 26).

1.3.1.1.3 Bile acids

Primary bile acids are synthesized in the liver from cholesterol. Bile acids can be converted to bile salts through taurine or glycine conjugation. Once bile salts are synthesized, they are accumulated in the gallbladder and then released in the small intestine where they favour dietary fat emulsion and absorption. The gut microbiota is able to synthesize secondary bile acids from primary bile acids. Examples of secondary bile acids produced by the gut microbiota are deoxycholic acid and lithocholic acid, which are absorbed with remaining primary bile acids and transported to the liver. Bile acids are able to activate farnesoid X receptor (FXR), a nuclear receptor which downregulates bile acids synthesis and increases cholesterol levels. High ratio of secondary bile acids to primary bile acids has been involved in dysbiosis-related heart failure, reduction of heart rate and regulation of vascular tone (Kazemian et al., 2020; Tang et al., 2017) (Figure 26).

1.3.1.1.4 Secondary metabolites

Among secondary metabolites synthesized by the gut microbiota which have shown a cardiovascular effect, phenylacetylglutamine (PAG), a byproduct in microbial phenylalanine metabolism, has been linked to the development of heart attack and stroke through the

interaction with α- and β- adrenergic receptors (Witkowski et al., 2020). Uremic toxins, such as indoxil sulfate and p-cresol sulfate have also been implicated in the development of CVD (Witkowski et al., 2020).

Tryptophane-derived metabolites have also been suggested as regulators of the cardiovascular system. In particular, indole-3-propionic acid (IPA), synthesized primarily by *Clostridium sporogenes*, modulates mitochondrial function in cultured HL-1 cardiomyocytes and improves cardiac contractility in isolated mouse hearts (Gesper et al., 2021). Furthermore, IPA increases blood pressure and cardiac metabolic activity (Konopelski et al., 2021).

Finally, microbiota conversion of cholesterol to coprostanol has been related to positive effects towards CVD, reducing cholesterol absorption and hypercholesterolemia development (Kazemian et al., 2020).

1.3.1.1.5 TMA and TMAO

New evidences suggest the already described microbiota-derived metabolite TMAO as a direct cause of CVD, showing, among all, its role in promoting atherosclerosis development (M. S. Thomas & Fernandez, 2021; Zhu et al., 2016). *In vitro* models point out that elevated levels of TMAO induce pro-inflammatory cytokines release via MAPK and NF-kB pathway, increase leukocytes and monocytes adhesion in cultured endothelial cells, reduce endothelial self-reparation and enhance endothelial dysfunction (Janeiro et al., 2018; Seldin et al., 2016). Direct TMAO platelet exposure induces Ca^{2+} release from intracellular stores, activating platelets hyperresponsiveness and showing a possible involvement of TMAO in *in vitro* thrombosis development (Zhu et al., 2016). Further studies also point out an involvement of the molecule in the development of cardiac damage and consequent CVD. Savi and collaborators show that TMAO causes impaired cardiomyocytes contractility, impaired intracellular calcium handling, accumulation of intracellular glycogen, increased mitochondria, metabolic changes and protein oxidative damage on isolated adult male rats cardiomyocytes (Savi et al., 2018). Moreover, isolated mice hearts show increased contractility after TMAO treatment suggesting an acute inotropic effect of the molecule (Oakley et al., 2020).

I*n vitro* models have also been supported by animal studies in which TMAO dietary supplementation accelerates atherosclerotic lesion, increases macrophage recruitment, induces CD36 expression and pro-inflammatory cytokines release, both in wild type (Organ et al., 2016) and Apolipoprotein E knock out ($ApoE^{-/-}$) mice models (Geng et al., 2018). Further *in vivo* studies underline that elevated plasma levels of TMAO in aged rats stricltly

correlate with endothelial dysfunction, pro-inflammatory cytokines release and superoxide production (T. Li et al., 2017).

Myocardial fibrosis, cardiac enlargement and worse ventricular ejection fraction develop in mice fed with a TMAO supplemented diet (Organ et al., 2016). Further evidences suggest that Western Diet causes augmented TMAO plasma levels which are strictly related to cardiac pro-inflammatory cytokines increase and the development of cardiac fibrosis and dysfunction (K. Chen et al., 2017).

Translational and clinical studies underline that higher TMAO plasma concentrations are related to increased risk of prevalent CVD and incident major adverse cardiac events, as myocardial infarction (Zununi Vahed et al., 2018), stroke or even death (Koeth et al., 2013; Tang et al., 2013), adjusted for traditional risk factors. Higher levels of TMAO were measured in chronic systolic heart failure patients and they were associated with advanced left ventricular diastolic dysfunction, and increased risk for 5-years adverse clinical events (Tang et al., 2015). Furthermore,Type 2 diabetes mellitus and chronic kidney disease patients have higher TMA-producing strains in their gut microbiota and show higher levels of plasma TMAO that directly correlate with chronic inflammation and endothelial dysfunction (Al-Obaide et al., 2017) (Figure 27).

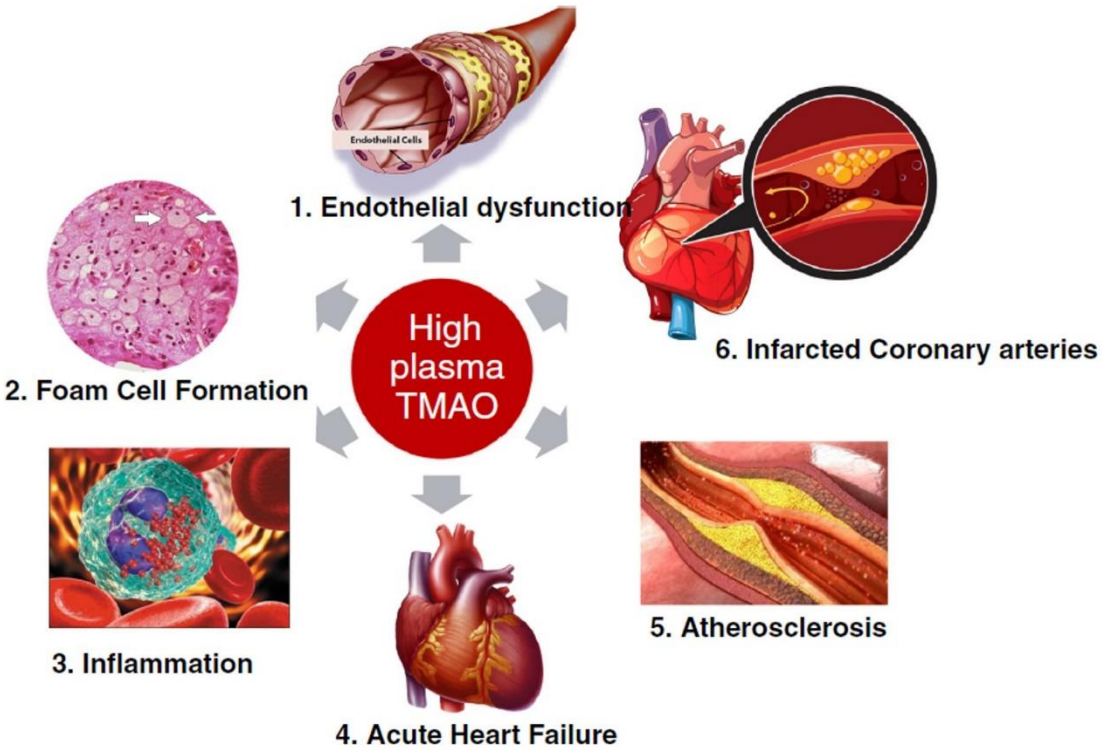

Figure 27. *Cardiovascular effects of trimethylamine N-oxide (TMAO). Elevated plasma levels of TMAO are related to different cardiac and vascular pathological conditions. Endothelial dysfunction, foam cell formation, inflammmation, acute heart failure atherosclerosis and coronary arteries infarction are the most studied TMAO-associated CVD. Figure from Thomas & Fernandez, 2021.*

On the other hand, studies suggest a neutral role of TMAO in CVD development, and motivate worse outcomes with existing risk factors that contribute to pathological manifestations. This hypothesis is supported by different *in vitro* works showing that TMA rather than TMAO is cytotoxic for cardiomyocytes (Jaworska et al., 2019) and that TMAO does not interfere with cardiomyocytes oxidative stress status (Querio et al., 2019). Furthermore, animal models show no effect of TMAO on cardiac functionality (Videja et al., 2020). TMAO supplementation of spontaneously hypertensive rats, increases plasma concentrations of the molecule, lowers NH2-terminal pro-B-type natriuretic peptide and vasopressin levels, reduces left ventricular end-diastolic pressure and cardiac fibrosis (Huc et al., 2018).

In this scenario, it is still unclear if TMAO higher plasma concentrations are direct cause or effect of a pre-exhisting pathological condition. Zeisel and Warrier propose this dual relationship between TMAO and CVD pointing out the possibility that both atherosclerosis and kidney disease can contribute to TMAO systemic accumulation. Moreover, deleterious effects seen in patients with higher TMAO plasma concentrations could not be directly mediated by the molecule, but they could be caused by exhisting pathologies (Figure 28) (Zeisel & Warrier, 2017).

Finally, it can also be underlined the role of diet and the controversial message that figures when meals with high fish content are suggested for patients with high risk of developing CVD. Considering, as already described, that fish products are rich in TMAO that could enter the sistemic circulation through direct absorbion by enterocytes, people eating diets rich in sea food products are exposed to higher concentrations of the molecule (Cho et al., 2017).

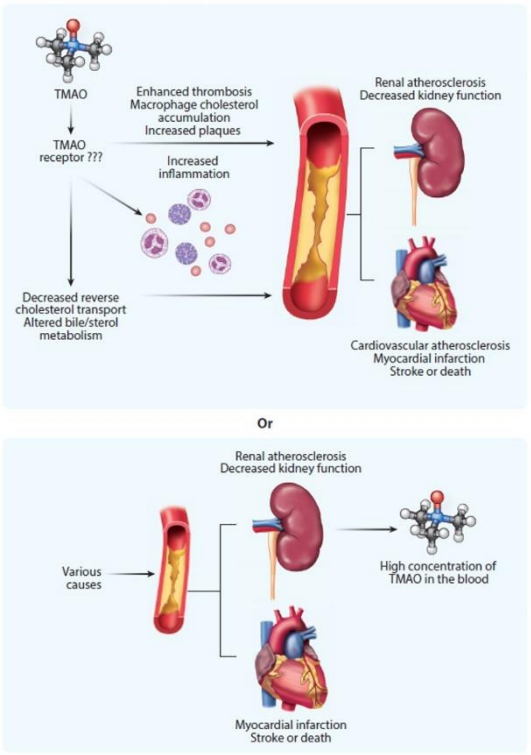

Figure 28. *Trimethylamine N-oxide (TMAO) and cardiovascular diseases relationship. It is still unknown if higher plasma concentrations of TMAO are a direct cause of cardiac and vascular outcomes or if exhisting vascular and renal diseases cause TMAO systemic accumulation. Figure from Zeisel & Warrier, 2017.*

1.3.1.2 Indirect microbiota-mediated effects in CVD

Indirect factors that influence microbiota-mediated CVD are those that affect the microbial diversity in the gut, thus favouring the proliferation of unwholesome pro-inflammatory bacterial strains that exacerbate pre-existing risk factors.

1.3.1.2.1 Diet

Diet is one of the primary factors involved in the modulation of microbiota population, and in the development of CVD. Indeed, a diet rich in lipids and carbohydrates is associated with tigh junctions loosening between enterocytes and mast cells activation, thus favouring LPS-mediated inflammatory response (Novakovic et al., 2020). Mediterranean Diet rich in unsaturated fatty acids, vegetables and legumes, has shown protective effects toward inflammation and metabolic alterations. Furthermore, a fiber-rich diet has been associated with higher SCFA production by the microbiota, thus favouring protection againsts CVD (Kazemian et al., 2020).

1.3.1.2.2 Demografic factors

Some factors that can influence microbiota homeostasis rely on host genetic, sex, ethnicity, age, smoking, physical activity and social position. These general CVD risk factors could influence also gut microbial populations, favouring dysbiosis.

As an example, people with lower education, those that live in poverty and have poor access or no access at all to healthcare support can easily develop wrong nutritional habits that contribute to the development of dysbiosis and a pro-inflammatory state (Kazemian et al., 2020).

Furthermore, aging promotes the development of dysbiosis and this physiological condition is related to a chronic inflammatory state that contributes to exacerbate CVD risk (Kazemian et al., 2020).

1.3.1.2.3 Drugs and pharmacological treatments

The use of drugs, and in particular antibiotics, is related to the development of dysbiosis and its linked pathologies. It is important to underline that microbiota and drugs strictly influence each other. Indeed, as already described, pharmacological treatment can alter microbial variety thus promoting dysbiosis, but also microbiota can interfere with drugs' systemic effects affecting both their absorption and function (Kazemian et al., 2020).

1.3.2 Strategies to prevent gut microbiota-mediated CVD

Several strategies have been proposed to prevent CVD through microbiota modulation. Contrasting results have been obtained between *in vitro* and *in vivo* studies regarding the efficacy of these different treatments. Further paragraphs will describe some proposed lines of intervention (Figure 29).

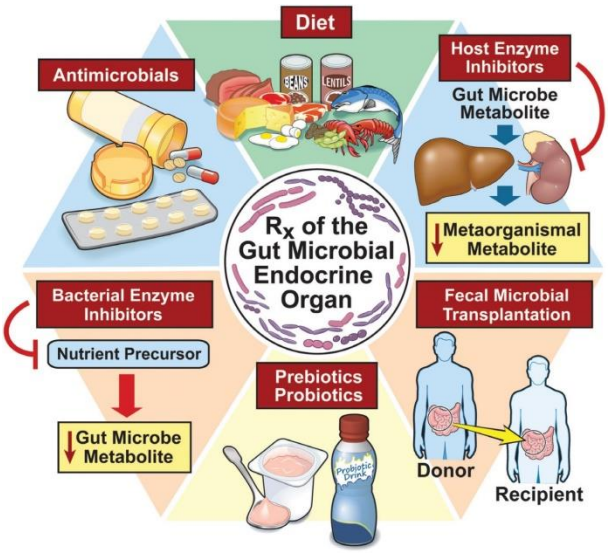

Figure 29. *Prevention of gut microbiota-derived cardiovascular diseases (CVD). Different lines of intervention have been suggested to prevent dysbiosis-derived CVD. In particular diet, prebiotics and probiotics figure as the primary lines of intervention. Faecal microbial transplantation and bacterial enzymes inhibitors, such as host enzyme inhibitors, have been suggested as pharmacological interventions with promising results in in vitro studies. Antimicrobials have been suggested but their related side effects discourage the large use in general population. Figure from Witkowski et al., 2020.*

1.3.2.1 Nutritional education

Among modifiable factors already explained in previous paragraphs, nutritional intervention figures as the primary and simplest way of prevention strategies. It has already underlined that Mediterranean Diet, rich in complex carbohydrates, low in animal proteins, rich in vegetables and fibers, figures as the most efficaceus life style intervention against CVD development. Mediterranean Diet reduces dysbiosis and promotes beneficial bacteria colonization. Furthermore, the use of microbial (probiotics) and non-microbial (prebiotics) supplements favor microbiota homeostasis (Witkowski et al., 2020).

1.3.2.2 Faecal transplantation

Clinical evidences have underlined different microbiota composition between healthy subjects and patients with overt or at high risk of developing CVD. Faecal transplantation from a healthy to a diseased subject has shown beneficial effects. The procedure consists in the administration of faecal solution from a donor to a recipient gut. Animal studies in atherosclerotic prone strains suggest a beneficial effect of the practice (Novakovic et al., 2020). Human studies are limited and they are primarily centered on obese subjects, who showed improved metabolic syndrome markers after faecal transplantation (Zhang et al., 2019). Even if faecal transplantation is a promising tool to prevent gut dysbiosis and its related pathological conditions, further investigations are needed to evaluate if long term side effects could develop in treated patients and if this therapeutic intervention could predispose to the development of further unexpected infections.

1.3.2.3 Specific enzyme target therapies

New therapies are addressed to the development of specific drugs that inhibit microbial enzymes, without toxic effects on microbiota and on the host. One of these new inhibitors, 1,3-dimethylbutanol, stops TMA synthesis from choline in the gut. Regarding TMAO as a possible risk factor in CVD development, *in vivo* studies demonstrated that orally

administered 1,3-dimethylbutanol reduces plasmatic TMAO levels, foam cell formation and atherosclerotic plaque formation (Novakovic et al., 2020; Witkowski et al., 2020). Furthermore, antibiotics have been suggested as possible pharmacological interventions, but their prolonged use can generate forms of microbial resistance likewise dangerous for human health (Tang et al., 2017).

2. AIM OF THE STUDY

Trimethylamine N-oxide (TMAO) is a diet derived compound that can be directly introduced through fish products or can be endogenously synthesized by the gut microbiota from its dietary precursors, in particular choline, L-carnitine and ergothioneine.

Recent evidences suggest a correlation between high plasma levels of TMAO and the development of cardiovascular diseases (CVD), highlighting a possible causal role of TMAO in atherosclerosis progression. On the other hand, fish products, that are high in TMAO content, are strongly recommended to patients at high risk of CVD, thus presenting a controversial role of the molecule in the development of cardiac and vascular pathologies. Furthermore, considering the physiological properties of TMAO in deep-sea fishes and its biosynthetic pathway that involves the detoxifying enzyme flavin containing monooxygenase 3 (FMO3), it has been proposed that its precursor, TMA, rather than TMAO could be the principal actor of cardiovascular damage.

TMAO's role in cardiac and vascular pathologies are still under investigation, but available data present controversial results about its pathophysiological functions, making it difficult to classify the molecule as a direct cause of pathology rather than a marker of disease.

Aim of the present project was to study in two *in vitro* models cardiac and vascular effects of TMAO.

The first part of the work was centered on the effect of the molecule in isolated adult rat cardiomyocytes in primary culture. Cells viability, reactive oxygen species increase and mitochondrial membrane potential ($\Delta\Psi m$) were monitored after TMAO treatment both in basal conditions and in presence of stressors.

For this cellular model different stressors have been used: doxorubicin and H_2O_2 in order to perform a direct pro-oxidant stimulation, while an ischemia/reperfusion protocol have been applied in order to simulate a pathological condition *in vitro*.

The second part of the project has been centered on bovine aortic endothelial cells, already used to study endothelial dysfunction development *in vitro*.

Also for this set of experiments cells were treated with TMAO both in basal conditions and in presence of a stressor, menadione, used as inducer of oxidative stress-mediated endothelial dysfunction. First experiments were centered on the evaluation of cells viability, reactive oxygen species production and $\Delta\Psi m$. Further analyses were performed in order to evaluate a possible role of TMAO in modulating purinergic response to ATP. Intracellular calcium, nitric oxide release and eNOS phosphorylation at Ser1179 ($eNOS^{Ser1179}$) were monitored after acute or prolonged treatment with TMAO and subsequent ATP stimulation.

3. MATERIALS AND METHODS

3.1 Study on adult rat cardiomyocytes

3.1.1 Solutions and reagents

Trimethylamine N-oxide (Sigma-Aldrich, Saint Louis, MO, USA) solubilized in culture medium or Tyrode standard solution according to the protocol used, was freshly prepared for each experiment.

Tyrode standard solution contained (in mM): 154 NaCl, 4 KCl, 1 $MgCl_2$, 5.5 D-glucose, 5 HEPES, 2 $CaCl_2$, pH adjusted to 7.34 with NaOH. Ca^{2+}-free Tyrode solution contained (in mM): 154 NaCl, 4 KCl, 1 $MgCl_2$, 5.5 D-glucose, 5 HEPES, 10 2,3-Butanedione monoxime, 5 taurine, pH adjusted to 7.34 with NaOH. All drug-containing solutions were prepared fresh before the experiments and the Tyrode solutions were oxygenated (O_2 100%) before each experiment.

Ischemic buffer (IB) used to simulate *in vitro* ischemia/reperfusin injury contained (in mM): 123 NaCl, 20 HEPES, 0.9 NaH_2PO_4, 2.5 $CaCl_2$-$2H_2O$, 0.5 $MgSO_4$, 20 Na-lactate, 8 KCl, pH adjusted to 6.2 with NaOH. Before each experiment IB was nitrogenated (N_2 100%) for 30 minutes.

Unless otherwise specified, all reagents for cell isolation and experiments were purchased from Sigma-Aldrich (St. Louis, MO, USA).

3.1.2 Animal care and sacrifice

Experiments were performed with female adult (3-5 months, 200-300 g body weight) Sprague-Dawley rats purchased from Charles River Laboratories (Wilmington, MA, USA). Animals were allowed to access water and standard rodent diet *ad libidum* and were maintained at constant room temperature with 12h dark/light cycles. Animal care was given according to the Guide for the Care and Use of Laboratory Animals published by the US National Institutes of Health (8^{th} edition) (National Research Council (US) Committee for the Update of the Guide for the Care and Use of Laboratory Animals, 2011) and in accordance with the Italian law (DL-116, Jan. 27, 1992). All experiments on animals were supervised and approved by the Italian Ministry of Health (Rome, Italy), and by the Ethical Committee of the University of Torino (approval code 116/2017-PR, 3/2/2017). Preceding hearts isolation, rats received 4 units of heparin (Epsodilave 250 U.I./5ml) to avoid blood clots formation in coronary vessels. After 20 minutes from heparin administration animals were anesthetized by intraperitoneal injection of tiletamine (Zoletil 100, Virbac, Carros, France) and sacrificed by stunning and cervical dislocation. Isolated heart was put in sterile cold Tyrode Ca^{2+}-free solution in order to avoid irreversible contraction of the organ. Heart was then cannulated in a Langendorff perfusion system mounted in a laminar flow hood.

3.1.3 Ventricular cell isolation

Isolated ventricular cardiomyocytes were obtained after heart cannulation through the aorta. Heart was perfused at constant flow rate of 10 ml/min with Tyrode Ca^{2+}-free solution maintained at 37°C with a peristaltic pump. After all blood was washed away, 10 ml of Tyrode Ca^{2+}-free solution containing collagenase (0.3 mg/ml) and protease (0.02 mg/ml) was added in the perfusion system. Further enzymatic dissociation was performed with other 20 ml of the same enzymatic solution in which 50 µM $CaCl_2$ was added. After the enzymatic digestion also a mechanical dissociation was performed and only ventricles were cut in small pieces to favour single cell separation. Calcium ion concentration was slowly increased to 0.8 mM to allow further treatments.

3.1.4 Cardiomyocytes viability in basal treatment

Once single cells have been isolated, cardiomyocytes viability after TMAO treatment was assessed. Cardiomyocytes were plated on glass cover slides treated with laminin to allow cell adhesion. Cells were treated for 1h or 24h with different concentrations of TMAO (1 µM, 10 µM, 100 µM, 1 mM, 10 mM). At the end of the treatment, cells were incubated in dark conditions with propidium iodide (PI, 10 µg/ml, Invitrogen, Carlsband, CA, USA) for 5 minutes. After PI incubation cells were fixed with paraformaldehyde (PAF) 4% dissolved in 0.1 M phosphate buffer, pH 7.3, for 40 minutes. After two washes with phosphate buffered saline (PBS) cover slides were mounted on standard slides with DABCO. Prepared slides were maintained at room temperature and dark overnight and then conserved at 4°C until acquisitions. Nuclei of suffering cells were labeled with PI, which is not permeant to live cells, and intercalates between damaged DNA bases with little or no sequence preference. Labeled nuclei were detected with confocal microscopy at excitation wavelength of 568nm using an Olympus Fluoview 200 laser scanning confocal system (Olympus America Inc., Melville, NY, USA) mounted on an inverted IX70 Olympus microscope, and all acquisitions were performed with a 20X objective. Bright field and fluorescence merged images were created with ImageJ software (Rasband, W. S., ImageJ, U. S. National Institutes of Health, Bethesda, Maryland, USA; https://imagej.nih.gov/ij/, 1997-2017) and cardiomyocytes viability was expressed as the mean percentage of not labeled cells for each experimental condition of three independent experiments.

3.1.5 Cardiomyocytes viability in ischemia/reperfusion injury

Isolated cardiomyocytes viability after TMAO treatment in an *in vitro* ischemia/reperfusion model was evaluated. Ischemia/reperfusion protocol was performed according to Louch and

collaborators (Louch et al., 2002) with minor modifications. Cardiomyocytes were plated on glass bottom dishes 35 mm diameter (Ibidi, Martinsried, Germany) treated with laminin to allow cell adhesion. During all acquisitions solutions used contained propidium iodide (PI, 10 µg/ml, Invitrogen, Carlsband, CA, USA). According to the scheme presented in Figure 30, cells acquisitions were performed in 100% oxygenated Tyrode standard solution before starting all treatments (t0), 45 minutes after incubation with the ischemic buffer (IB) or corresponding experimental condition (Tyrode standard for CTRL, Tyrode standard containing TMAO 100 µM or IB containing TMAO 100 µM) (t1), and 15 minutes after reperfusion with 100% oxygenated Tyrode standard solution (t2). Labeled nuclei were detected with live cells acquisition using confocal microscopy at excitation wavelength of 568nm using an Olympus Fluoview 200 laser scanning confocal system (Olympus America Inc., Melville, NY, USA) mounted on an inverted IX70 Olympus microscope, and all acquisitions were performed with a 20X objective. Bright field and fluorescence merged images were created with ImageJ software. Cardiomyocytes viability was expressed as mean percentage of not labeled cells at t2 in a total of three independent experiments.

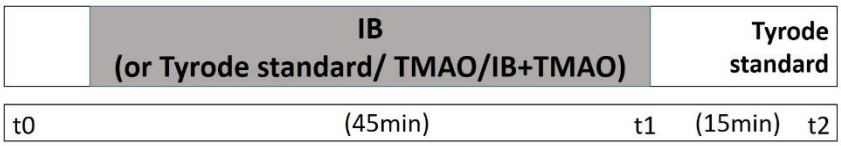

Figure 30. *Scheme of ischemia/reperfusion protocol. Acquisitions were performed at different times: immediately before (t0), after 45 min incubation with IB or corresponding treatment solution (t1), and after 15 min of reperfusion with Tyrode standard solution (t2).*

3.1.6 Sarcomere length

To evaluate if TMAO has any effect on sarcomere length, immunostaining for sarcomeric α-actinin was performed. Isolated cardiomyocytes were plated on glass cover slides treated with laminin to allow cell adhesion. Cells were treated with TMAO 100 µM, H_2O_2 50 µM, TMAO 100 µM + H_2O_2 50 µM, DOXO 1 µM and TMAO 100 µM + DOXO 1 µM for 24h. At the end of the treatments cells were fixed with PAF 4% dissolved in 0.1 M phosphate buffer, pH 7.3, for 40 minutes. After three washes with PBS cells were incubated with 0.3% Triton, 1% bovine serum albumin (BSA) in PBS for 20 minutes and then stained with mouse monoclonal anti-α-actinin primary antibody (1:800 dilution) for 24h at 4°C. Cells were washed twice with PBS and incubated with the secondary antibody, anti-mouse Alexa Fluor 568 (1:2000 dilution, Thermo Fisher Scientific, Waltham, MA, USA) for 1h at room temperature. Cover slides were then washed twice with PBS and mounted on standard slides

with DABCO, leaved overnight at room temperature and dark conditions and then at 4°C before the acquisitions. Confocal fluorimetric measurements at 568nm were performed using a Leica SP2 laser scanning confocal system (Wetzlar, Germany), equipped with a 40X water-immersion objective. Image processing and analysis were performed with ImageJ software. Sarcomere length was evaluated measuring the mean distance between Z lanes labeled with α-actinin in n = 10 sarcomeres/cell, obtained values from three independent experiments were used to calculate mean sarcomere length.

3.1.7 Intracellular reactive oxygen species

Production of reactive oxygen species (ROS) was monitored through the use of 2'-7'-dichlorofluorescein diacetate probe (DCF-DA). Isolated cardiomyocytes were plated on glass bottom dishes 35mm diameter (Ibidi) treated with laminin to allow cell adhesion. After incubation cells were treated with TMAO 100 µM, H_2O_2 50 µM and TMAO 100 µM + H_2O_2 50 µM for 1h, to simulate acute exposure to the compound, and treated with TMAO 100 µM, DOXO 1 µM and TMAO 100 µM + DOXO 1 µM for 24h, to simulate prolonged exposure to the compound. Thirty minutes before the end of each treatment DCF-DA (10 µM) was added in each dish and incubated in dark conditions, then cells were washed twice with Tyrode standard solution before the acquisitions. Cells fluorescence was detected at 488nm with an inverted IX70 Olympus microscope, and all acquisitions were performed with a 60X Uplan FI (NA 1.25) oil-immersion objective. Fluorescence variations, indicative of ROS production, were calculated through the definition of the Regions Of Interest (ROIs) using the software ImageJ. All measurements were expressed as mean fluorescence compared to CTRL condition of three independent experiments.

3.1.8 Mitochondrial membrane potential

Mitochondrial membrane potential (ΔΨm) was monitored through confocal microscopy and the 5,5′,6,6′-tetrachloro-1,1′,3,3′-tetraethyl-imidacarbocyanine iodide (JC-1) probe. JC-1 is a ratiometric indicator of ΔΨm, it is able to shift its fluorescence from red to green when a depolarization of the mitochondrial membrane occurs. Isolated cardiomyocytes were plated on glass bottom dishes 35mm diameter (Ibidi) treated with laminin to allow cell adhesion. After incubation cells were treated with TMAO 100 µM, H_2O_2 50 µM and TMAO100 µM + H_2O_2 50 µM for 1h to simulate acute exposure to the compound, and treated with TMAO 100 µM, DOXO 1 µM and TMAO 100 µM + DOXO 1 µM for 24h, to simulate prolonged exposure to the compound. Thirty minutes before the end of each treatment JC-1 probe (10 µM) was added in each dish and incubated in dark conditions, then cells were washed three times with Tyrode standard solution before the acquisitions. Cell images were obtained at

488nm and 568nm with an Olympus Fluoview 200 laser scanning confocal system (Olympus America Inc., Melville, NY, USA) mounted on an inverted IX70 Olympus microscope, and all acquisitions were performed with a 60X Uplan FI (NA 1.25) oil-immersion objective. ΔΨm was calculated through the red/green fluorescence ratio and the definition of the ROIs using the ImageJ software and expressed as mean value of the resulting ratios for each condition compared to control of three independent experiments.

3.1.9 Statistical analysis

Data are presented as mean±SEM. All data were analyzed with GraphPad Prims 8 software using ANOVA followed by Bonferroni's multiple comparison for post hoc tests. Differences with $p<0.05$ were considered statistically significant.

3.2 Study on bovine aortic endothelial cells

3.2.1 Solutions and reagents

Trimethylamine N-oxide (Sigma-Aldrich, Saint Louis, MO, USA) solubilized in culture medium or Tyrode standard solution according to the protocol used, was freshly prepared for each experiment. Menadione (MEN) (Sigma-Aldrich, Saint Louis, MO, USA) was solubilized in Dimethyl sulfoxide (DMSO) at the initial concentration of 100 mM and then diluted in culture medium at the final concentration of 100 µM. ATP was prepared in Tyrode standard solution at the concentration of 10 mM and diluted in culture medium at the final concentration of 100 µM. Tyrode standard solution used in different experiments contained (in mM): 154 NaCl, 4 KCl, 1 $MgCl_2$, 5.5 D-glucose, 5 HEPES, 2 $CaCl_2$, pH adjusted to 7.34 with NaOH. Unless otherwise specified, all reagents for cell culture and experiments were purchased from Sigma-Aldrich.

3.2.2 Cell culture

Bovine aortic endothelial cells-1 (BAE-1, ECACC, Salisbury, UK) used for this part of the project were maintained in Dulbecco's Modified Eagle Medium (DMEM) 1 g/L glucose supplemented with 10% Fetal Bovine Serum (FBS), 2 mM L-Glutamine and 50 µg/ml Gentamycin. Cells were incubated at 37°C, in humified atmosphere containing 5% CO_2 during all experiments. BAE-1 were used from passage 2 to 7.

3.2.3 BAE-1 viability in basal treatment

To assess cells viability after TMAO treatment, BAE-1 were seeded (3.3×10^4 cells/200 µl/ well) into a 96-well plate in culture medium and incubated at 37°C for 24h. Following incubation and cells adhesion, BAE-1 were treated for 24h, 48h and 72h with different concentrations of TMAO (1 µM, 10 µM, 100 µM, 1 mM, 10 mM). Assessment of cell viability was performed with CellTiter 96® AQueous One Solution Cell Proliferation Assay, using the tetrazolium compound 3-(4,5-dimethylthiazol-2-yl)-5-(3-carboxymethoxyphenyl)-2-(4-sulfophenyl)-2H-tetrazolium, inner salt (MTS, Promega, Madison, WI, USA). The Assay is based on the bioreduction by metabolically active cells of MTS into a colored formazan product soluble in culture medium. Three hours before the end of the treatment MTS (20 µl/100 µl) was added in each well. Formazan product formation was measured with FilterMax™ F5 Multi-Mode microplate reader (Molecular Devices, Sunnyvale, CA, USA) at 450nm, and the detected absorbance was considered proportional to the number of viable cells. Data from three independent experiments were expressed as mean percentage referred to the control condition.

3.2.4 Intracellular reactive oxygen species

Reactive oxygen species variations were monitored through the microplate reader and the CellROX® green probe (Thermo Fisher Scientific, Waltham, MA, USA). BAE-1 were seeded ($3.3x10^4$ cells/200 µl/well) on Greiner black clear bottom 96-well plate in culture medium and incubated at 37°C for 24h. Following incubation cells were treated according to experimental conditions: TMAO 100 µM for 1h, MEN 100 µM for 1h, TMAO 100 µM + MEN 100 µM for 1h, for acute stimulation tests, and TMAO 100 µM for 24h, MEN 100 µM for 1h, TMAO 100 µM for 24h + MEN 100 µM for 1h, for prolonged stimulation tests. CellROX® green (5 µM) was added in each well 30 minutes before the end of the treatment, cells were then washed two times with PBS containing Ca^{2+} and Mg^{2+} to avoid cell loss. Fluorescence intensity variations were measured at 485nm through FilterMax™ F5 Multi-Mode microplate reader (Molecular Devices, Sunnyvale, CA, USA). ROS production was expressed as mean fluorescence compared to control condition of three independent experiments.

3.2.5 Mitochondrial membrane potential

Mitochondrial membrane potential was monitored through confocal microscopy and the JC-1 probe. BAE-1 were seeded ($3.3x10^4$ cells/ml) on uncoated glass bottom dishes of 35 mm diameter (Ibidi) in culture media and incubated at 37°C for 24h. Following incubation cells were treated according to experimental conditions: TMAO 100 µM for 1h, MEN 100 µM for 1h, TMAO 100 µM + MEN 100 µM for 1h, for acute stimulation tests, and TMAO 100 µM for 24h, MEN 100 µM for 1h, TMAO 100 µM for 24h + MEN 100 µM for 1h, for prolonged stimulation tests. JC-1 (10 µM) was added in each dish 30 minutes before the end of the treatment, cells were then washed three times with PBS containing Ca^{2+} and Mg^{2+} to avoid cell loss. Fluorescence intensity variations were measured at 568nm and 488nm through an Olympus Fluoview 200 laser scanning confocal system (Olympus America Inc., Melville, NY, USA) mounted on an inverted IX70 Olympus microscope, and all acquisitions were performed with a 60X Uplan FI (NA 1.25) oil-immersion objective. $\Delta\Psi m$ was calculated through the red/green fluorescence ratio and the definition of the ROIs using the ImageJ software and expressed as mean value of the resulting ratios for each condition compared to the control of three independent experiments.

3.2.6 Intracellular calcium variations in purinergic response to ATP

Intracellular calcium variations were monitored through time course acquisitions in confocal microscopy and Fluo-3 AM probe (Thermo Fisher Scientific). BAE-1 were seeded ($3.3x10^4$ cells/ml) on uncoated glass bottom dishes of 35 mm diameter (Ibidi) in culture media and

incubated at 37°C for 24h. Following incubation, cells were treated for 1h or 24h with TMAO 100 μM or were leaved in culture medium. Fluo-3 AM (2 μM) was added in each dish 30 minutes before the end of the treatments, cells were then washed two times with Tyrode standard solution. Fluorescence intensity variations in time were measured at 488nm through an Olympus Fluoview 200 laser scanning confocal system (Olympus America Inc., Melville, NY, USA) mounted on an inverted IX70 Olympus microscope, and all acquisitions were performed with a 60X Uplan FI (NA 1.25) oil-immersion objective. During the experiments BAE-1 were maintained in Tyrode standard solution, ATP 100 μM and ATP 100 μM + TMAO 100 μM used for cell stimulation were added through a microperfusion system (pipette diameter 200 μm). Intracellular calcium variations in time were analyzed through the definition of the ROIs using the ImageJ software. Changes in intracellular calcium concentration were calculated as F/F_0 to normalize the traces; moreover, an additional analysis was applied in order to highlight changes in ATP-induced calcium signal profile between control and TMAO-treated cells. First, traces of the same dish were mediated; from each of four independent experiments, mean traces from every condition (ATP, TMAO 1h + ATP, TMAO 24h + ATP) were aligned respect to the peak value (F_{max}). Then, the mean difference between F_{max} and the fluorescence at t/2 ($F_{t/2}$), (F_{max} - $F_{t/2}$), of the aligned curves were compared in order to evaluate if any perturbation in calcium curves occurred during each treatment.

3.2.7 Nitric oxide release in purinergic response to ATP

Nitric oxide (NO) release was monitored through time course acquisitions in confocal microscopy and DAR-4M AM probe (Thermo Fisher Scientific). BAE-1 were seeded ($3.3x10^4$ cells/ml) on uncoated glass bottom dishes of 35mm diameter (Ibidi) in culture media and incubated at 37°C for 24h. Following incubation cells were treated for 1h or 24h with TMAO 100 μM or were leaved in culture medium. DAR-4M AM (5 μM) was added in each dish 30 minutes before the end of the treatments, cells were then washed two times with Tyrode standard solution. Fluorescence intensity variations in time were measured at 568nm through an Olympus Fluoview 200 laser scanning confocal system (Olympus America Inc., Melville, NY, USA) mounted on an inverted IX70 Olympus microscope, and all acquisitions were performed with a 60X Uplan FI (NA 1.25) oil-immersion objective. During the experiments BAE-1 were maintained in Tyrode standard solution. ATP 100 μM and ATP 100 μM + TMAO 100 μM used for cell stimulation were added through a microperfusion system (pipette diameter 200 μm). NO release variations in time were analyzed through the definition of the ROIs using the ImageJ software. NO release after different treatments was

calculated as percentage change in mean fluorescence detected $((F_{max}-F_0)/F_0)x100$ for each trace. Normalized percentage change values of three independent experiments were then mediated and expressed as folds toward basal ATP treatment to verify if any variation in NO release could be detected in different treatments.

3.2.8 Western Blot

To evaluate if TMAO treatment influences eNOS phosphorylation at Ser1179 ($eNOS^{Ser1179}$) during purinergic stimulation with ATP, Western Blot analysis were performed. BAE-1 were seeded ($4x10^4$ cells/ml) on plastic petri dishes 22.1cm^2 of growth area (TPP®) in culture media and incubated at 37°C for 24h. Following incubation, cells were treated for 1h or 24h with TMAO 100 μM or were leaved in culture medium. After the treatment with ATP 100 μM for 1 minute cells were lysed with RIPA lysis buffer containing phosphatase inhibitor (PhosSTOP diluted in RIPA Buffer according to the manifacturer instructions), forced through a 1 ml syringe needle for several times, centrifuged at 10000rpm for 5 minutes at 4°C and then stored at -80°C. Protein lysates (20 μg per lane) were run on 8% gradient SDS-PAGE gel, transferred to a polyvinylidene fluoride membrane (PVDF) and blocked for 1h in TBST (10 mM Tris–HCl, pH 7.5, 0.1 M NaCl, 0.1% Tween 20) plus 5% non-fat dry milk. PVDF were incubated overnight at 4°C with primary antibodies (mouse monoclonal anti-eNOS, 1:500 dilution, BD, Biosciences; rabbit polyclonal anti-$eNOS^{Ser1179}$, 1:250 dilution, Thermo Fisher Scientific; mouse monoclonal anti-β-actin, 1:2000 dilution, Sigma-Aldrich). Membranes were then washed three times with TBST and incubated for 1h at room temperature with horseradish peroxidase-conjugated secondary antibodies (anti-mouse, 1:20000 dilution, Amersham, for total eNOS and total β-actin; anti-rabbit, 1:10000 dilution, Amersham for $eNOS^{Ser1179}$) and washed again three times with TBST. Protein bands were localized by chemiluminescence with Western Lightning Plus-ECL (Perkin Elmer, Waltham, MA, USA). Protein levels were determined using the ImageJ software and expressed as mean percentage toward ATP condition of four independent experiments.

3.2.9 Statistical analysis

Data are presented as mean±SEM. All data were analyzed with GraphPad Prism 8 using ANOVA followed by Bonferroni's multiple comparison for post hoc tests, while only NO release variations were analyzed with Kruskal-Wallis test. Differences with $p<0.05$ were considered statistically significant.

4. RESULTS

4.1 Study on adult rat cardiomyocytes

4.1.1 Cardiomyocytes viability in basal treatment

To assess if TMAO is toxic for cardiac cells in basal conditions, isolated adult rat cardiomyocytes were treated with different concentrations of the molecule (1 μM, 10 μM, 100 μM, 1 mM, 10 mM) and stained with propidium iodide (PI). As shown in Figure 31, after 1h (Figure 31A) and 24h (Figure 31B) of treatment TMAO was not toxic for cardiac cells, that maintained their rod shape throughout all treatments.

From these first results we decided to use TMAO 100 μM in following experiments, as this concentration has been accepted as the threshold for the pathological condition (Gatarek & Kaluzna-Czaplinska, 2021).

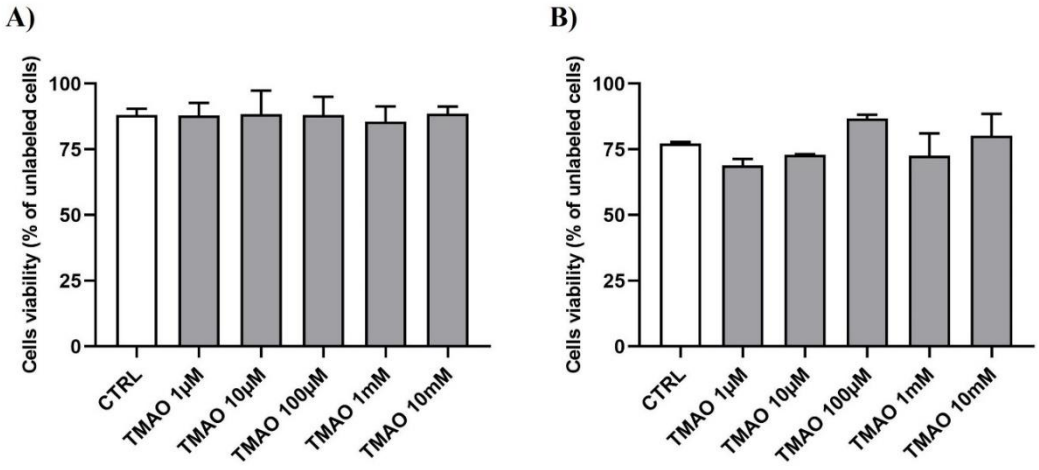

Figure 31. *Cardiomyocytes viability is not affected by TMAO treatment. TMAO showed no cytotoxic effect after* ***A)*** *1h (CTRL: 88.15±2.29; TMAO 1 μM: 87.98±4.75; TMAO 10 μM: 88.45±8.92; TMAO 100 μM: 88.14±6.87; TMAO 1 mM: 85.66±5.69; TMAO 10 mM:88.52±2.80. Cells number for each condition in a total of three independent experiments: CTRL: 198; TMAO 1 μM: 41; TMAO 10 μM: 96; TMAO 100 μM: 49; TMAO 1 mM: 199; TMAO 10 mM:52) and* ***B)*** *24h (CTRL: 77.22±0.54; TMAO 1 μM: 68.85±2.55; TMAO 10 μM: 72.89±0.28; TMAO 100 μM: 86.69±1.56; TMAO 1 mM: 72.56±8.56; TMAO 10 mM: 80.24±8.26. Cells number for each condition in a total of three independent experiments: CTRL: 100; TMAO 1 μM: 185; TMAO 10 μM: 202; TMAO 100 μM: 94; TMAO 1 mM: 195; TMAO 10 mM:119) of treatment.*

4.1.2 Cardiomyocytes viability in ischemia/reperfusion injury

In order to assess if TMAO has any effect on cell viability in a stressed condition, *in vitro* ischemia/reperfusion protocol has been used to treat cardiomyocytes, both in presence or absence of TMAO. As shown in Figure 32A, at t0, cells incubated with Tyrode standard solution (first column of acquisitions) were only partially labeled by propidium iodide and

maintained their characteristic rod shape. At t1, cardiomyocytes treated with Tyrode, or TMAO 100 µM or IB or IB + TMAO 100 µM for 45 minutes, showed no change from the t0 condition, indeed the cells majority was not labeled with PI and maintained the rod shape (second column of acquisitions). Then, the reperfusion with Tyrode standard solution showed a cytotoxic effect after 15 minutes (t2) in cells treated with IB containing or not TMAO (third column of acquisitions). Treatment with basal TMAO 100 µM showed no effects at any endpoint, underlining comparable results as those obtained for the control. Bar graph of panel B shows cells viability at t2, and as already seen for confocal images, TMAO had no effects in basal conditions and it was not able to balance or exacerbate the effect of the reperfusion injury (Figure 32).

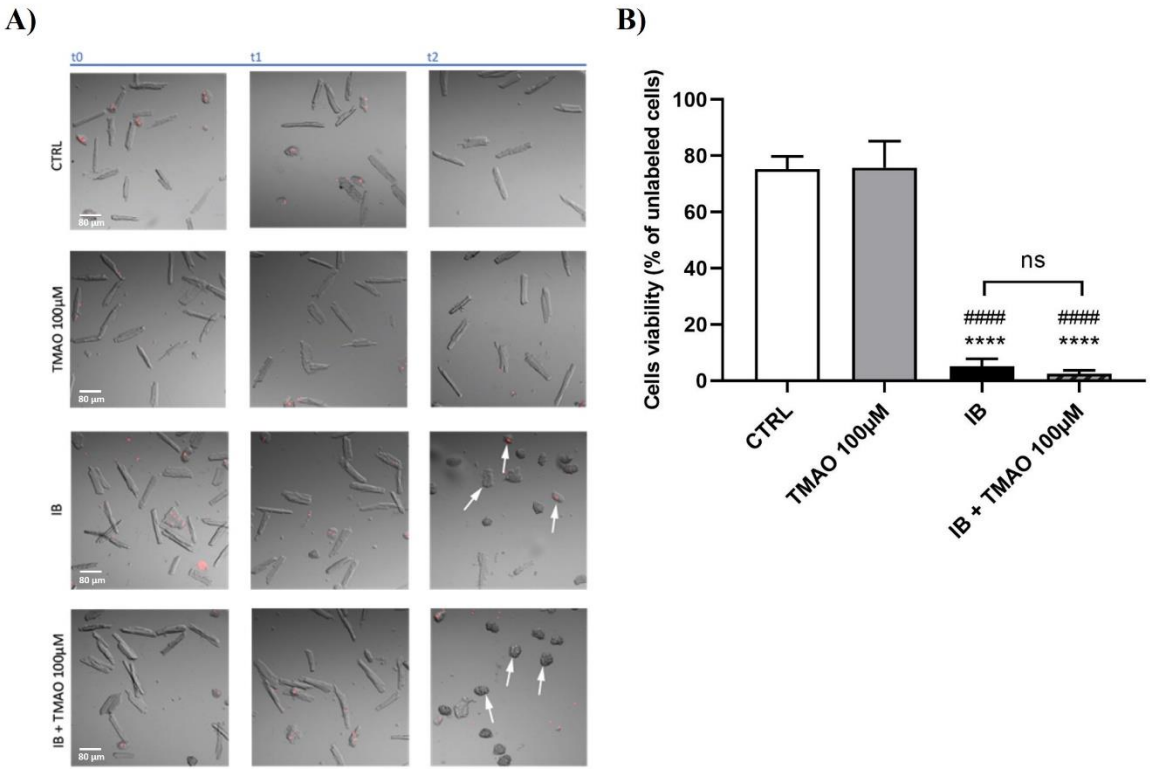

Figure 32. *TMAO does not interfere with ischemia/reperfusion injury.* ***A)*** *Confocal microscopy merged images of adult cardiomyocytes in bright field and 568nm fluorescence (magnification 20X). XY acquisitions were performed before (t0), 45 minutes after (t1) incubation with ischemic buffer (IB) (or Tyrode standard or TMAO 100 μM or IB + TMAO 100 μM) and 15 minutes after reperfusion (t2). White arrows show PI labeled suffering cells after the reperfusion step.* ***B)*** *Bar graph showing cell viability after reperfusion. As expected, treatment with the IB induced cell death after the restoration of physiological medium, and this effect was not modified in presence of TMAO 100 μM. Moreover, treatment with TMAO alone did not induce any effect and cells viability was comparable with that of the control. (CTRL: 75.22±4.58; TMAO 100 μM: 75.81±9.36; IB: 5.12±2.63; IB + TMAO 100 μM: 2.14±1.23). ****p< 0.0001 (vs CTRL); $^{\#\#\#\#}$p<0.0001 (vs TMAO 100 μM).*

4.1.3 Sarcomere length

To evaluate the potential role of TMAO in affecting contractile function of cardiomyocytes, both in basal and stressed conditions, sarcomere length was evaluated through immunofluorescence technique after 24h of treatment. In particular, cells were stained with the sarcomeric α-actinin antibody and bands distance was calculated as index of cell shrinkage.

As shown in Figure 33, basal treatment with TMAO 100 μM did not induce cell shortening. Results obtained with DOXO 1 μM evidenced no effect of the stressor on sarcomere length and this effect was not modified by TMAO simultaneous treatment. On the contrary, H_2O_2 50 μM induced cell shrinkage, and this effect was maintained during TMAO simultaneous treatment. These results showed that TMAO was not able to influence sarcomere length both in basal conditions and in presence of different stressors.

A)

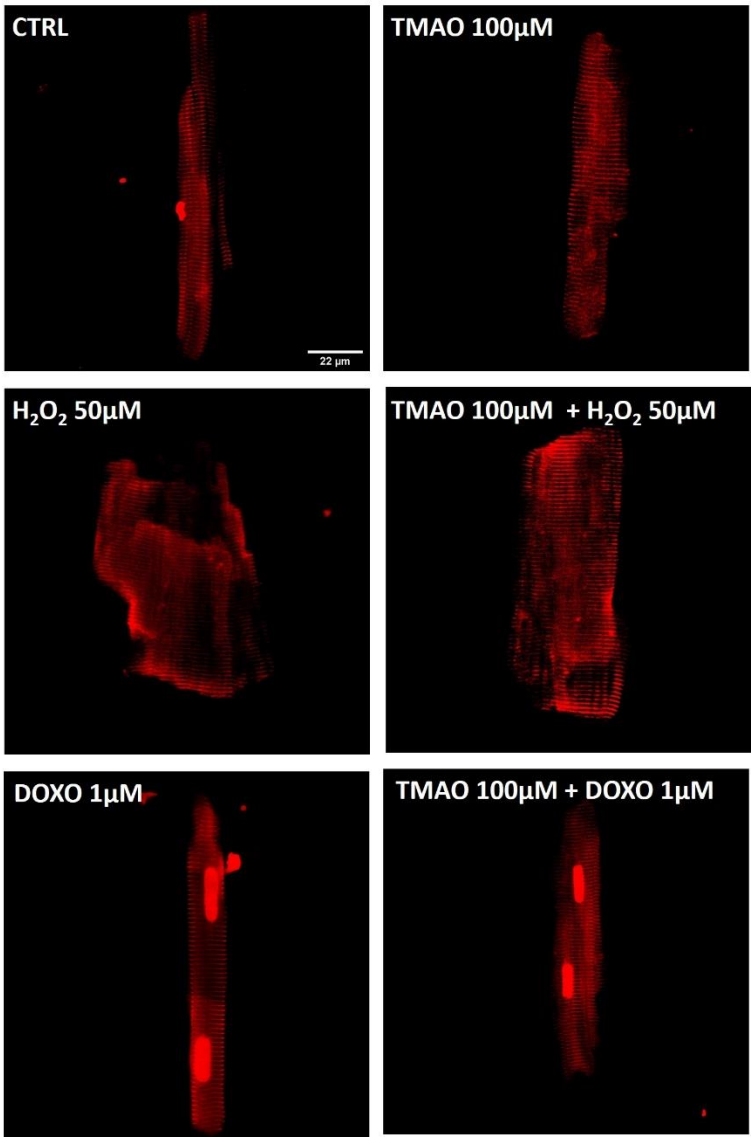
CTRL
22 µm
TMAO 100µM
H_2O_2 50µM
TMAO 100µM + H_2O_2 50µM
DOXO 1µM
TMAO 100µM + DOXO 1µM

B)

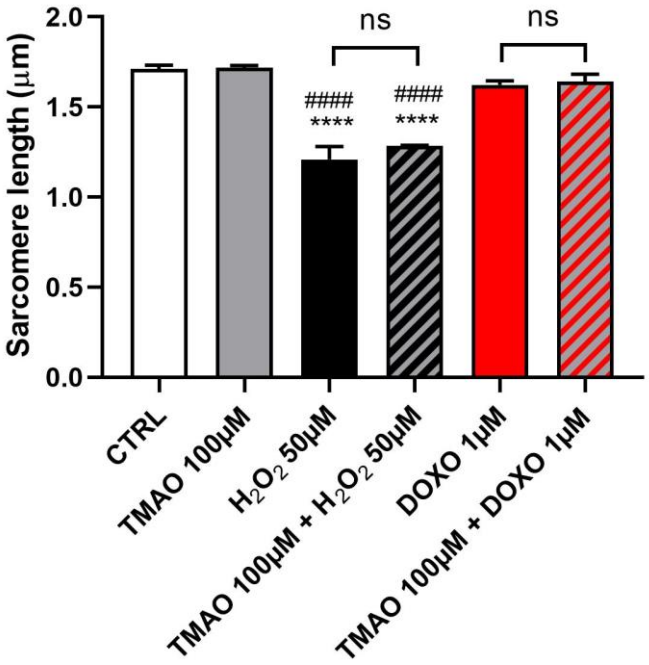

Figure 33. *Sarcomere length is not affected by TMAO treatment.* ***A)*** *Confocal microscopy acquisitions of single cardiomyocytes stained for sarcomeric α-actinin (568nm; magnification 40X).* ***B)*** *Bar graphs showing sarcomere length after different treatments. Basal treatment with TMAO 100 μM did not induce sarcomere length variations. Only H_2O_2 50 μM induced a reduction in sarcome length that was not balanced nor exacerbated by the simultaneous treatment with TMAO. As expected, DOXO 1 μM treatment did not induce cell shrinkage and this effect was not changed by the simultaneous treatment with TMAO. (CTRL: 1.71±0.02; TMAO 100 μM: 1.71±0.02; H_2O_2 50 μM: 1.21±0.07; TMAO 100 μM + H_2O_2 50 μM: 1.28±0.01; DOXO 1 μM: 1.62±5.69; TMAO 100 μM + DOXO 1 μM: 1.65±0.04. Cells number for each condition in a total of three independent experiments: CTRL: 28; TMAO 100 μM: 40; H_2O_2 50 μM: 34; TMAO 100 μM + H_2O_2 50 μM: 49; DOXO 1 μM: 32; TMAO 100 μM + DOXO 1 μM:30). ****p< 0.0001 (vs CTRL); $^{\#\#\#\#}$p<0.0001 (vs TMAO 100 μM).*

4.1.4 Intracellular reactive oxygen species

Rise of reactive oxygen species after TMAO treatment was monitored through the DCF-DA probe. After 1h of treatment, TMAO 100 μM did not induce ROS production, while H_2O_2 50 μM treatment increased cells fluorescence, directly associated with the rise of ROS. Simultaneous treatment with H_2O_2 50 μM and TMAO 100 μM did not change the effect of the stressor (Figure 34). Cells fluorescence variations due to different treatments is shown in Figure 34A in which increased and comparable fluorescence in H_2O_2 50μM and TMAO 100μM + H_2O_2 50μM treatments is visible.

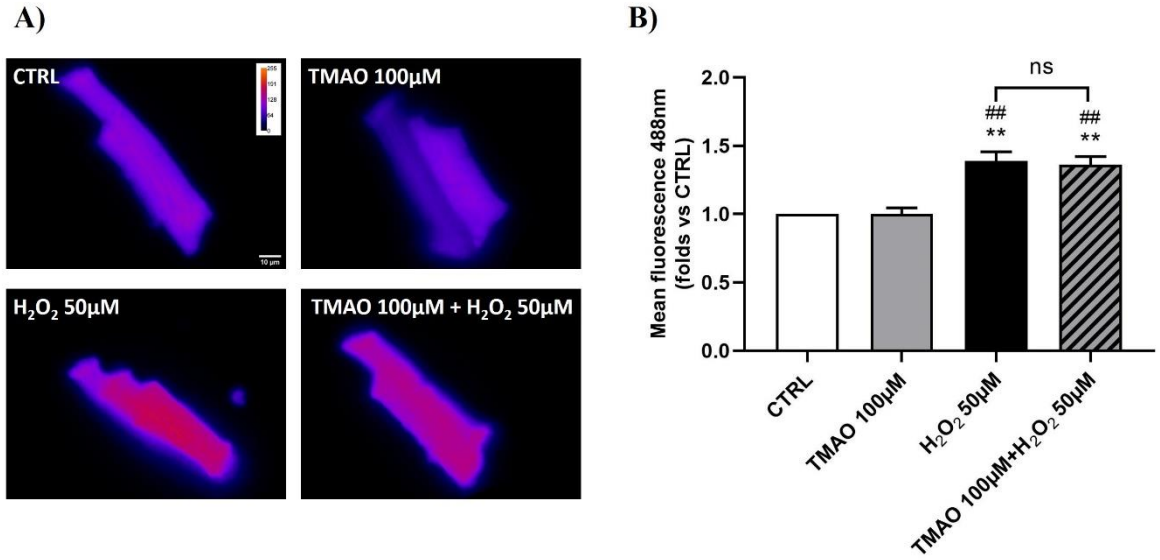

Figure 34. *TMAO treatment for 1h does not induce the rise of reactive oxygen species (ROS) in cardiomyocytes.* ***A)*** *Representative single cell fluorescence images of isolated cardiomyocytes treated for 1h with TMAO 100 μM, H_2O_2 50 μM or simultaneously treated with TMAO 100 μM and the stressor (488 nm; magnification 60X).* ***B)*** *TMAO treatment for 1h did not induce ROS increase, the effect of H_2O_2 50 μM was not changed by simultaneous treatment with TMAO. (CTRL: 1.00±0.00; TMAO 100 μM: 1.00±0.04; H_2O_2 50 μM: 1.39±0.07; TMAO 100 μM + H_2O_2 50 μM: 1.36±0.06. Cells number for each condition in a total of three independent experiments: CTRL: 16; TMAO 100 μM: 16; H_2O_2 50 μM: 16; TMAO 100 μM + H_2O_2 50 μM: 16). **p< 0.01 (vs CTRL); $^{\#\#}$p<0.01 (vs TMAO 100 μM).*

Cardiomyocytes oxidative stress was evaluated also after 24h of TMAO treatment. As shown in Figure 35, basal treatment with TMAO 100 μM did not induce any variation in cells mean fluorescence, suggesting no direct role of the molecule in inducing the rise of ROS. Furthermore, the effects of TMAO were monitored in presence of DOXO 1 μM. DOXO, as expected, induced ROS increase and this effect was not changed in a simultaneous treatment

with TMAO. These results showed that also for prolonged exposure time TMAO did not change the effect of the used stressor.

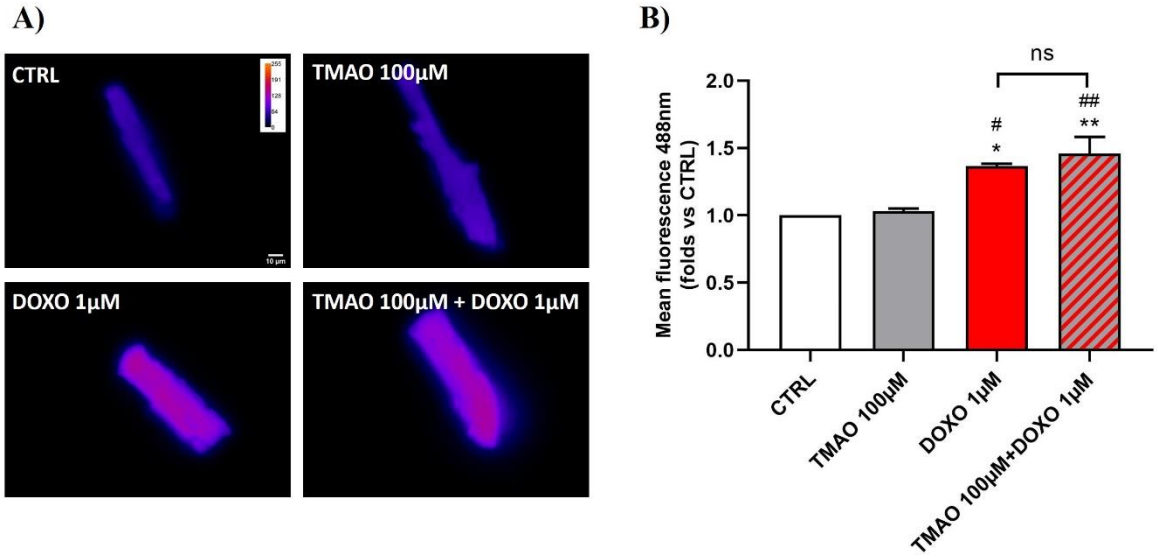

Figure 35. *TMAO treatment for 24h does not induce the rise of reactive oxygen species (ROS) in cardiomyocytes.* ***A)*** *Representative single cell fluorescence images of isolated cardiomyocytes treated for 24h with TMAO 100µM, DOXO 1µM or simultaneously treated with TMAO 100 µM and the stressor (488 nm; magnification 60X).* ***B)*** *TMAO treatment for 24h did not induce ROS increase, the effect of DOXO 1 µM was not changed by simultaneous treatment with TMAO. (CTRL: 1.00±0.00; TMAO 100 µM: 1.03±0.02; DOXO 1 µM: 1.37±0.02; TMAO 100 µM + DOXO 1 µM: 1.46±0.12. Cells number for each condition in a total of three independent experiments: CTRL: 12; TMAO 100 µM: 12; DOXO 1 µM: 12; TMAO 100 µM + DOXO 1 µM: 12). *p<0.05 and **p< 0.01 (vs CTRL); $^{\#}p<0.05$ and $^{\#\#}p<0.01$ (vs TMAO 100 µM).*

4.1.5 Mitochondrial membrane potential

To assess if TMAO induces or worsens an exhisting mitochondrial stress, cardiomyocytes were treated in basal condition or simultaneously with H_2O_2 50 µM for 1h, and mitochondrial membrane depolarization was monitored with the JC-1 probe in confocal microscopy.

As illustrated in Figure 36, cells teated for 1h did not show mitochondrial depolarization following basal treatment with TMAO 100 µM, while H_2O_2 50 µM induced a partial loss of the mitochondrial membrane potential, and this effect was unchanged by the simultaneous treatment with TMAO.

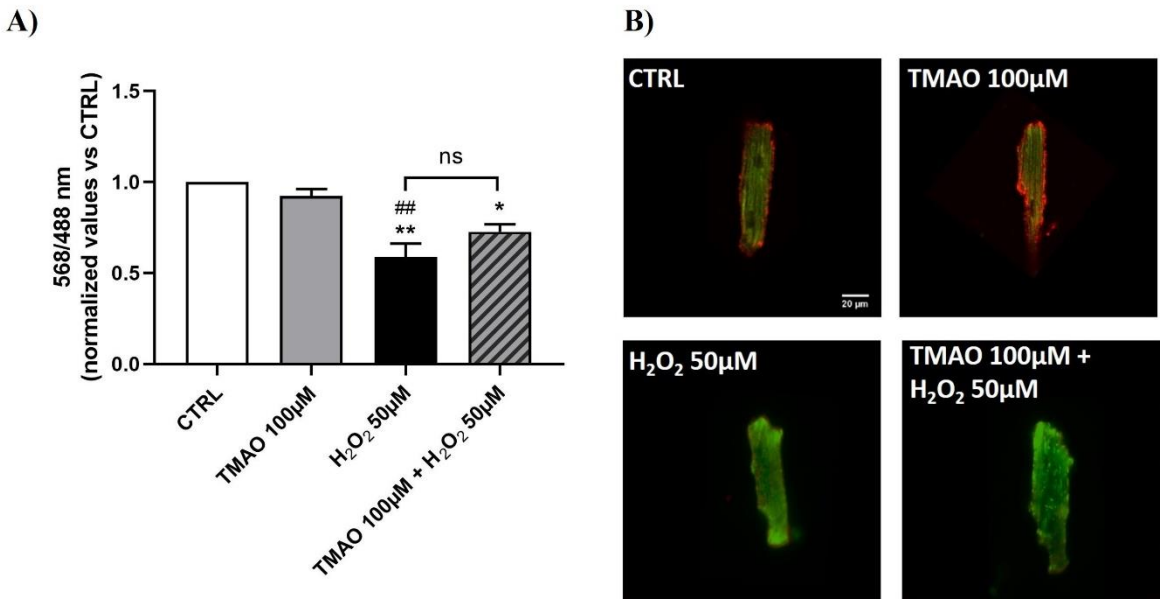

Figure 36. *TMAO treatment for 1h does not induce mitochondrial membrane depolarization in cardiomyocytes.* ***A)*** *TMAO 100 µM treatment for 1h did not induce mitochondrial membrane depolarization, while the effect of H_2O_2 50 µM induced a partial reduction in 568/488nm fluorescence ratio that was maintained in the simultaneous treatment with TMAO. (CTRL: 1.00±0.00; TMAO 100µM: 0.92±0.04; H_2O_2 50µM: 0.59±0.07; TMAO 100µM + H_2O_2 50µM: 0.72±0.04. Cells number for each condition in a total of three independent experiments CTRL: 8; TMAO 100 µM: 8; H_2O_2 50 µM: 8; TMAO 100 µM + H_2O_2 50 µM: 8). *p<0.05 and **p<0.01 (vs CTRL); $^{\#\#}$p<0.01 (vs TMAO 100 µM)* ***B)*** *Merged confocal microscopy images of isolated cardiomyocytes treated for 1h with TMAO 100 µM, H_2O_2 50 µM or simultaneously treated with TMAO 100 µM and H_2O_2 50 µM (488 and 568nm; magnification 60X).*

Moreover, in order to verify if TMAO induces any effect on mitochondrial membrane potential after prolonged treatments, cardiomyocytes were treated for 24h, both in basal conditions and in presence of DOXO 1 µM. Also in this set of experiments TMAO had no effects alone and it was not able to balance or exacerbate the effect of the stressor, that partially reduced the mitochondrial membrane potential (Figure 37).

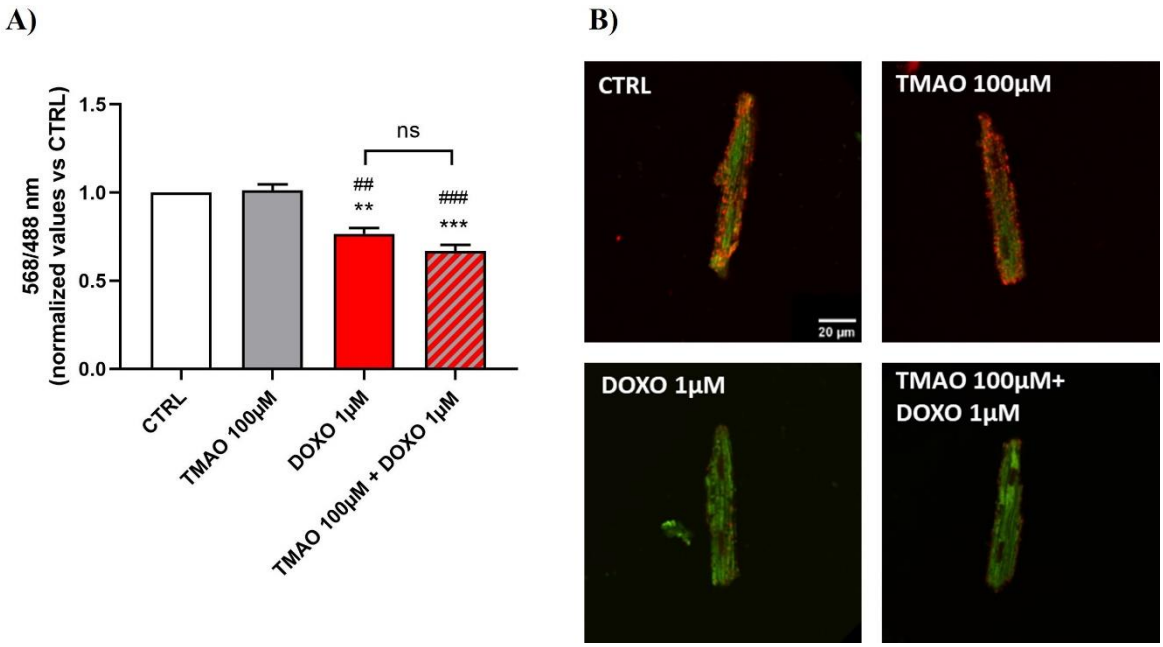

Figure 37. *TMAO treatment for 24h does not induce mitochondrial membrane depolarization in cardiomyocytes.* ***A)*** *TMAO 100 µM treatment for 24h did not induce mitochondrial membrane depolarization, while the effect of DOXO 1 µM induced a reduction in 568/488nm fluorescence ratio that was maintained in the simultaneous treatment with TMAO. (CTRL: 1.00±0.00; TMAO 100µM: 1.02±0.03; DOXO 1µM: 0.77±0.03; TMAO 100µM + DOXO 1µM: 0.67±0.03. Cells number for each condition in a total of three independent experiments: CTRL: 24; TMAO 100 µM: 24; DOXO 1 µM: 24; TMAO 100 µM + DOXO 1 µM: 24). **p< 0.01 and ***p< 0.001 (vs CTRL); $^{\#\#}$p<0.01 and $^{\#\#\#}$p< 0.001 (vs TMAO 100 µM)* ***B)*** *Merged* ***c****onfocal microscopy images of isolated cardiomyocytes treated for 24h with TMAO 100 µM, DOXO 1 µM or simultaneously treated with TMAO 100 µM and DOXO 1 µM (488 and 568nm; magnification 60X).*

4.2 Study on bovine aortic endothelial cells

4.2.1 BAE-1 viability in basal treatment

Bovine aortic endothelial cells viability was assessed through the MTS assay after 24h, 48h and 72h of treatment with different concentrations of TMAO (1 μM, 10 μM, 100 μM, 1 mM, 10 mM). As Figure 38 shows, none of the concentrations used was toxic for BAE-1 at any time tested. According with these results, further experiments using BAE-1 were performed only with the concentration 100 μM, assessed as the pathological threshold for vascular dysfunction (Gatarek & Kaluzna-Czaplinska, 2021).

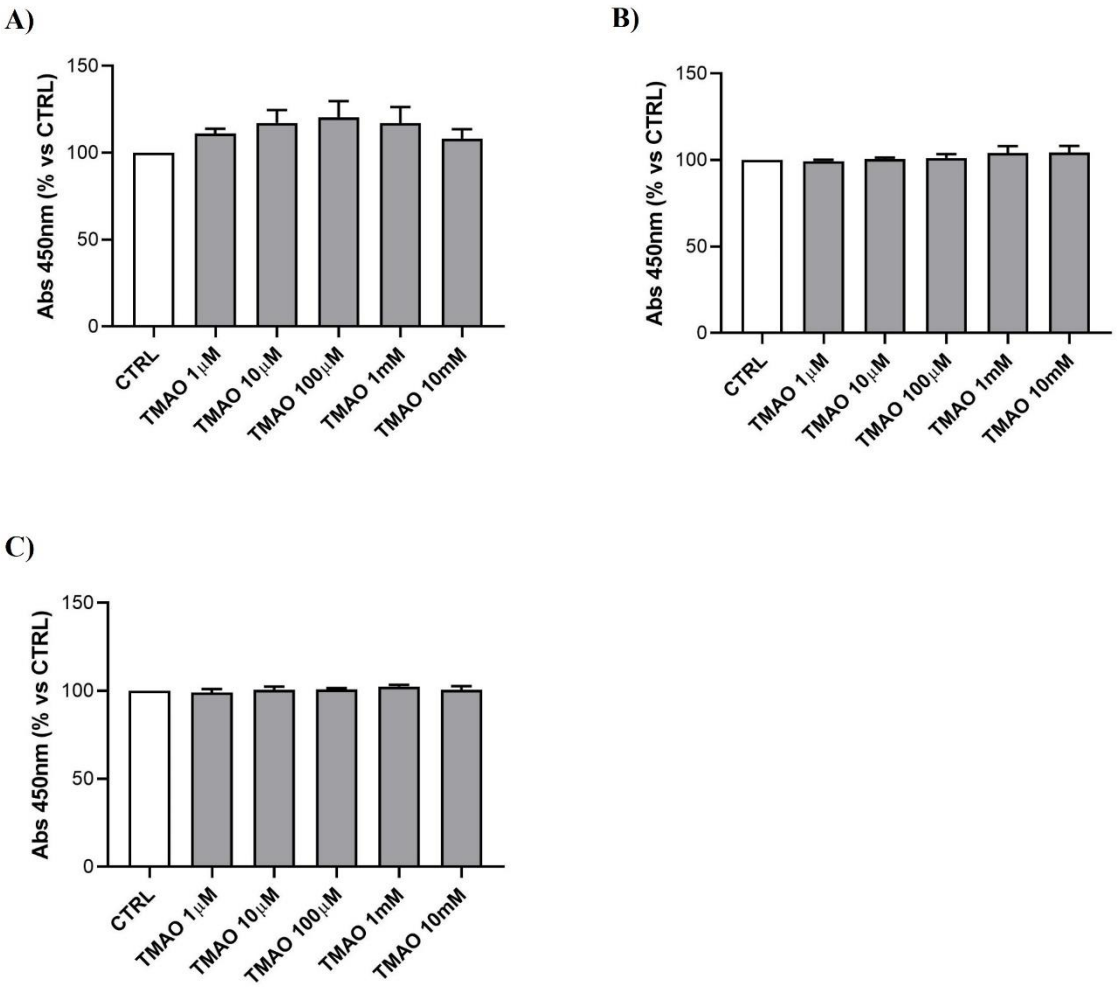

Figure 38. *BAE-1 viability is not affected by TMAO treatment. TMAO showed no cytotoxic effect after* ***A)*** *24h (CTRL: 100±0.00; TMAO 1 μM: 111.05±2.81; TMAO 10 μM: 117.25±7.34; TMAO 100 μM: 120.49±9.16; TMAO 1 mM: 117.08±9.18; TMAO 10 mM: 108.23±5.29),* ***B)*** *48h (CTRL: 100±0.00; TMAO 1 μM: 99.49±0.72; TMAO 10 μM: 100.53±0.86; TMAO 100 μM: 101.18±2.29; TMAO 1 mM: 104.02±3.99; TMAO 10 mM: 104.28±3.86) and* ***C)*** *72h (CTRL: 100±0.00; TMAO 1 μM: 99.12±1.92; TMAO 10 μM: 100.67±1.78; TMAO 100 μM: 100.90±0.71; TMAO 1 mM: 102.43±0.99; TMAO 10 mM: 100.60±2.04) of treatment.*

4.2.2 Intracellular reactive oxygen species

To evaluate if TMAO impacts the oxidative status of endothelial cells, ROS were monitored with the CellROX® green probe after 1h or 24h of treatment with TMAO 100 μM, in basal condition and in presence of MEN 100 μM. As explained in material and methods section, for 1h treatment experiments, both drugs were given simultaneously; while in the 24h treatment experiments, MEN was added in the last hour of TMAO incubation. TMAO alone was not able to induce the rise of ROS both at 1h and 24h, while MEN treated cells showed, as expected, a higher mean fluorescence considered directly proportional to intracellular ROS. Simultaneous treatment with TMAO and the stressor at both 1h and 24h did not induce any change in intracellular ROS, indeed, mean fluorescence was comparable to that of cells treated with MEN alone (Figure 39).

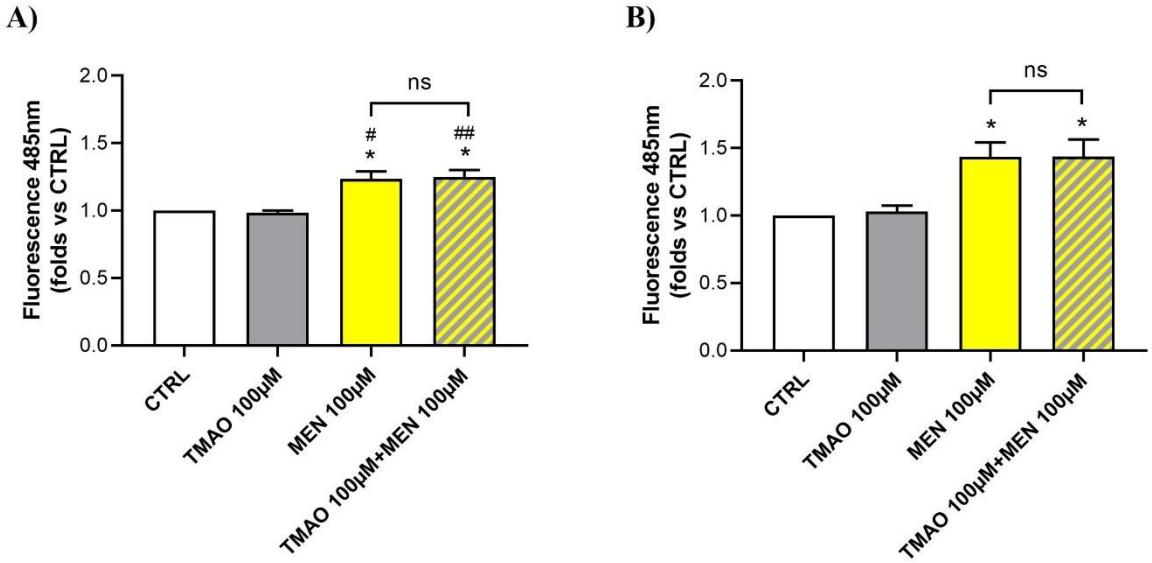

Figure 39. *TMAO treatment does not induce the rise of reactive oxygen species (ROS) in BAE-1.* ***A)*** *TMAO 100 μM treatment for 1h did not induce the rise of ROS in basal condition. As expected, MEN induced ROS production, and this effect was not changed in the simultaneous treatment with TMAO (CTRL: 1.00±0.00; TMAO 100 μM: 0.98±0.02; MEN 100 μM: 1.24±0.06; TMAO 100 μM + MEN 100 μM: 1.25±0.05). *p<0.05 (vs CTRL), $^{\#}$p<0.05 and $^{\#\#}$p<0.01 (vs TMAO).* ***B)*** *TMAO 100 μM treatment for 24h did not induce the rise of ROS in basal condition. As expected, MEN induced ROS production, and this effect was not changed in the simultaneous treatment with TMAO (CTRL: 1.00±0.00; TMAO 100 μM: 1.03±0.04; MEN 100 μM: 1.43±0.11; TMAO 100 μM + MEN 100 μM: 1.43±0.13). *p<0.05 (vs CTRL).*

4.2.3 Mitochondrial membrane potential

Mitochondrial membrane potential after BAE-1 treatment with TMAO was monitored through confocal microscopy and the JC-1 probe. BAE-1 were treated for 1h or 24h with TMAO 100 μM, in basal condition or in presence of MEN 100 μM. Also for this set of experiments, for 1h treatment, both drugs were given simultaneously; while in the 24h treatment, MEN was added in the last hour of TMAO incubation. Quantitative variations in fluorescence ratio 568/488nm is presented in Figure 40A and B, in which mitochondrial membrane depolarization was only visible in MEN treated cells, and the simultaneous treatment with TMAO did not affect this condition, at both time tested. Figure 40C shows representative confocal microscopy images of cells after 1h of the indicated treatment: the increase in green fluorescence intensity after MEN treatment, sign of mitochondrial depolarization, is not dampened or exacerbated by TMAO.

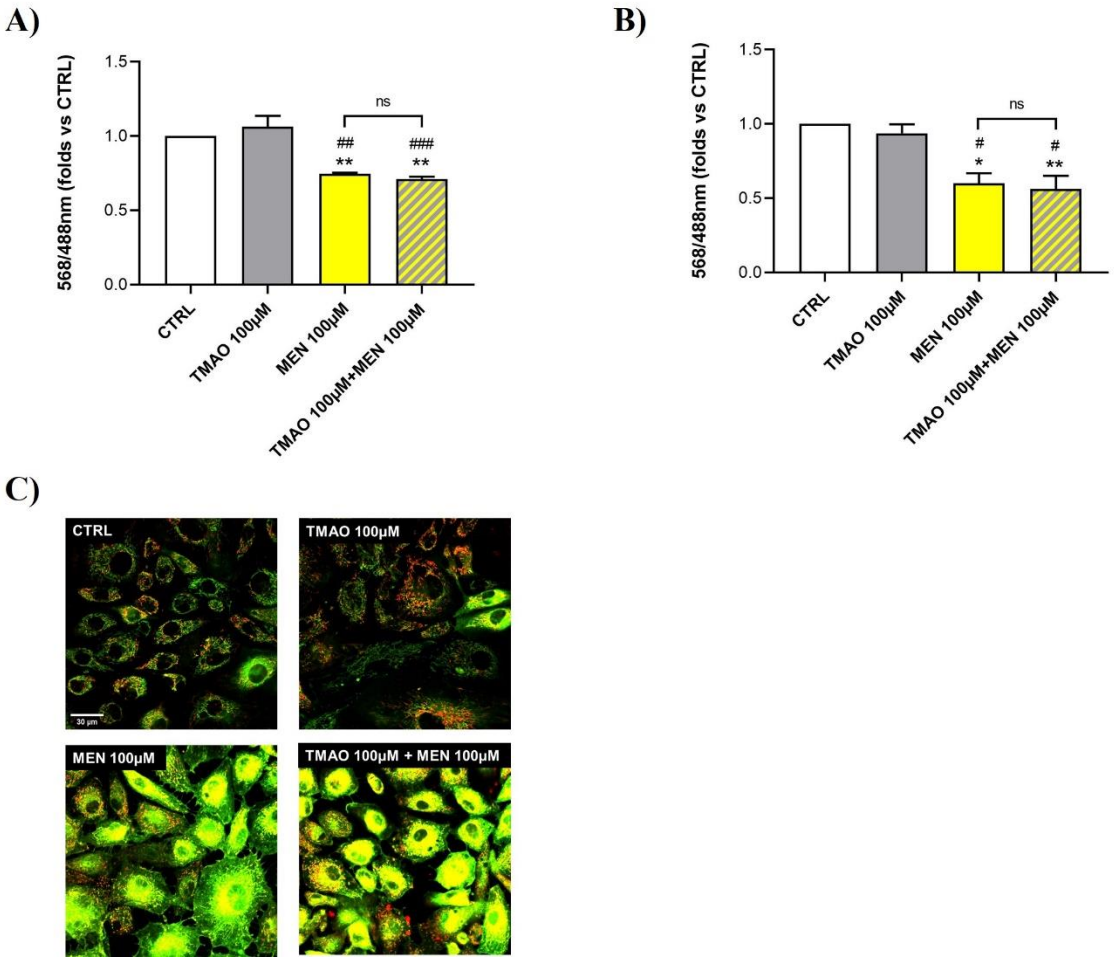

Figure 40. *TMAO treatment does not induce mitochondrial membrane depolarization in BAE-1.* ***A)*** *TMAO 100 µM treatment for 1h did not induce a reduction of mitochondrial membrane potential. While the effect of MEN 100 µM induced a reduction in 568/488nm fluorescence ratio that was maintained in the simultaneous treatment with TMAO (CTRL: 1.00±0.00; TMAO 100 µM: 1.06±0.07; MEN 100 µM: 0.75±0.01; TMAO 100 µM + MEN 100 µM: 0.71±0.02. Cells number for each condition in a total of three independent experiments: CTRL: 160; TMAO 100 µM: 180; MEN 100 µM: 180; TMAO 100 µM + MEN 100 µM: 180). **p<0.01 (vs CTRL), $^{\#\#}$p<0.01 and $^{\#\#\#}$p<0.001 (vs TMAO).* ***B)*** *TMAO 100 µM treatment for 24h did not induce a reduction of mitochondrial membrane potential. While the effect of MEN 100 µM induced a reduction in 568/488nm fluorescence ratio that was maintained in the simultaneous treatment with TMAO. (CTRL: 1.00±0.00; TMAO 100 µM: 0.93±0.06; MEN 100 µM: 0.60±0.07; TMAO 100 µM + MEN 100 µM: 0.56±0.09. Cells number for each condition in a total of three independent experiments: CTRL: 83; TMAO 100 µM: 83; MEN 100 µM: 83; TMAO 100 µM + MEN 100 µM: 83). *p<0.05 and **p<0.01 (vs CTRL), $^{\#}$p<0.05 (vs TMAO).* ***C)*** *Merged confocal microscopy images of BAE-1 treated for 1h with TMAO 100 µM, MEN 100 µM or simultaneously treated with TMAO 100 µM and MEN 100 µM (568 and 488nm, magnification 60X).*

4.2.4 Intracellular calcium variations in purinergic response to ATP

In order to assess if TMAO is involved in endothelial dysfuction, intracellular calcium variations participating in the purinergic response to ATP were monitored through confocal microscopy, by using the fluorescent probe Fluo-3 AM. As expected, basal stimulation with ATP induced prolonged calcium signal; indeed, both intracellular stores opening and extracellular influx of Ca^{2+} (da Silva et al., 2009) are involved in the intracellular pathway activated by ATP. Pretreatment for 24h with TMAO 100 µM, before stimulation with ATP, induced a significant reduction in the plateau phase of the curve, suggesting a possible implication of TMAO in modulating calcium signal in response to ATP (Figure 41A). Fluorescence variations between the peak value and the fluorescence at t/2 (F_{max}-$F_{t/2}$), highlighted with the dotted line in panel A, showed a significant shortening of the calcium signal in 24h TMAO pretreated cells; otherwise, 1h of pretreatment was not able to induce any substantial change in purinergic response to ATP (Figure 41).

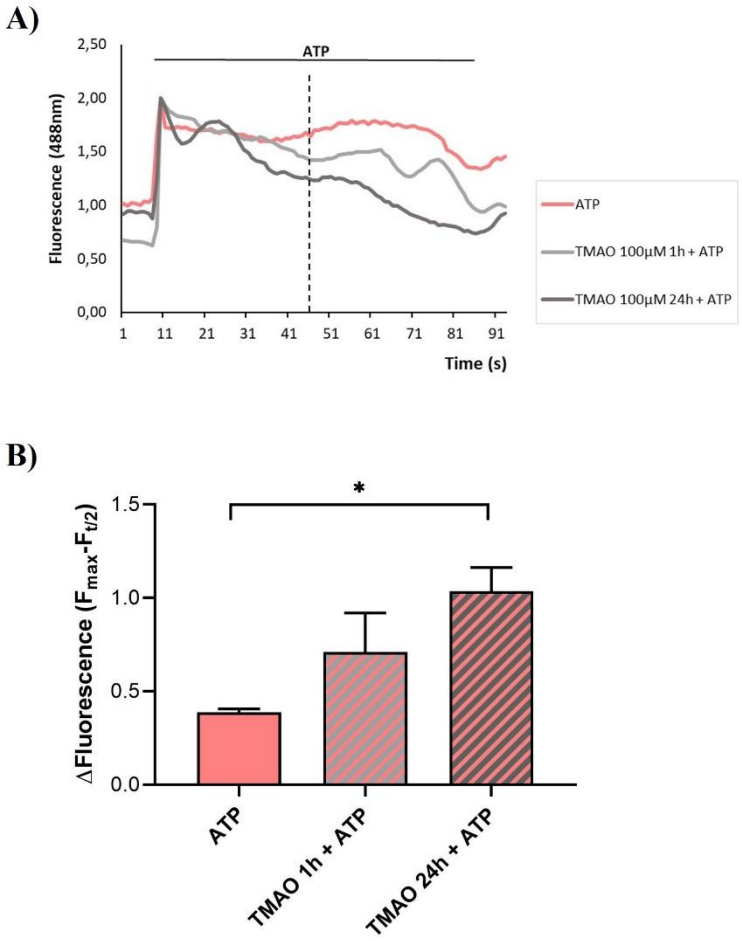

Figure 41. *TMAO treatment alters intracellular calcium in purinergic response to ATP.* ***A)*** *Mean fluorescence variations of normalized curves aligned respect to the peak value (F_{max}) after ATP stimulation in a single representative experiment. Dotted line indicates the t/2 at which curves differences were considered.* ***B)*** *Plot representing mean F_{max}-$F_{t/2}$ fluorescence of four independent experiments during ATP stimulation in basal condition (ATP) or after treatment with TMAO 100 μM for 1h or 24h. As shown, treatment with TMAO for 24h reduced intracellular calcium after ATP stimulation as expressed by the higher value of the difference between F_{max} and $F_{t/2}$. (ATP: 0.48±0.02; TMAO 1h+ATP: 0.55±0.21; TMAO 24h+ATP: 0.85±0.13. Cells number for each condition in a total of four independent experiments: ATP: 47; TMAO 1h+ATP: 47; TMAO 24h+ATP: 47). *p<0.05.*

4.2.5 Nitric oxide release in purinergic response to ATP

Previous results regarding calcium signal shortening, suggested a possible involvement of TMAO in modulating nitric oxide release in response to ATP, as the rise of intracellular calcium represents the essential trigger for eNOS activation (da Silva et al., 2009; Förstermann & Sessa, 2012). To analyze this issue, nitric oxide production in BAE-1 cells was monitored with the NO-fluorescent probe DAR-4M AM, and time course acquisitions in confocal microscopy. Figure 42 shows representative time course fluorescence variations of single cells, in basal condition (ATP) or after TMAO 100 µM treatment for 1h or 24h before ATP stimulation. As expected, basal treatment with ATP induced a slow continuous rise in fluorescence intensity, directly associated with NO release; this effect was preserved when cells were treated for 1h with TMAO before purinergic stimulation. Otherwise, treatment with TMAO for 24h induced a reduction in NO production, thus confirming a possible involvement of TMAO in the Ca^{2+}- NO pathway (Figure 42A). These results were quantified by the measument of fluorescence variation before and after ATP stimulation (Figure 42B).

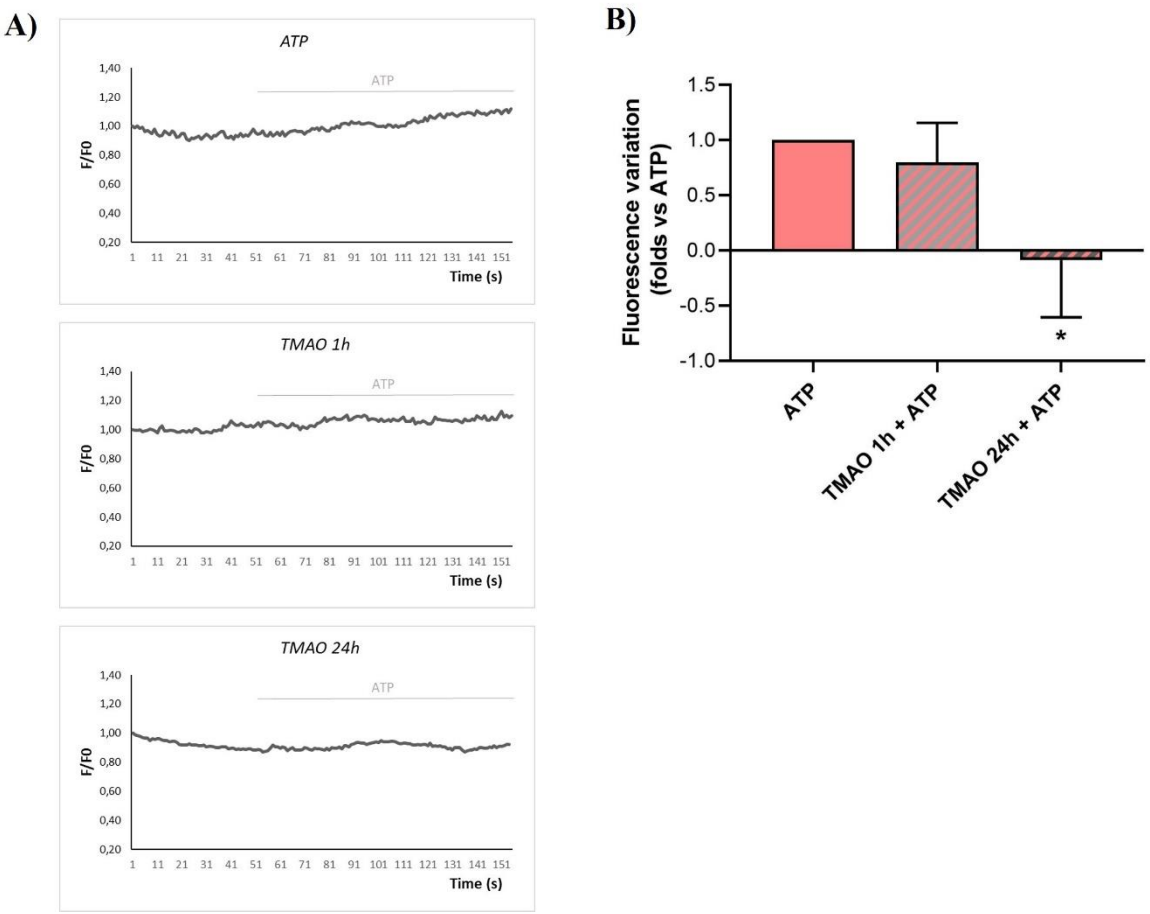

Figure 42. *TMAO treatment influences nitric oxide (NO) release in purinergic response to ATP.* ***A)*** *Normalized traces of fluorescence variations at 568 nm of single cells stimulated with ATP in basal condition (ATP) and after 1h or 24h of treatment with TMAO 100 µM before purinergic stimulation.* ***B)*** *Bar graph showing fluorescence variations before and after ATP stimulation. Treatment with TMAO 100 µM for 24h before purinergic stimulation with ATP influenced NO release. (ATP: 1.00±0.00; TMAO 1h + ATP: 0.79±0.36; TMAO 24h + ATP: -0.09±0.52. Cells number for each experimental condition in a total of three independent experiments: ATP 63; TMAO 1h + ATP:63; TMAO 24h + ATP:57). *p<0.05 (vs ATP).*

4.2.6 Endothelial nitric oxide synthase phosphorylation in ATP stimulation

As reported by several authors, ATP-induced rise of intracellular calcium activates eNOS by setting-up the Ca^{2+}-Calmodulin complex, wich leads to eNOS phosphorylation at Ser1179. To assess if TMAO impairment of ATP-induced NO release was dependent from a decrease of eNOS phosphorylation at Ser1179 ($eNOS^{Ser1179}$), Western Blot experiments were performed, in cells stimulated with ATP and pretreated or not with TMAO 100 μM, for 1h and 24h. As Figure 43 shows, pretreatment of BAE-1 with TMAO 100 μM for 1h did not influence $eNOS^{Ser1179}$/eNOS ratio after purinergic stimulation, while treatment for 24h with TMAO 100 μM significantly reduced eNOS phosphorylation. These data were aligned with previous results on NO release, and suggested a possible involvement of TMAO in the impairment of vasodilatory mechanisms.

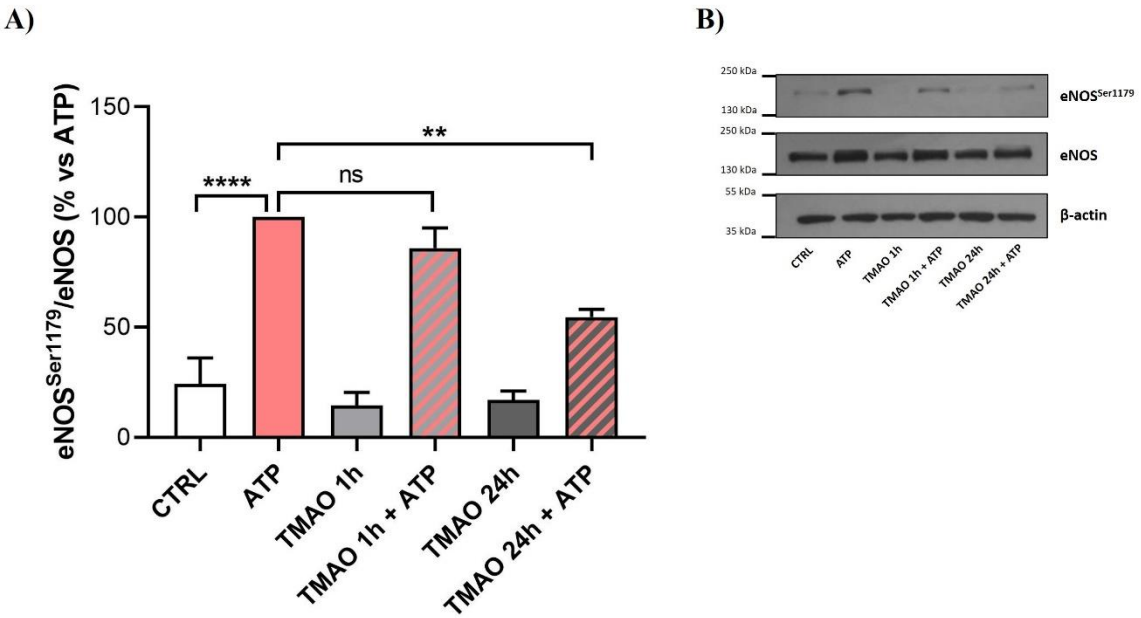

Figure 43. *TMAO impacts on eNOS phosphorylation in purinergic stimulation with ATP.* ***A)*** *Bar graph showing mean percentage of $eNOS^{Ser1179}$/eNOS ratio related to ATP condition of four independent experiments. Basal treatment with TMAO for 1h and 24h did not induce any variation in eNOS phosphorylation, while treatment for 24h induced a reduction of $eNOS^{Ser1179}$/eNOS ratio in purinergic response to ATP. (CTRL: 24.27±11.76; ATP: 100.00±0.00; TMAO 1h: 14.40±6.02; TMAO 1h + ATP: 85.98±9.06; TMAO 24h: 16.95±4.17; TMAO 24h + ATP: 54.63±3.62). **p<0.01 and ****p<0.0001.* ***B)*** *Representative Western Blots showing the effect of TMAO treatment for 1h and 24h in eNOS phosphorylation at Ser1179 in basal condition and after ATP stimulation.*

5. DISCUSSION

Cardiovascular diseases (CVD) are the leading cause of death worldwide. In particular, last data available, that refer to the period from 2007 to 2016, register 17.8 million deaths caused by this group of pathological conditions. Major cardiovascular fatal outcomes were caused by ischemic heart disease and stroke (Townsend et al., 2021). Clinical evidences now support the definition of a sexual dimophism in the development and outcome of CVD. Indeed, women in post-menopausal period show more critical, and even fatal, outcomes than men, probably due to the lack of physiological estrogen-mediated cardioprotection (Querio, Antoniotti, et al., 2021). Furthermore, clinical manifestations of CVD are different between women and men, and only in this last period scientific and epidemiological evidences point out the need to set up specific guidelines for proper clinical intervention in the two sexes.

Cardiovascular diseases are multifactorial chronic conditions that can develop through the influence of both intrinsic and extrinsic factors. In particular, CVD risk factors can be classified as non-modifiable and modifiable. The first group is characterized by age, sex, genetic factors that cannot be changed and represent the starting points to control modifiable risk factors. Life-style habits, smoke, diet-derived conditions, such as obesity, diabetes, hyperlipidemia, hypertension, physical inactivity and drugs, as some chemotherapeutic agents, are the most relevant examples of modifiable risk factors (Francula-Zaninovic & Nola, 2018). Preventive strategies in this last group of risk factors is one of the approaches developed in last years in order to limit both CVD incidence and prevalence.

New evidences suggest a possible relationship between microbial population that resides in the gut, the microbiota, and the development of several pathological conditions, and, among others, CVD seem to be strictly related to host-microbiota interactions.

Gut microbiota carries out different physiological functions that contribute to the maintainance of a homeostatic state in the host. Indeed, microbes residing in the gut are involved in the regulation of intestinal barrier, contributing to the defence against pathogens and activating the immune response; and in the metabolic transformation of nutrients, facilitating their absorption by the host (Tang et al., 2017). Moreover, new studies point out that imbalanced microbial population in the gut, the so called dysbiosis, can induce secondary metabolites increase that can enter the systemic circulation and mediate different functions in peripheral tissues before being excreted through urine. Among all the molecules that are synthesized by the gut microbiota, trimethylamine (TMA) is emerging as a multifactorial agent when released in systemic circulation. Trimethylamine is a diet-derived compound that can be synthesized from different precursors, in particular, choline, L-carnitine and ergothioneine (Simó & García-Cañas, 2020). Once synthesized through the action of bacteria expressing the enzymes directly involved in TMA precursors metabolism,

such as *CutC/CutD*, *CntA/CntB* and *YeaW/X* (Falony et al., 2015), TMA could be absorbed by enterocytes or freely cross the intestinal barrier thanks to its volatility. Once TMA enters the portal circulation it is driven to the liver where it is N-oxidized by flavin containing monooxygenase 3 to form trimethylamine N-oxide (TMAO) (Zeisel & Warrier, 2017).

TMAO has already been studied in deep-sea animals in which its high concentrations are linked to its physiological functions related to osmotic and hydrostatic pressures contrast (Ufnal et al., 2015). Indeed, it is involved in protein stabilization against these environmental denaturing forces (Catucci et al., 2019; Ufnal et al., 2015).

Controversial results concerning patho-physiological roles of TMAO in human organism are recently rising and TMAO direct effect in pathological development is still under investigation.

Recent evidences suggest a possible implication of TMAO in the development of CVD, in particular, it has been underlined that higher plasma concentrations of TMAO are linked to CVD outcome and chronic kidney disease development (Gatarek & Kaluzna-Czaplinska, 2021).

On the other hand, evidences support a positive or neutral effect of TMAO. Studies suggest that its precursor, TMA, represents the toxic agent, while TMAO is its metabolically inactive byproduct of detoxification (Catucci et al., 2019; Jaworska et al., 2019). Moreover, high TMAO plasmatic concentration in marine organisms has several protective effects, thus suggesting a similar role of the molecule also in human body (Ufnal et al., 2015).

Aim of this study was to evaluate TMAO-mediated effects in the cardiovascular system, in two *in vitro* models. The project was divided in two parts: the first set of experiments was focused on adult rat cardiomyocytes in primary culture, while the second part was developed using bovine aortic endothelial cells (BAE-1).

First experiments evaluated TMAO toxicity in adult rat cardiomyocytes in basal conditions: different concentrations of the molecule (1 µM, 10 µM, 100 µM, 1 mM and 10 mM) were tested for 1h and 24h without any effect on cells viability (Figure 31). Further studies were addressed to the evaluation of TMAO cytotoxicity in stressed cardiomyocytes, in order to evaluate if the molecule is able to balance or worsen the effect of a known insult.

Several stressed conditions were applied: ischemia-reperfusion, H_2O_2-induced oxidative stress and DOXO-induced damage.

Cardiomyocytes were subjected to an ischemia/reperfusion *in vitro* protocol, following the scheme presented in Figure 30. As expected, after incubation for 45 minutes with the ischemic buffer and the successive reperfusion with Tyrode standard solution, an high cell loss was evident and this is in agreement with specialistic literature concerning the

deleteriuos effects of both ischemic and reperfusion insults (Heusch, 2020). Treatment with TMAO 100 µM, considered the threshold for the onset of pathological effects and used for all subsequent experiments in both cell models (Gatarek & Kaluzna-Czaplinska, 2021), was uneffective in basal condition and in the ischemia-reperfusion condition did not modify the detrimental consequence of reperfusion (Figure 32). These are first results concerning TMAO effects on primary adult cardiomyocytes viability, showing that the molecule is uneffective within 24h of treatment. According to these first results, Jaworska and collaborators showed no toxic effects of TMAO in H9c2 cardiomyocytes treated for 24h and 72h in a concentration range between 0.2 mM and 10 mM (Jaworska et al., 2019).

Further experiments were linked to the evaluation of a possible TMAO-mediated modulation of cardiomyocytes functionality, so, cell shrinkage was monitored after 24h of treatment with TMAO 100 µM in basal condition or in presence of two different stressors, DOXO and H_2O_2. Results obtained in the study, showed no direct effect of the molecule in modulating sarcomere length, furthermore it was not able to change the effect of the two stressors when simultaneously present (Figure 33). These results are in agreement with those obtained by Savi and collaborators (Savi et al., 2018), showing that both TMAO 20 µM and 100 µM did not impact on cardiomyocytes sarcomere length. The same study also evidenced a decreased sarcomere fraction of shortening and a decreased maximal rate of shortening and re-lengthening induced by TMAO, which impaired cell contraction (Savi et al., 2018). Moreover, contrasting results were obtained by Oakley and collaborators, that showed impairment in human cardiac muscle and mouse isolated hearts contraction. Indeed, increased contractile tension, increased maximum slope and increased minimum slope after acute treatment with TMAO 300 µM and 3 mM was shown (Oakley et al., 2020).

Oxidative stress is one of the primary response to cardiac insults and it is involved in inflammatory response activation with the principal aim to limit heart's damage. Oxidative stress is a condition related to uncontrolled ROS and other free radicals rising and a reduction in the cellular antioxidant systems, with a resultant cellular structural and functional impairment. So, further experiments were directed toward the evaluation of TMAO induction of reactive oxygen species increase, both in basal condition and in presence of stressors, using the DCF-DA probe. After 1h of treatment with TMAO 100 µM, ROS were not detectable in cardiomyocytes, while H_2O_2 induced fluorescence increase that was considered as direct indicator of ROS production. This same result was obtained in the simultaneous treatment with TMAO and the stressor (Figure 34). Similarly, after 24h of treatment, TMAO 100 µM alone was not able to induce ROS increase, while DOXO 1 µM induced ROS production and its effect was not worsened by simultaneous administration of

TMAO (Figure 35), thus underlining a neutral role of the molecule that was not able to balance or exacerbate the effect of a known cardiac insult (Al-Malky et al., 2020). Further experiments centered on TMAO role in oxidative stress evaluated its effect on mitochondrial membrane potential, using the JC-1 probe. Results obtained showed no direct effects of TMAO 100 µM after 1h or 24h of treatment. Moreover, TMAO was not able to modify the mitochondrial depolarization induced by different stressors (Figure 36 and 37). These last results are not supported by data obtained by Li and coworkers, that showed the rise of ROS after TMAO treatment in cardiac fibroblasts. Probably these contrasting results are linked to differences in cell models and protocols used for ROS detection (X. Li et al., 2019).

As data obtained on adult cardiomyocytes highlighted the lack of TMAO impact in all conditions and parameters tested, further experiments were developed on bovine aortic endothelial cells (BAE-1), in order to evaluate if any cardiac damage ascribed to TMAO could be endothelium mediated.

First experiments on BAE-1 were centered on the evaluation of cells viability, using the MTS assay, after treatment with different concentrations of TMAO (1 µM, 10 µM, 100 µM, 1 mM and 10 mM) for 24h, 48h and 72h. Also in this set of experiments, cells viability was not modified by TMAO even for prolonged times of treatment (Figure 38). These results are supported by other studies, as an example Ma and collaborators, showed that different concentrations of TMAO (0, 10, 50, 100 µmol/l) had no toxic effects on human umbilical vein endothelial cells (HUVEC) after 24h of treatment and these results were confirmed both with the MTT assay and the lactate dehydrogenase (LDH) test (Ma et al., 2017).

Endothelial cells oxidative stress can favour the development of endothelial dysfunction, and vascular impairment (Incalza et al., 2018). Furthermore, different studies underlined TMAO involvement in endothelial dysfunction, and in particular Brunt and collaborators pointed out that TMAO-mediated oxidative stress could be cause of this pathological condition (Brunt et al., 2020). Further experiments using BAE-1 were then performed to evaluate the rise of ROS and mitochondrial membrane potential both in basal condition and in presence of menadione (MEN), a vitamin K3 precursor involved in oxidative stress enhancement and endothelial damage, as already underlined in paragraph 1.4.1.1 of the introduction (Bik et al., 2021; Burdette et al., 2002; N. O. Thomas et al., 2016). As Figures 39 and 40 show, also for endothelial cells basal treatment with TMAO 100 µM for 1h and 24h did not induce ROS production and mitochondrial membrane depolarization. Treatment with MEN 100 µM induced cells oxidative damage, underlined by both the rise of ROS and mitochondrial membrane depolarization, and these effects were maintained in the simultaneous treatment with TMAO. Contrasting results have been obtained by Sun and collaborators, who

demonstrated ROS production after TMAO 300 µM treatment in HUVEC (Sun et al., 2016). Probably these different results have been obtained due to higher TMAO concentrations used for experiments, different cellular model and different protocol to detect ROS production.

Endothelial dysfunction is characterized by vasodilatory mechanisms impairment, resulting in particular from a detrimental reduction of NO release. Therefore, further experiments were addressed to the evaluation in BAE-1 cells of TMAO impact on the ATP-induced NO release. Starting experiments were focused on the first step of the purinergic intracellular pathway, that is the rise of intracellular calcium. Thus, time course imaging of intracellular calcium was monitored, in cells pretreated with TMAO (1h and 24h) and acutely perfused with ATP. Results obtained showed a significant reduction in the calcium wave lengthening when cells were pretreated with TMAO for 24h and then stimulated with ATP, thus suggesting a possible role of the molecule in interfering with the intracellular Ca^{2+} signal and with its dependent pathways (Figure 41). In particular, TMAO-dependent inhibition of ATP-evoked intracellular Ca^{2+} signal suggests a possible involvement of store-operated Ca^{2+} entry (SOCE). These results open an interesting comparison with data obtained in platelets, showing that TMAO enahnces the ATP-dependent intracellular calcium release from intracellular stores, thus favoring platelets activation and thrombosis onset (Zhu et al., 2016). In our model TMAO seems to affect intracellular calcium signal in terms of dampening its duration, but, like in platelets, also this calcium alteration could be associated with vascular dysfunction.

To further underline a possible involvement of TMAO in ATP-induced NO release, production of the gasotransmitter was evaluated with the fluorescent probe DAR-4M AM. As Figure 42 shows, a slow but continuous release of nitric oxide was detected during perfusion with ATP, both in basal condition and in cells pretreated for 1h with TMAO 100 µM. Otherwise, pretreatment with TMAO 100 µM for 24h induced a reduction in NO release after ATP stimulation, thus confirming previuos presented data on intracellular calcium. These results fit with those obtained by Sun and collaborators, that, by using a total nitric oxide assay kit, showed a reduction in NO release in HUVEC treated with TMAO 300 µM (Sun et al., 2016).

To clearly detect a role of TMAO in modulating calcium-induced NO release, Western Blot experiments were performed to evaluate activation of the principal enzyme involved in NO synthesis, endothelial nitric oxide synthase (eNOS). Reduction in eNOS phosphorylation at Ser1179 ($eNOS^{Ser1179}$) when cells were treated with TMAO for 24h and subsequently stimulated with ATP was outlined, thus confirming a reduction in enzymatic activity, and suggesting TMAO-mediated endothelial dysfunction after prolonged treatments (Figure 43).

Similar results were obtained by Brunt and collaborators, that showed in an *in vivo* model of TMAO supplemented diet, a reduction in eNOS phosphorylation (Brunt et al., 2020).

This work presents some limitations that have to be underlined before final conclusions. In particular, rat used were only female animals and, considering the sexual dimophism already underlined between sexes, obviously female derived cardiomyocytes could have endogeous estrogen-mediated defence against different stressors. Furthermore, experiments performed with cardiomyocytes in primary culture underline another weakness because treatments were no longer than 24h due to cells vulnerability after their isolation. Points of strenght could also reside in the cellular model used in the first part of the study, because primary cardiomyocytes are difficult to maintain in culture and difficult to obtain in a successful organ dissociation, thus underlining the originality of presented data.

In conclusion, obtained results on direct effects of TMAO in adult rat cardiomyocytes and bovine aortic endothelial cells, show no direct effects of the molecule in impacting cell viability and oxidative stress status, and these effects were maintained in presence of cardiac and vascular stressors, thus showing a neutral role of the molecule on these general indicators of damage. Intringuing results were however obtained in BAE-1 on the purinergic vasodilatory pathway, showing a role of TMAO, after 24h of treatment, in impairing calcium handling and nitric oxide release.

Clinical data and further *in vitro* and *in vivo* studies are certainly needed to elucidate the specific molecular targets affected by TMAO in vascular endothelium, that could represent the trigger points of its detrimental cardiovascular, and more broadly, muoltiorgan outcome.

6. ACKNOWLEDGMENTS

In queste ultime pagine vorrei ringraziare le persone che mi hanno accompagnata in questo bellissimo percorso.

Prima di tutto vorrei ringraziare la mia Tutor, *Maria Pia*, perché mi ha accolta nel suo laboratorio permettendomi di approfondire diverse tecniche e argomenti. In questi anni è stata un esempio per me sia dal punto di vista professionale che personale. Il confronto, che non è mai mancato durante tutto il mio percorso di dottorato, mi ha permesso di crescere e imparare ad osservare le cose con occhi nuovi. L'interesse, l'entusiasmo e la dedizione che ha nel suo lavoro sono fonte di continua ispirazione per me.

Il mio punto di riferimento in laboratorio, *Susanna*, che mi ha sempre affiancata e sostenuta durante gli esperimenti, insegnandomi ogni volta una cosa nuova senza mai farmi sentire inadeguata. Spero di aver imparato e interiorizzato parte della sua attenzione e sensibilità verso il prossimo e la sua serietà e rigore sul lavoro.

Un grazie speciale a *Renzo* che mi ha sempre sostenuta e qualche volta messa alla prova. Le sue domande e riflessioni nelle nostre lunghe chiacchierate fin dal mio ingresso in laboratorio sono state stimolo di continua ricerca. Un confronto diretto e multi tematico che mi ha permesso di crescere e sviluppare nuovi interessi.

La mia compagna di avventure e disavventure *Federica*, che ho imparato a conoscere pian piano e con cui ormai c'è un rapporto di vera amicizia e reciproco rispetto.

Tiziana che con la sua mitezza mi ha insegnato il lavoro in stabulario e *Alessandra* che con le sue fette biscottate e risate mi ha rasserenata anche nelle giornate più buie.

Un grazie speciale ai miei genitori, *Laura* e *Angelo*, e mio fratello, *Stefano*, che mi hanno sempre sostenuta in questi anni e hanno sempre creduto nelle mie capacità, non mettendomi mai in secondo piano o facendomi sentire scontata.

Gaia, che con grande pazienza ha riletto il lavoro e verso cui ho da sempre provato sincera di stima.

In ultimo, ma non per questo meno importante, *Andrea*, che da anni ormai mi sta vicino e con il quale ho vissuto tanti momenti belli, quelli in cui si capisce cosa vuol dire stare bene con una persona. Un compagno su cui poter contare in qualsiasi circostanza, anche nei momenti di maggiore sconforto, confusione o tristezza.

Sono tante le persone che vorrei ringraziare, nell'attesa di farlo di persona, le porto tutte nel cuore.

7. REFERENCES

Al-Malky, H. S., Al Harthi, S. E., & Osman, A.-M. M. (2020). Major obstacles to doxorubicin therapy: Cardiotoxicity and drug resistance. *Journal of Oncology Pharmacy Practice: Official Publication of the International Society of Oncology Pharmacy Practitioners*, *26*(2), 434–444. https://doi.org/10.1177/1078155219877931

Al-Obaide, M. A. I., Singh, R., Datta, P., Rewers-Felkins, K. A., Salguero, M. V., Al-Obaidi, I., Kottapalli, K. R., & Vasylyeva, T. L. (2017). Gut Microbiota-Dependent Trimethylamine-N-oxide and Serum Biomarkers in Patients with T2DM and Advanced CKD. *Journal of Clinical Medicine*, *6*(9). https://doi.org/10.3390/jcm6090086

Andrews, A. M., Jaron, D., Buerk, D. G., & Barbee, K. A. (2014). Shear stress-induced NO production is dependent on ATP autocrine signaling and capacitative calcium entry. *Cellular and molecular bioengineering*, *7*(4), 510–520. https://doi.org/10.1007/s12195-014-0351-x

Bik, E., Mateuszuk, L., Stojak, M., Chlopicki, S., Baranska, M., & Majzner, K. (2021). Menadione-induced endothelial inflammation detected by Raman spectroscopy. *Biochimica Et Biophysica Acta. Molecular Cell Research*, *1868*(2), 118911. https://doi.org/10.1016/j.bbamcr.2020.118911

Brunt, V. E., Gioscia-Ryan, R. A., Casso, A. G., VanDongen, N. S., Ziemba, B. P., Sapinsley, Z. J., Richey, J. J., Zigler, M. C., Neilson, A. P., Davy, K. P., & Seals, D. R. (2020). Trimethylamine-N-Oxide Promotes Age-Related Vascular Oxidative Stress and Endothelial Dysfunction in Mice and Healthy Humans. *Hypertension (Dallas, Tex.: 1979)*, *76*(1), 101–112. https://doi.org/10.1161/HYPERTENSIONAHA.120.14759

Burdette, J. E., Chen, S.-N., Lu, Z.-Z., Xu, H., White, B. E. P., Fabricant, D. S., Liu, J., Fong, H. H. S., Farnsworth, N. R., Constantinou, A. I., Van Breemen, R. B., Pezzuto, J. M., & Bolton, J. L. (2002). Black cohosh (Cimicifuga racemosa L.) protects against menadione-induced DNA damage through scavenging of reactive oxygen species: Bioassay-directed isolation and characterization of active principles. *Journal of Agricultural and Food Chemistry*, *50*(24), 7022–7028. https://doi.org/10.1021/jf020725h

Cale, J. M., & Bird, I. M. (2006). Dissociation of endothelial nitric oxide synthase phosphorylation and activity in uterine artery endothelial cells. *American Journal of Physiology-Heart and Circulatory Physiology*, *290*(4), H1433–H1445. https://doi.org/10.1152/ajpheart.00942.2005

Catucci, G., Querio, G., Sadeghi, S. J., Gilardi, G., & Levi, R. (2019). Enzymatically Produced Trimethylamine N-Oxide: Conserving It or Eliminating It. *Catalysts*, *9*(12), 1028. https://doi.org/10.3390/catal9121028

Chen, K., Zheng, X., Feng, M., Li, D., & Zhang, H. (2017). Gut Microbiota-Dependent Metabolite Trimethylamine N-Oxide Contributes to Cardiac Dysfunction in Western Diet-Induced Obese Mice. *Frontiers in Physiology*, *8*, 139. https://doi.org/10.3389/fphys.2017.00139

Chen, S., & Li, S. (2012). The Na+/Ca2+ exchanger in cardiac ischemia/reperfusion injury. *Medical Science Monitor*, *18*(11), RA161–RA165. https://doi.org/10.12659/MSM.883533

Chhibber-Goel, J., Gaur, A., Singhal, V., Parakh, N., Bhargava, B., & Sharma, A. (2016). The complex metabolism of trimethylamine in humans: Endogenous and exogenous sources. *Expert Reviews in Molecular Medicine*, *18*. https://doi.org/10.1017/erm.2016.6

Cho, C. E., Taesuwan, S., Malysheva, O. V., Bender, E., Tulchinsky, N. F., Yan, J., Sutter, J. L., & Caudill, M. A. (2017). Trimethylamine-N-oxide (TMAO) response to animal source foods varies among healthy young men and is influenced by their gut microbiota composition: A randomized controlled trial. *Molecular Nutrition & Food Research*, *61*(1). https://doi.org/10.1002/mnfr.201600324

da Silva, C. G., Specht, A., Wegiel, B., Ferran, C., & Kaczmarek, E. (2009). Mechanism of purinergic activation of endothelial nitric oxide synthase in endothelial cells. *Circulation*, *119*(6), 871–879. https://doi.org/10.1161/CIRCULATIONAHA.108.764571

Deanfield, J. E., Halcox, J. P., & Rabelink, T. J. (2007). Endothelial function and dysfunction: Testing and clinical relevance. *Circulation*, *115*(10), 1285–1295. https://doi.org/10.1161/CIRCULATIONAHA.106.652859

DeMartino, A. W., Kim-Shapiro, D. B., Patel, R. P., & Gladwin, M. T. (2019). Nitrite and nitrate chemical biology and signalling. *British Journal of Pharmacology*, *176*(2), 228–245. https://doi.org/10.1111/bph.14484

Despa, S., & Bers, D. M. (2013). Na^+ transport in the normal and failing heart—Remember the balance. *Journal of Molecular and Cellular Cardiology*, *61*, 2–10. https://doi.org/10.1016/j.yjmcc.2013.04.011

Dudzinski, D. M., & Michel, T. (2007). Life history of eNOS: Partners and pathways. *Cardiovascular Research*, *75*(2), 247–260. https://doi.org/10.1016/j.cardiores.2007.03.023

Falony, G., Vieira-Silva, S., & Raes, J. (2015). Microbiology Meets Big Data: The Case of Gut Microbiota-Derived Trimethylamine. *Annual Review of Microbiology*, *69*, 305–321. https://doi.org/10.1146/annurev-micro-091014-104422

Fennema, D., Phillips, I. R., & Shephard, E. A. (2016). Trimethylamine and Trimethylamine N-Oxide, a Flavin-Containing Monooxygenase 3 (FMO3)-Mediated Host-Microbiome Metabolic Axis Implicated in Health and Disease. *Drug Metabolism*

and Disposition: The Biological Fate of Chemicals, *44*(11), 1839–1850. https://doi.org/10.1124/dmd.116.070615

Förstermann, U., & Sessa, W. C. (2012). Nitric oxide synthases: Regulation and function. *European Heart Journal*, *33*(7), 829–837, 837a–837d. https://doi.org/10.1093/eurheartj/ehr304

Francula-Zaninovic, S., & Nola, I. A. (2018). Management of Measurable Variable Cardiovascular Disease' Risk Factors. *Current Cardiology Reviews*, *14*(3), 153–163. https://doi.org/10.2174/1573403X14666180222102312

Frank, A., Bonney, M., Bonney, S., Weitzel, L., Koeppen, M., & Eckle, T. (2012). Myocardial ischemia reperfusion injury—From basic science to clinical bedside. *Seminars in cardiothoracic and vascular anesthesia*, *16*(3), 123–132. https://doi.org/10.1177/1089253211436350

Fulton, D., Ruan, L., Sood, S. G., Li, C., Zhang, Q., & Venema, R. C. (2008). Agonist-stimulated endothelial nitric oxide synthase activation and vascular relaxation. Role of eNOS phosphorylation at Tyr83. *Circulation Research*, *102*(4), 497–504. https://doi.org/10.1161/CIRCRESAHA.107.162933

Gatarek, P., & Kaluzna-Czaplinska, J. (2021). Trimethylamine N-oxide (TMAO) in human health. *EXCLI Journal*, *20*, 301–319. https://doi.org/10.17179/excli2020-3239

Geng, J., Yang, C., Wang, B., Zhang, X., Hu, T., Gu, Y., & Li, J. (2018). Trimethylamine N-oxide promotes atherosclerosis via CD36-dependent MAPK/JNK pathway. *Biomedicine & Pharmacotherapy = Biomedecine & Pharmacotherapie*, *97*, 941–947. https://doi.org/10.1016/j.biopha.2017.11.016

Gesper, M., Nonnast, A. B. H., Kumowski, N., Stoehr, R., Schuett, K., Marx, N., & Kappel, B. A. (2021). Gut-Derived Metabolite Indole-3-Propionic Acid Modulates Mitochondrial Function in Cardiomyocytes and Alters Cardiac Function. *Frontiers in Medicine*, *8*. https://www.frontiersin.org/article/10.3389/fmed.2021.648259

Gisladottir, R. S., Ivarsdottir, E. V., Helgason, A., Jonsson, L., Hannesdottir, N. K., Rutsdottir, G., Arnadottir, G. A., Skuladottir, A., Jonsson, B. A., Norddahl, G. L., Ulfarsson, M. O., Helgason, H., Halldorsson, B. V., Nawaz, M. S., Tragante, V., Sveinbjornsson, G., Thorgeirsson, T., Oddsson, A., Kristjansson, R. P., … Stefansson, K. (2020). Sequence Variants in TAAR5 and Other Loci Affect Human Odor Perception and Naming. *Current Biology*, *30*(23), 4643-4653.e3. https://doi.org/10.1016/j.cub.2020.09.012

Godo, S., & Shimokawa, H. (2017). Endothelial Functions. *Arteriosclerosis, Thrombosis, and Vascular Biology*, *37*(9), e108–e114. https://doi.org/10.1161/ATVBAHA.117.309813

Hadi, H. A. R., Carr, C. S., & Al Suwaidi, J. (2005). Endothelial dysfunction: Cardiovascular risk factors, therapy, and outcome. *Vascular Health and Risk Management*, *1*(3), 183–198.

Halilovic, A., Schmedt, T., Benischke, A.-S., Hamill, C., Chen, Y., Santos, J. H., & Jurkunas, U. V. (2016). Menadione-Induced DNA Damage Leads to Mitochondrial Dysfunction and Fragmentation During Rosette Formation in Fuchs Endothelial Corneal Dystrophy. *Antioxidants & Redox Signaling*, *24*(18), 1072–1083. https://doi.org/10.1089/ars.2015.6532

Hausenloy, D. J., & Yellon, D. M. (2013). Myocardial ischemia-reperfusion injury: A neglected therapeutic target. *The Journal of Clinical Investigation*, *123*(1), 92–100. https://doi.org/10.1172/JCI62874

Heianza, Y., Ma, W., Manson, J. E., Rexrode, K. M., & Qi, L. (2017). Gut Microbiota Metabolites and Risk of Major Adverse Cardiovascular Disease Events and Death: A Systematic Review and Meta-Analysis of Prospective Studies. *Journal of the American Heart Association*, *6*(7), e004947. https://doi.org/10.1161/JAHA.116.004947

Henninger, C., & Fritz, G. (2017). Statins in anthracycline-induced cardiotoxicity: Rac and Rho, and the heartbreakers. *Cell Death & Disease*, *8*(1), e2564. https://doi.org/10.1038/cddis.2016.418

Heusch, G. (2020). Myocardial ischaemia–reperfusion injury and cardioprotection in perspective. *Nature Reviews Cardiology*, *17*(12), 773–789. https://doi.org/10.1038/s41569-020-0403-y

Hoyles, L., Jiménez-Pranteda, M. L., Chilloux, J., Brial, F., Myridakis, A., Aranias, T., Magnan, C., Gibson, G. R., Sanderson, J. D., Nicholson, J. K., Gauguier, D., McCartney, A. L., & Dumas, M.-E. (2018). *Metabolic retroconversion of trimethylamine N-oxide and the gut microbiota*. 1–14. https://doi.org/10.1186/s40168-018-0461-0

Huc, T., Drapala, A., Gawrys, M., Konop, M., Bielinska, K., Zaorska, E., Samborowska, E., Wyczalkowska-Tomasik, A., Pączek, L., Dadlez, M., & Ufnal, M. (2018). Chronic, low-dose TMAO treatment reduces diastolic dysfunction and heart fibrosis in hypertensive rats. *American Journal of Physiology. Heart and Circulatory Physiology*, *315*(6), H1805–H1820. https://doi.org/10.1152/ajpheart.00536.2018

Incalza, M. A., D'Oria, R., Natalicchio, A., Perrini, S., Laviola, L., & Giorgino, F. (2018). Oxidative stress and reactive oxygen species in endothelial dysfunction associated with cardiovascular and metabolic diseases. *Vascular Pharmacology*, *100*, 1–19. https://doi.org/10.1016/j.vph.2017.05.005

Jameson, E., Quareshy, M., & Chen, Y. (2018). Methodological considerations for the identification of choline and carnitine-degrading bacteria in the gut. *Methods (San Diego, Calif.)*, *149*, 42–48. https://doi.org/10.1016/j.ymeth.2018.03.012

Janeiro, M. H., Ramírez, M. J., Milagro, F. I., Martínez, J. A., & Solas, M. (2018). Implication of Trimethylamine N-Oxide (TMAO) in Disease: Potential Biomarker or New Therapeutic Target. *Nutrients*, *10*(10). https://doi.org/10.3390/nu10101398

Jaworska, K., Hering, D., Mosieniak, G., Bielak-Zmijewska, A., Pilz, M., Konwerski, M., Gasecka, A., Kapłon-Cieślicka, A., Filipiak, K., Sikora, E., Hołyst, R., & Ufnal, M. (2019). TMA, A Forgotten Uremic Toxin, but Not TMAO, Is Involved in Cardiovascular Pathology. *Toxins*, *11*(9). https://doi.org/10.3390/toxins11090490

Jl, L., V, B., Y, Z., & Ra, S. (2013). Endothelial nitric-oxide synthase activation generates an inducible nitric-oxide synthase-like output of nitric oxide in inflamed endothelium. *The Journal of Biological Chemistry*, *288*(6). https://doi.org/10.1074/jbc.M112.436022

Kalogeris, T., Baines, C. P., Krenz, M., & Korthuis, R. J. (2012). Cell Biology of Ischemia/Reperfusion Injury. *International review of cell and molecular biology*, *298*, 229–317. https://doi.org/10.1016/B978-0-12-394309-5.00006-7

Kazemian, N., Mahmoudi, M., Halperin, F., Wu, J. C., & Pakpour, S. (2020). Gut microbiota and cardiovascular disease: Opportunities and challenges. *Microbiome*, *8*(1), 36. https://doi.org/10.1186/s40168-020-00821-0

Kiouptsi, K., Ruf, W., & Reinhardt, C. (2018). Microbiota-Derived Trimethylamine. *Circulation Research*, *123*(10), 1112–1114. https://doi.org/10.1161/CIRCRESAHA.118.314039

Koeth, R. A., Wang, Z., Levison, B. S., Buffa, J. A., Org, E., Sheehy, B. T., Britt, E. B., Fu, X., Wu, Y., Li, L., Smith, J. D., DiDonato, J. A., Chen, J., Li, H., Wu, G. D., Lewis, J. D., Warrier, M., Brown, J. M., Krauss, R. M., … Hazen, S. L. (2013). Intestinal microbiota metabolism of L-carnitine, a nutrient in red meat, promotes atherosclerosis. *Nature medicine*, *19*(5), 576–585. https://doi.org/10.1038/nm.3145

Kolluru, G. K., Siamwala, J. H., & Chatterjee, S. (2010). ENOS phosphorylation in health and disease. *Biochimie*, *92*(9), 1186–1198. https://doi.org/10.1016/j.biochi.2010.03.020

Kondo, T., Nakano, Y., Adachi, S., & Murohara, T. (2019). Effects of Tobacco Smoking on Cardiovascular Disease. *Circulation Journal: Official Journal of the Japanese Circulation Society*, *83*(10), 1980–1985. https://doi.org/10.1253/circj.CJ-19-0323

Konopelski, P., Chabowski, D., Aleksandrowicz, M., Kozniewska, E., Podsadni, P., Szczepanska, A., & Ufnal, M. (2021). Indole-3-propionic acid, a tryptophan-derived bacterial metabolite, increases blood pressure via cardiac and vascular mechanisms

in rats. *American Journal of Physiology-Regulatory, Integrative and Comparative Physiology*. https://doi.org/10.1152/ajpregu.00142.2021

Kossenjans, W., Rymaszewski, Z., Barankiewicz, J., Bobst, A., & Ashraf, M. (1996). Menadione-induced oxidative stress in bovine heart microvascular endothelial cells. *Microcirculation (New York, N.Y.: 1994)*, *3*(1), 39–47. https://doi.org/10.3109/10739689609146781

Lang, D. H., Yeung, C. K., Peter, R. M., Ibarra, C., Gasser, R., Itagaki, K., Philpot, R. M., & Rettie, A. E. (1998). Isoform specificity of trimethylamine N-oxygenation by human flavin-containing monooxygenase (FMO) and P450 enzymes: Selective catalysis by FMO3. *Biochemical Pharmacology*, *56*(8), 1005–1012. https://doi.org/10.1016/s0006-2952(98)00218-4

Lavie, C. J., Ozemek, C., Carbone, S., Katzmarzyk, P. T., & Blair, S. N. (2019). Sedentary Behavior, Exercise, and Cardiovascular Health. *Circulation Research*, *124*(5), 799–815. https://doi.org/10.1161/CIRCRESAHA.118.312669

Lee, J. Y., Bae, O. N., Chung, S. M., Lee, M. Y., & Chung, J. H. (2001). Menadione induces endothelial dysfunction mediated by oxidative stress and arylation. *Chemico-Biological Interactions*, *137*(2), 169–183. https://doi.org/10.1016/s0009-2797(01)00235-6

Lee, J. Y., Lee, M. Y., Chung, S. M., & Chung, J. H. (1999). Menadione-induced vascular endothelial dysfunction and its possible significance. *Toxicology and Applied Pharmacology*, *161*(2), 140–145. https://doi.org/10.1006/taap.1999.8795

Li, T., Chen, Y., Gua, C., & Li, X. (2017). Elevated Circulating Trimethylamine N-Oxide Levels Contribute to Endothelial Dysfunction in Aged Rats through Vascular Inflammation and Oxidative Stress. *Frontiers in Physiology*, *8*. https://doi.org/10.3389/fphys.2017.00350

Li, X., Geng, J., Zhao, J., Ni, Q., Zhao, C., Zheng, Y., Chen, X., & Wang, L. (2019). Trimethylamine N-Oxide Exacerbates Cardiac Fibrosis via Activating the NLRP3 Inflammasome. *Frontiers in Physiology*, *10*, 866. https://doi.org/10.3389/fphys.2019.00866

Louch, W. E., Ferrier, G. R., & Howlett, S. E. (2002). Changes in excitation-contraction coupling in an isolated ventricular myocyte model of cardiac stunning. *American Journal of Physiology-Heart and Circulatory Physiology*, *283*(2), H800–H810. https://doi.org/10.1152/ajpheart.00020.2002

Lovatt, M., Adnan, K., Peh, G. S. L., & Mehta, J. S. (2018). Regulation of Oxidative Stress in Corneal Endothelial Cells by Prdx6. *Antioxidants (Basel, Switzerland)*, *7*(12), E180. https://doi.org/10.3390/antiox7120180

Lundberg, J. O., Weitzberg, E., & Gladwin, M. T. (2008). The nitrate–nitrite–nitric oxide pathway in physiology and therapeutics. *Nature Reviews Drug Discovery*, *7*(2), 156–167. https://doi.org/10.1038/nrd2466

Ma, G., Pan, B., Chen, Y., Guo, C., Zhao, M., Zheng, L., & Chen, B. (2017). Trimethylamine N-oxide in atherogenesis: Impairing endothelial self-repair capacity and enhancing monocyte adhesion. *Bioscience Reports*, *37*(2). https://doi.org/10.1042/BSR20160244

Martínez-González, M. A., Gea, A., & Ruiz-Canela, M. (2019). The Mediterranean Diet and Cardiovascular Health. *Circulation Research*, *124*(5), 779–798. https://doi.org/10.1161/CIRCRESAHA.118.313348

May, J. M., Qu, Z., & Li, X. (2003). Ascorbic acid blunts oxidant stress due to menadione in endothelial cells. *Archives of Biochemistry and Biophysics*, *411*(1), 136–144. https://doi.org/10.1016/s0003-9861(02)00715-4

Méjean, V., Lobbi-Nivol, C., Lepelletier, M., Giordano, G., Chippaux, M., & Pascal, M.-C. (1994). TMAO anaerobic respiration in Escherichia coli: Involvement of the tor operon. *Molecular Microbiology*, *11*(6), 1169–1179. https://doi.org/10.1111/j.1365-2958.1994.tb00393.x

Mitchell, S. C., & Smith, R. L. (2003). Trimethylamine and odorous sweat. *Journal of Inherited Metabolic Disease*, *26*(4), 415–416. https://doi.org/10.1023/a:1025179708708

Mitchell, S. C., & Smith, R. L. (2016). Trimethylamine-The Extracorporeal Envoy. *Chemical Senses*, *41*(4), 275–279. https://doi.org/10.1093/chemse/bjw001

Miyake, T., Mizuno, T., Mochizuki, T., Kimura, M., Matsuki, S., Irie, S., Ieiri, I., Maeda, K., & Kusuhara, H. (2017). Involvement of Organic Cation Transporters in the Kinetics of Trimethylamine N-oxide. *Journal of Pharmaceutical Sciences*, *106*(9), 2542–2550. https://doi.org/10.1016/j.xphs.2017.04.067

Murabito, A., Hirsch, E., & Ghigo, A. (2020). Mechanisms of Anthracycline-Induced Cardiotoxicity: Is Mitochondrial Dysfunction the Answer? *Frontiers in Cardiovascular Medicine*, *7*, 35. https://doi.org/10.3389/fcvm.2020.00035

National Research Council (US) Committee for the Update of the Guide for the Care and Use of Laboratory Animals. (2011). *Guide for the Care and Use of Laboratory Animals* (8th ed.). National Academies Press (US). http://www.ncbi.nlm.nih.gov/books/NBK54050/

Negri, S., Faris, P., Pellavio, G., Botta, L., Orgiu, M., Forcaia, G., Sancini, G., Laforenza, U., & Moccia, F. (2020). Group 1 metabotropic glutamate receptors trigger glutamate-induced intracellular Ca2+ signals and nitric oxide release in human brain microvascular endothelial cells. *Cellular and Molecular Life Sciences: CMLS*, *77*(11), 2235–2253. https://doi.org/10.1007/s00018-019-03284-1

Noutsias, M., & Maisch, B. (2011). Treatment of cardiovascular diseases in cancer patients. *Herz*, *36*(4), 340–345. https://doi.org/10.1007/s00059-011-3452-5

Novakovic, M., Rout, A., Kingsley, T., Kirchoff, R., Singh, A., Verma, V., Kant, R., & Chaudhary, R. (2020). Role of gut microbiota in cardiovascular diseases. *World Journal of Cardiology*, *12*(4), 110–122. https://doi.org/10.4330/wjc.v12.i4.110

Oakley, C. I., Vallejo, J. A., Wang, D., Gray, M. A., Tiede-Lewis, L. M., Shawgo, T., Daon, E., Zorn, G., Stubbs, J. R., & Wacker, M. J. (2020). Trimethylamine-N-oxide acutely increases cardiac muscle contractility. *American Journal of Physiology. Heart and Circulatory Physiology*, *318*(5), H1272–H1282. https://doi.org/10.1152/ajpheart.00507.2019

Organ, C. L., Otsuka, H., Bhushan, S., Wang, Z., Bradley, J., Trivedi, R., Polhemus, D. J., Tang, W. H. W., Wu, Y., Hazen, S. L., & Lefer, D. J. (2016). Choline Diet and Its Gut Microbe-Derived Metabolite, Trimethylamine N-Oxide, Exacerbate Pressure Overload-Induced Heart Failure. *Circulation. Heart Failure*, *9*(1), e002314. https://doi.org/10.1161/CIRCHEARTFAILURE.115.002314

Penna, C., Granata, R., Tocchetti, C. G., Gallo, M. P., Alloatti, G., & Pagliaro, P. (2015). Endogenous Cardioprotective Agents: Role in Pre and Postconditioning. *Current Drug Targets*, *16*(8), 843–867. https://doi.org/10.2174/1389450116666150309115536

Querio, G., Antoniotti, S., Geddo, F., Tullio, F., Penna, C., Pagliaro, P., & Gallo, M. P. (2021). Ischemic heart disease and cardioprotection: Focus on estrogenic hormonal setting and microvascular health. *Vascular Pharmacology*, *141*, 106921. https://doi.org/10.1016/j.vph.2021.106921

Querio, G., Antoniotti, S., Levi, R., & Gallo, M. P. (2019). Trimethylamine N-Oxide Does Not Impact Viability, ROS Production, and Mitochondrial Membrane Potential of Adult Rat Cardiomyocytes. *International Journal of Molecular Sciences*, *20*(12). https://doi.org/10.3390/ijms20123045

Querio, G., Geddo, F., Antoniotti, S., Gallo, M. P., & Penna, C. (2021). Sex and Response to Cardioprotective Conditioning Maneuvers. *Frontiers in Physiology*, *12*, 667961. https://doi.org/10.3389/fphys.2021.667961

Rajakovich, L. J., Fu, B., Bollenbach, M., & Balskus, E. P. (2021). Elucidation of an anaerobic pathway for metabolism of l-carnitine–derived γ-butyrobetaine to trimethylamine in human gut bacteria. *Proceedings of the National Academy of Sciences*, *118*(32). https://doi.org/10.1073/pnas.2101498118

Rath, S., Heidrich, B., Pieper, D. H., & Vital, M. (2017). Uncovering the trimethylamine-producing bacteria of the human gut microbiota. *Microbiome*, *5*(1), 54. https://doi.org/10.1186/s40168-017-0271-9

Roddy, D., McCarthy, P., Nerney, D., Mulligan-Rabbitt, J., Smith, E., & Treacy, E. P. (2020). Impact of trimethylaminuria on daily psychosocial functioning. *JIMD Reports*, *57*(1), 67–75. https://doi.org/10.1002/jmd2.12170

Rowland, I., Gibson, G., Heinken, A., Scott, K., Swann, J., Thiele, I., & Tuohy, K. (2018). Gut microbiota functions: Metabolism of nutrients and other food components. *European Journal of Nutrition*, *57*(1), 1–24. https://doi.org/10.1007/s00394-017-1445-8

Rozenberg, M., Loewenschuss, A., & Nielsen, C. J. (2012). H-Bonded Clusters in the Trimethylamine/Water System: A Matrix Isolation and Computational Study. *The Journal of Physical Chemistry A*, *116*(16), 4089–4096. https://doi.org/10.1021/jp3020035

Saleh, Y., Abdelkarim, O., Herzallah, K., & Abela, G. S. (2021). Anthracycline-induced cardiotoxicity: Mechanisms of action, incidence, risk factors, prevention, and treatment. *Heart Failure Reviews*, *26*(5), 1159–1173. https://doi.org/10.1007/s10741-020-09968-2

Samodelov, S. L., Kullak-Ublick, G. A., Gai, Z., & Visentin, M. (2020). Organic Cation Transporters in Human Physiology, Pharmacology, and Toxicology. *International Journal of Molecular Sciences*, *21*(21), E7890. https://doi.org/10.3390/ijms21217890

Savi, M., Bocchi, L., Bresciani, L., Falco, A., Quaini, F., Mena, P., Brighenti, F., Crozier, A., Stilli, D., & Del Rio, D. (2018). Trimethylamine-N-Oxide (TMAO)-Induced Impairment of Cardiomyocyte Function and the Protective Role of Urolithin B-Glucuronide. *Molecules (Basel, Switzerland)*, *23*(3). https://doi.org/10.3390/molecules23030549

Schiffer, T. A., Lundberg, J. O., Weitzberg, E., & Carlström, M. (2020). Modulation of mitochondria and NADPH oxidase function by the nitrate-nitrite-NO pathway in metabolic disease with focus on type 2 diabetes. *Biochimica Et Biophysica Acta. Molecular Basis of Disease*, *1866*(8), 165811. https://doi.org/10.1016/j.bbadis.2020.165811

Schmidt, A. C., & Leroux, J.-C. (2020). Treatments of trimethylaminuria: Where we are and where we might be heading. *Drug Discovery Today*, *25*(9), 1710–1717. https://doi.org/10.1016/j.drudis.2020.06.026

Seldin, M. M., Meng, Y., Qi, H., Zhu, W., Wang, Z., Hazen, S. L., Lusis, A. J., & Shih, D. M. (2016). Trimethylamine N-Oxide Promotes Vascular Inflammation Through Signaling of Mitogen-Activated Protein Kinase and Nuclear Factor-κB. *Journal of the American Heart Association: Cardiovascular and Cerebrovascular Disease*, *5*(2). https://doi.org/10.1161/JAHA.115.002767

Simó, C., & García-Cañas, V. (2020). Dietary bioactive ingredients to modulate the gut microbiota-derived metabolite TMAO. New opportunities for functional food development. *Food & Function*, *11*(8), 6745–6776. https://doi.org/10.1039/D0FO01237H

Songbo, M., Lang, H., Xinyong, C., Bin, X., Ping, Z., & Liang, S. (2019). Oxidative stress injury in doxorubicin-induced cardiotoxicity. *Toxicology Letters*, *307*, 41–48. https://doi.org/10.1016/j.toxlet.2019.02.013

Strassheim, D., Verin, A., Batori, R., Nijmeh, H., Burns, N., Kovacs-Kasa, A., Umapathy, N. S., Kotamarthi, J., Gokhale, Y. S., Karoor, V., Stenmark, K. R., & Gerasimovskaya, E. (2020). P2Y Purinergic Receptors, Endothelial Dysfunction, and Cardiovascular Diseases. *International Journal of Molecular Sciences*, *21*(18), E6855. https://doi.org/10.3390/ijms21186855

Sun, X., Jiao, X., Ma, Y., Liu, Y., Zhang, L., He, Y., & Chen, Y. (2016). Trimethylamine N-oxide induces inflammation and endothelial dysfunction in human umbilical vein endothelial cells via activating ROS-TXNIP-NLRP3 inflammasome. *Biochemical and Biophysical Research Communications*, *481*(1–2), 63–70. https://doi.org/10.1016/j.bbrc.2016.11.017

Tang, W. H. W., Kitai, T., & Hazen, S. L. (2017). Gut Microbiota in Cardiovascular Health and Disease. *Circulation Research*, *120*(7), 1183–1196. https://doi.org/10.1161/CIRCRESAHA.117.309715

Tang, W. H. W., Wang, Z., Levison, B. S., Koeth, R. A., Britt, E. B., Fu, X., Wu, Y., & Hazen, S. L. (2013). Intestinal microbial metabolism of phosphatidylcholine and cardiovascular risk. *The New England Journal of Medicine*, *368*(17), 1575–1584. https://doi.org/10.1056/NEJMoa1109400

Tang, W. H. W., Wang, Z., Shrestha, K., Borowski, A. G., Wu, Y., Troughton, R. W., Klein, A. L., & Hazen, S. L. (2015). Intestinal microbiota-dependent phosphatidylcholine metabolites, diastolic dysfunction, and adverse clinical outcomes in chronic systolic heart failure. *Journal of Cardiac Failure*, *21*(2), 91–96. https://doi.org/10.1016/j.cardfail.2014.11.006

Teft, W. A., Morse, B. L., Leake, B. F., Wilson, A., Mansell, S. E., Hegele, R. A., Ho, R. H., & Kim, R. B. (2017). Identification and Characterization of Trimethylamine-N-oxide Uptake and Efflux Transporters. *Molecular Pharmaceutics*, *14*(1), 310–318. https://doi.org/10.1021/acs.molpharmaceut.6b00937

Temple, N. J., Guercio, V., & Tavani, A. (2019). The Mediterranean Diet and Cardiovascular Disease: Gaps in the Evidence and Research Challenges. *Cardiology in Review*, *27*(3), 127–130. https://doi.org/10.1097/CRD.0000000000000222

Thomas, M. S., & Fernandez, M. L. (2021). Trimethylamine N-Oxide (TMAO), Diet and Cardiovascular Disease. *Current Atherosclerosis Reports*, *23*(4), 12. https://doi.org/10.1007/s11883-021-00910-x

Thomas, N. O., Shay, K. P., Kelley, A. R., Butler, J. A., & Hagen, T. M. (2016). Glutathione maintenance mitigates age-related susceptibility to redox cycling agents. *Redox Biology*, *10*, 45–52. https://doi.org/10.1016/j.redox.2016.09.010

Townsend, N., Kazakiewicz, D., Lucy Wright, F., Timmis, A., Huculeci, R., Torbica, A., Gale, C. P., Achenbach, S., Weidinger, F., & Vardas, P. (2021). Epidemiology of cardiovascular disease in Europe. *Nature Reviews. Cardiology*. https://doi.org/10.1038/s41569-021-00607-3

Treberg, J. R. (2006). The accumulation of methylamine counteracting solutes in elasmobranchs with differing levels of urea: A comparison of marine and freshwater species. *Journal of Experimental Biology*, *209*(5), 860–870. https://doi.org/10.1242/jeb.02055

Ufnal, M. (2020). Trimethylamine, a Toxic Precursor of Trimethylamine Oxide, Lost in Medical Databases. *The Journal of Nutrition*, *150*(2), 419. https://doi.org/10.1093/jn/nxz265

Ufnal, M., Zadlo, A., & Ostaszewski, R. (2015). TMAO: A small molecule of great expectations. *Nutrition*, *31*(11), 1317–1323. https://doi.org/10.1016/j.nut.2015.05.006

Videja, M., Vilskersts, R., Korzh, S., Cirule, H., Sevostjanovs, E., Dambrova, M., & Makrecka-Kuka, M. (2020). Microbiota-Derived Metabolite Trimethylamine N-Oxide Protects Mitochondrial Energy Metabolism and Cardiac Functionality in a Rat Model of Right Ventricle Heart Failure. *Frontiers in Cell and Developmental Biology*, *8*, 622741. https://doi.org/10.3389/fcell.2020.622741

Wallrabenstein, I., Kuklan, J., Weber, L., Zborala, S., Werner, M., Altmüller, J., Becker, C., Schmidt, A., Hatt, H., Hummel, T., & Gisselmann, G. (2013). Human Trace Amine-Associated Receptor TAAR5 Can Be Activated by Trimethylamine. *PLoS ONE*, *8*(2), e54950. https://doi.org/10.1371/journal.pone.0054950

Witkowski, M., Weeks, T. L., & Hazen, S. L. (2020). Gut Microbiota and Cardiovascular Disease. *Circulation Research*, *127*(4), 553–570. https://doi.org/10.1161/CIRCRESAHA.120.316242

Yamamoto, K., Imamura, H., & Ando, J. (2018). Shear stress augments mitochondrial ATP generation that triggers ATP release and Ca2+ signaling in vascular endothelial cells. *American Journal of Physiology - Heart and Circulatory Physiology*, *315*(5), H1477–H1485. https://doi.org/10.1152/ajpheart.00204.2018

Zeisel, S. H., & Warrier, M. (2017). Trimethylamine N-Oxide, the Microbiome, and Heart and Kidney Disease. *Annual Review of Nutrition*, *37*, 157–181. https://doi.org/10.1146/annurev-nutr-071816-064732

Zhang, Z., Mocanu, V., Cai, C., Dang, J., Slater, L., Deehan, E. C., Walter, J., & Madsen, K. L. (2019). Impact of Fecal Microbiota Transplantation on Obesity and Metabolic Syndrome—A Systematic Review. *Nutrients*, *11*(10), 2291. https://doi.org/10.3390/nu11102291

Zhao, Y., Vanhoutte, P. M., & Leung, S. W. S. (2015). Vascular nitric oxide: Beyond eNOS. *Journal of Pharmacological Sciences*, *129*(2), 83–94. https://doi.org/10.1016/j.jphs.2015.09.002

Zhu, W., Gregory, J. C., Org, E., Buffa, J. A., Gupta, N., Wang, Z., Li, L., Fu, X., Wu, Y., Mehrabian, M., Sartor, R. B., McIntyre, T. M., Silverstein, R. L., Tang, W. H. W., DiDonato, J. A., Brown, J. M., Lusis, A. J., & Hazen, S. L. (2016). Gut Microbial Metabolite TMAO Enhances Platelet Hyperreactivity and Thrombosis Risk. *Cell*, *165*(1), 111–124. https://doi.org/10.1016/j.cell.2016.02.011

Zununi Vahed, S., Barzegari, A., Zuluaga, M., Letourneur, D., & Pavon-Djavid, G. (2018). Myocardial infarction and gut microbiota: An incidental connection. *Pharmacological Research*, *129*, 308–317. https://doi.org/10.1016/j.phrs.2017.11.008

International Journal of
Molecular Sciences

MDPI

Article

Trimethylamine N-Oxide Does Not Impact Viability, ROS Production, and Mitochondrial Membrane Potential of Adult Rat Cardiomyocytes

Giulia Querio, Susanna Antoniotti, Renzo Levi and Maria Pia Gallo *

Department of Life Sciences and Systems Biology, University of Turin, Via Accademia Albertina 13, 10123 Turin, Italy; giulia.querio@unito.it (G.Q.); susanna.antoniotti@unito.it (S.A.); renzo.levi@unito.it (R.L.)
* Correspondence: mariapia.gallo@unito.it; Tel.: +39-011-670-4671

Received: 17 May 2019; Accepted: 19 June 2019; Published: 21 June 2019

Abstract: Trimethylamine N-oxide (TMAO) is an organic compound derived from dietary choline and L-carnitine. It behaves as an osmolyte, a protein stabilizer, and an electron acceptor, showing different biological functions in different animals. Recent works point out that, in humans, high circulating levels of TMAO are related to the progression of atherosclerosis and other cardiovascular diseases. However, studies on a direct role of TMAO in cardiomyocyte parameters are still limited. The purpose of this work is to study the effects of TMAO on isolated adult rat cardiomyocytes. TMAO in both 100 μM and 10 mM concentrations, from 1 to 24 h of treatment, does not affect cell viability, sarcomere length, intracellular ROS, and mitochondrial membrane potential. Furthermore, the simultaneous treatment with TMAO and known cardiac insults, such as H_2O_2 or doxorubicin, does not affect the treatment's effect. In conclusion, TMAO cannot be considered a direct cause or an exacerbating risk factor of cardiac damage at the cellular level in acute conditions.

Keywords: trimethylamine N-oxide; cardiomyocytes; cardiotoxicity; ROS; mitochondrial membrane potential

1. Introduction

Trimethylamine N-oxide (TMAO) is an amine oxide directly introduced through diet or synthetized from its precursors, primarily L-carnitine and choline, that are transformed into trimethylamine (TMA) by the gut microbiota. Once absorbed, TMA in most mammals is oxidized by hepatic FMOs to form TMAO which enters the systemic circulation. Several studies illustrate different biological functions of TMAO in other animals. In elasmobranchs and deep-sea fishes, it acts as an osmolyte able to counteract either osmotic or hydrostatic pressure. It is a protein stabilizer preserving protein folding and it also acts as an electron acceptor balancing oxidative stress [1,2]. TMAO is also reduced to TMA in the anaerobic metabolism of a number of bacteria. Although TMAO is involved in several reactions within cells, recent studies highlight its detrimental role when present in high plasmatic concentrations in some mammals. In fact, TMAO seems to be involved in accelerating endothelial cell senescence, enhancing vascular inflammation and oxidative stress [3,4]; it also could be involved in the stimulation of platelet hyperreactivity and in the onset of thrombosis, exacerbating atherosclerotic lesions [5]. Several studies also underline the role of TMAO in the pathogenesis of type 2 diabetes mellitus [6]. There are limited data on its function in mediating direct cardiac injuries, and those studies are mainly focused on its role in the impairment of mitochondrial metabolism [7] and calcium handling [8]. On the contrary, recent papers are re-evaluating the role of TMAO, underlining the emerging debate on its direct effect in causing or exacerbating cardiovascular diseases (CVD) [9,10]. First criticisms point out that populations having diets with high concentrations of TMAO, like those rich in fish products, when

compared to Western diets rich in its precursors, have reduced risks of CVD or diseases assumed to be related to high TMAO plasma levels [11]. Another study demonstrates that TMAO does not affect macrophage foam cell formation and lesion progression in $ApoE^{-/-}$ mice expressing human cholesteryl ester transfer protein, suggesting that the molecule does not worsen atherosclerosis [12]. Furthermore, administration of TMAO seems to improve symptoms related to streptozotocin-induced diabetes in rats and mice, highlighting no direct contribution of the molecule in exacerbating this condition [13]. Finally, data about TMAO plasma concentrations in healthy and pathological subjects are not clear: the lack of plasma concentration ranges of the molecule highlights the difficulties in referring to TMAO as a protective or a damaging factor in CVD. Starting from these conflicting considerations, the aim of this work was to evaluate for the first time the effect of TMAO in an in vitro model of adult rat cardiomyocytes exposed to different concentrations of the compound from 1 h to 24 h of treatment. To show whether TMAO exacerbates or reduces induced cell stress, cardiomyocytes were simultaneously treated with TMAO and H_2O_2 or doxorubicin (DOX). Investigations were focused on cell viability after TMAO or TMAO and stressors co-treatment, assessing cell morphology and functionality with α-actinin staining and specific probes that measure oxidative stress status and mitochondrial membrane potential.

2. Results

2.1. TMAO and Cell Viability

In order to investigate the effect of TMAO on cell viability, cardiomyocytes were treated with TMAO 100 μM, TMAO 10 mM, H_2O_2 50 μM, and H_2O_2 50 μM + TMAO 100 μM. After 1 h or 24 h of treatment, cardiomyocytes were labeled with propidium iodide (PI) and marked nuclei of suffering cells were detected by confocal microscopy at 568 nm. Concentrations used were taken from the literature: TMAO 100 μM is recognized as a marker of cardiovascular risk, TMAO 10 mM is over the physiological range and was tested here to detect any effect induced by high concentrations of the compound [14]. As shown in Figure 1a, there is no effect of TMAO 100 μM or TMAO 10 mM at either time of treatment, whereas H_2O_2, used here as a positive control, had effects only after 24 h. Simultaneous treatment with H_2O_2 and TMAO did not improve or worsen the effect of the stressor on cell viability (1 h—CTRL: 83.95 ± 6.59, n = 3, 52 cells; TMAO 100 μM: 85.52 ± 7.01, n = 5, 81 cells; TMAO 10 mM: 84.08 ± 5.84, n = 5, 92 cells; H_2O_2: 52.92 ± 16.46, n = 3, 56 cells; H_2O_2 + TMAO: 50.93 ± 18.50, n = 3, 58 cells. 24 h—CTRL: 83.42 ± 2.29, n = 3, 101 cells; TMAO 100 μM: 85.66 ± 6.48, n = 3, 91 cells; TMAO 10 mM: 62.22 ± 10.47, n = 3, 119 cells; H_2O_2: 2.38 ± 2.38, n = 3, 82 cells (*** $p < 0.001$); H_2O_2 + TMAO: 1.33 ± 1.33, n = 3, 41 cells (*** $p < 0.001$)). Figure 1b displays confocal images of cardiomyocytes from a representative experiment of PI staining after 24 h of treatment. White arrows point out PI-stained, damaged cardiomyocytes.

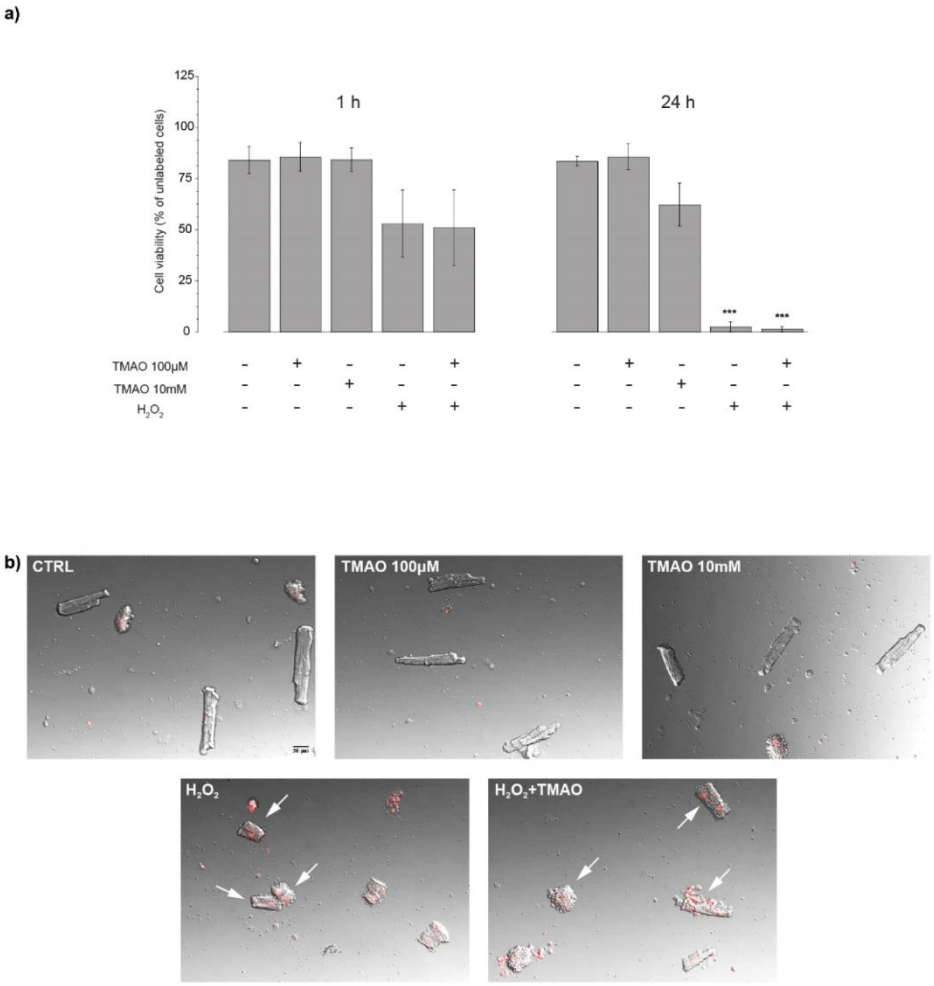

Figure 1. Cell viability after trimethylamine N-oxide (TMAO) exposure. (**a**) Bar graph of cell viability after 1 h and 24 h of treatment. Cell viability results reduced only after H_2O_2 treatment for 24 h, condition not improved or worsened by the simultaneous treatment with TMAO (refer to the main text for numerical values). (**b**) Merged images in bright field and fluorescence of cells treated for 24 h with TMAO 100 µM and TMAO 10 mM, H_2O_2, and H_2O_2+TMAO and labeled with propidium iodide (PI) (20× magnification). White arrows point out PI-stained, damaged cardiomyocytes.

2.2. TMAO and Sarcomere Length

To evaluate if TMAO was able to alter sarcomere structures after 24 h of treatment, sarcomere length was measured in α-actinin-stained cardiomyocytes. As shown in Figure 2, no changes in sarcomere length were observed in cells treated with TMAO, while H_2O_2 50 µM used as a positive control caused cardiomyocyte shrinkage, a condition that was not improved or worsened by the simultaneous treatment with TMAO. In cardiomyocytes treated with DOX 1 µM for 24 h, no sarcomere length variations were observed, because the DOX treatment in our model was designed to induce mild damage preceding cell shortening. Even so, TMAO 100 µM did not modify DOX-treated cardiomyocytes (sarcomere length in µm—CTRL: 1.69 ± 0.01, $n = 7$, 42 cells; TMAO 100 µM: 1.69 ± 0.01, $n = 6$, 34 cells; TMAO 10 mM: 1.67 ± 0.02, $n = 3$, 19 cells; H_2O_2: 1.22 ± 0.04, $n = 5$, 33 cells (*** $p < 0.001$); H_2O_2 + TMAO: 1.28 ± 0.03, $n = 3$, 24 cells (*** $p < 0.001$); DOX: 1.62 ± 0.02, $n = 3$, 16 cells; DOX + TMAO: 1.65 ± 0.01, $n = 3$, 15 cells).

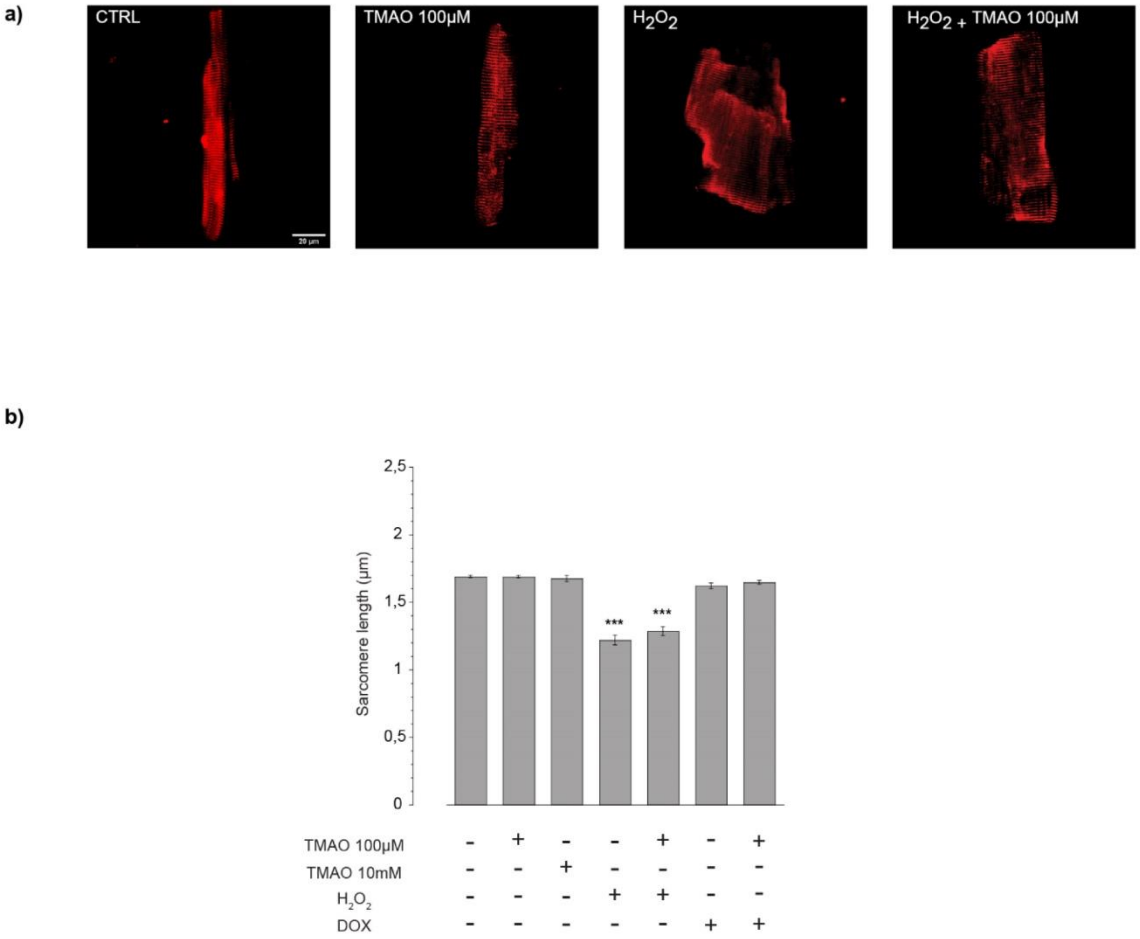

Figure 2. Sarcomere length after TMAO treatment. (**a**) Confocal microscopy images of fixed cells labeled for α-actinin protein (40× magnification). (**b**) Bar graph showing sarcomere length after 24 h of treatment with TMAO and other stressors: no cell shrinkage is measured when cells are exposed to different TMAO concentrations (refer to the main text for numerical values).

2.3. TMAO and Intracellular Reactive Oxygen Species (ROS)

In order to determine a variation in total ROS produced after treatment with TMAO for 1 h, 3 h, or 24 h, cells were labeled with the DCF-DA probe and its fluorescence was quantified and related to the control. As shown in Figure 3 (1 h, 3 h) and 4 (24 h), no fluorescence variations after TMAO treatment were detected at any concentration and time used. As a positive control, we employed DOX 1 μM for 24 h [15]; this drug caused a significant variation in ROS production with respect to the control condition. TMAO 100 μM did not modify ROS production in the DOX-treated cardiomyocytes (Figure 4) (1 h—TMAO 100 μM: 1.30 ± 0.21, n = 3, 34 cells; TMAO 10 mM: 1.32 ± 0.23, n = 3, 40 cells, vs. CTRL; 3 h—TMAO 100 μM: 0.96 ± 0.05, n = 3, 45 cells; TMAO 10 mM: 1.15 ± 0.09, n = 3, 52 cells, vs. CTRL; 24 h—TMAO 100 μM: 1.18 ± 0.04, n = 5, 40 cells; TMAO 10 mM: 1.24 ± 0.16, n = 3, 52 cells; DOX: 1.33 ± 0.11, n = 4, 21 cells (** $p < 0.01$); DOX+TMAO: 1.27 ± 0.01, n = 6, 31 cells (*** $p < 0.001$), vs. CTRL).

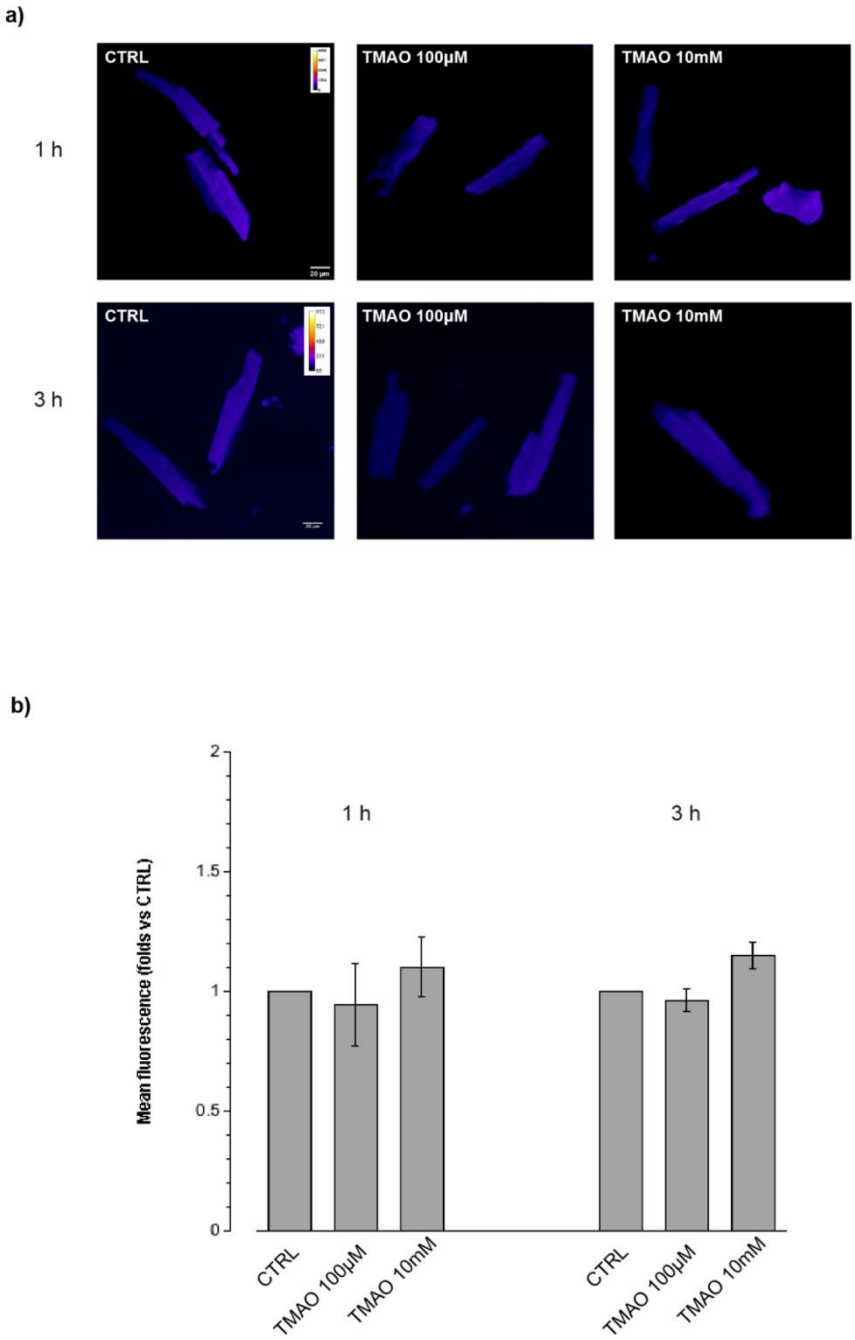

Figure 3. ROS production after 1 h and 3 h of treatment. (**a**) Confocal microscopy images of cells treated with TMAO 100 μM and TMAO 10 mM for 1 h and 3 h and labeled with the DCF-DA probe (60× magnification). (**b**) Bar graph showing mean fluorescence after 1 h and 3 h of treatment, no variations or ROS produced are detectable (refer to the main text for numerical values).

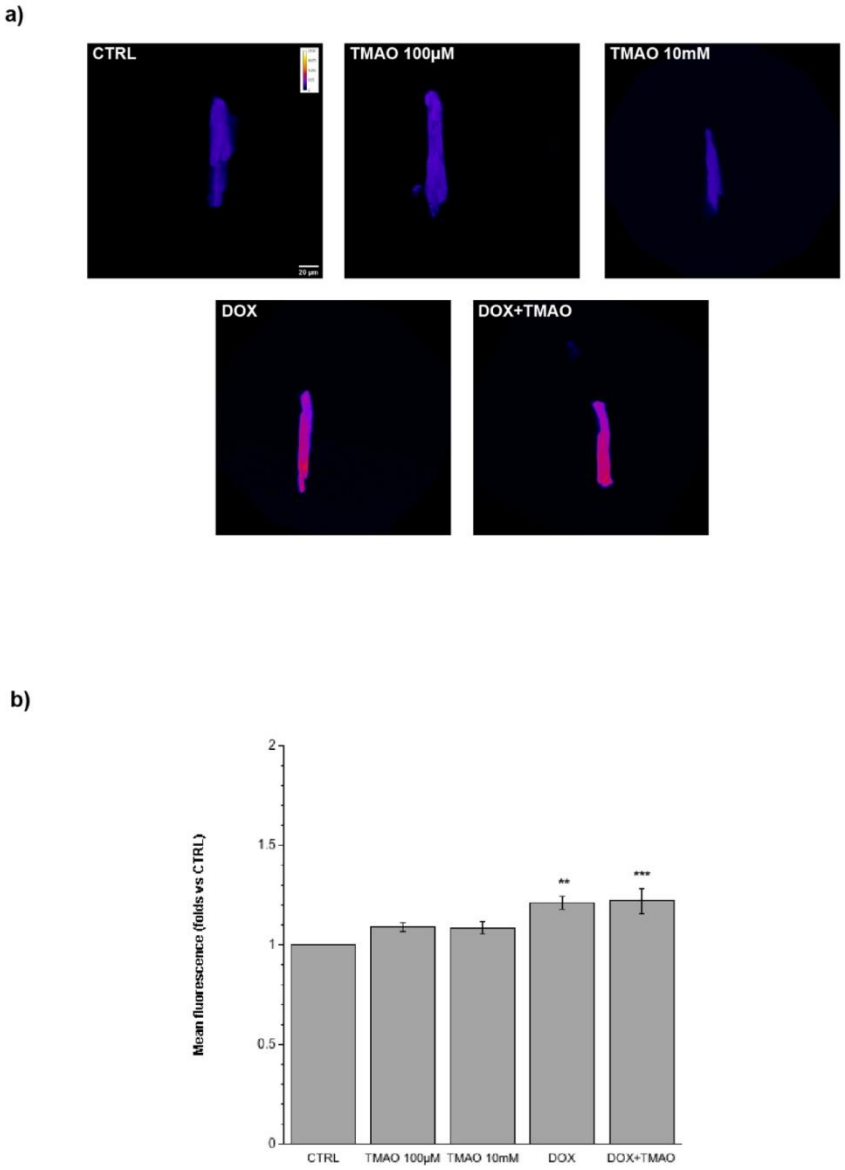

Figure 4. ROS production after 24 h of treatment. (**a**) Confocal microscopy images of cells treated with TMAO 100 µM and TMAO 10 mM for 24 h and labeled with the DCF-DA probe. In these experiments, doxorubicin (DOX) is used as a positive control (60× magnification). (**b**) Bar graph showing mean fluorescence after 24 h of treatment. No variations of ROS produced are detectable after TMAO treatment, and a small but significant increase is visible after DOX treatment (used here as a positive control); this increase is not changed by a simultaneous treatment with TMAO (refer to the main text for numerical values).

2.4. TMAO and Mitochondrial Membrane Potential

To investigate the potential metabolic damage induced by TMAO, cardiomyocytes treated with TMAO 100 µM and 10 mM for 1 h, 3 h, or 24 h were labeled with the JC-1 probe. Figure 5 (1 h, 3 h) and 6 (24 h) show variations in mitochondrial membrane potential (red/green fluorescence ratio) detected by confocal microscopy in living cells. TMAO treatment from 1 to 24 h did not cause any difference with respect to the control, indicating no mitochondrial effect of the molecule, whereas, as expected, DOX caused a depolarization of mitochondrial membrane potential after 24 h of treatment. TMAO 100 µM did not modify mitochondrial membrane potential in DOX-treated cardiomyocytes (Figure 6)

(1 h—TMAO 100 μM: 1.09 ± 0.08, n = 5, 65 cells; TMAO 10 mM: 1.11 ± 0.11, n = 3, 49 cells, vs. CTRL. 3 h—TMAO 100 μM: 1.02 ± 0.06, n = 3, 26 cells; TMAO 10 mM: 0.88 ± 0.05, n = 4, 39 cells, vs. CTRL; 24 h—TMAO 100 μM: 1.08 ± 0.11, n = 3, 21 cells; TMAO 10 mM: 0.95 ± 0.15, n = 3, 54 cells; DOX: 0.73 ± 0.02, n = 3, 24 cells (** $p < 0.01$); DOX + TMAO: 0.69 ± 0.05, n = 3, 22 cells (** $p < 0.01$), vs. CTRL).

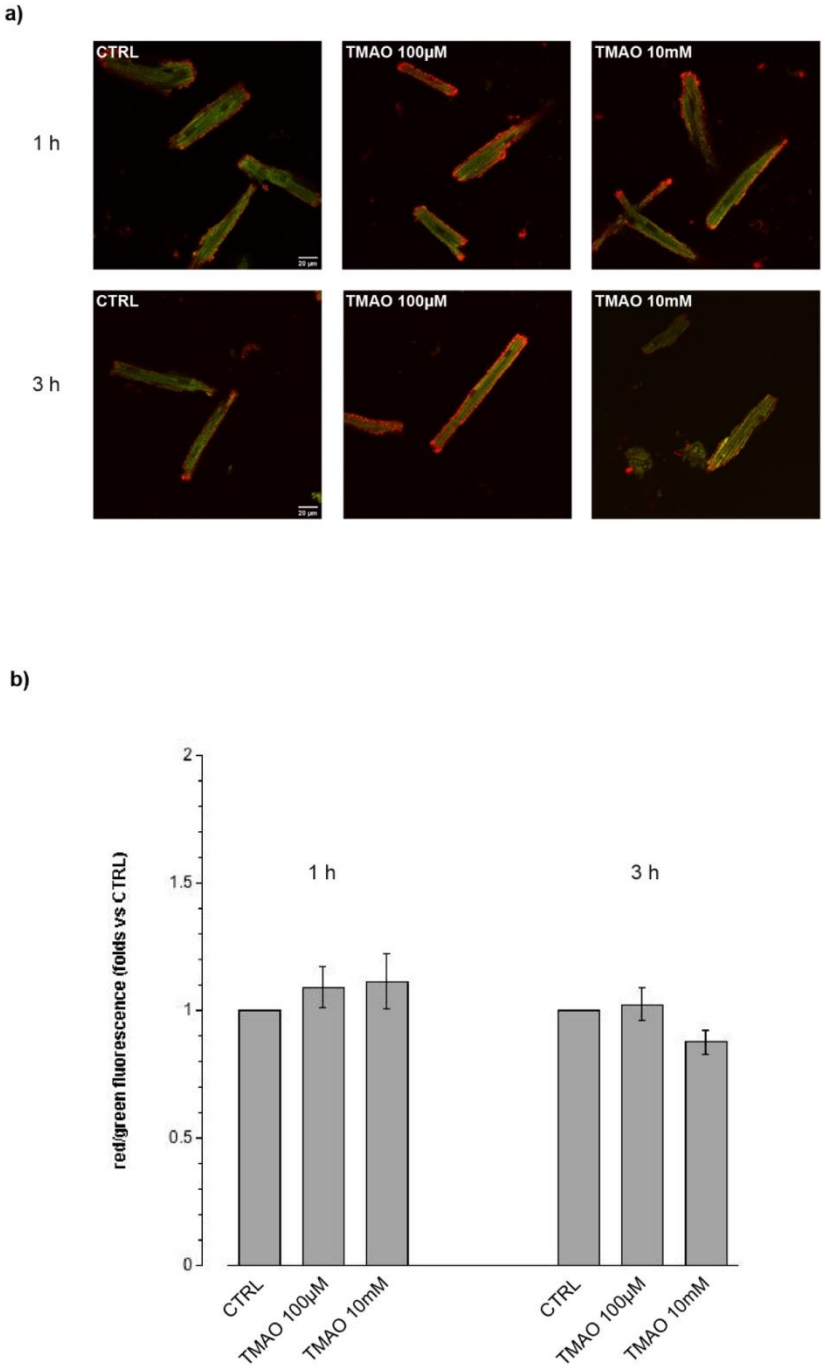

Figure 5. Mitochondrial membrane potential variation following 1 h and 3 h of treatment. (**a**) Confocal microscopy images of cells treated with TMAO 100 μM and TMAO 10 mM for 1 h and 3 h and labeled with the JC-1 probe (60× magnification). (**b**) Bar graph showing red/green fluorescence after 1 h and 3 h of treatment, no variations of mitochondrial membrane potential are detected (refer to the main text for numerical values).

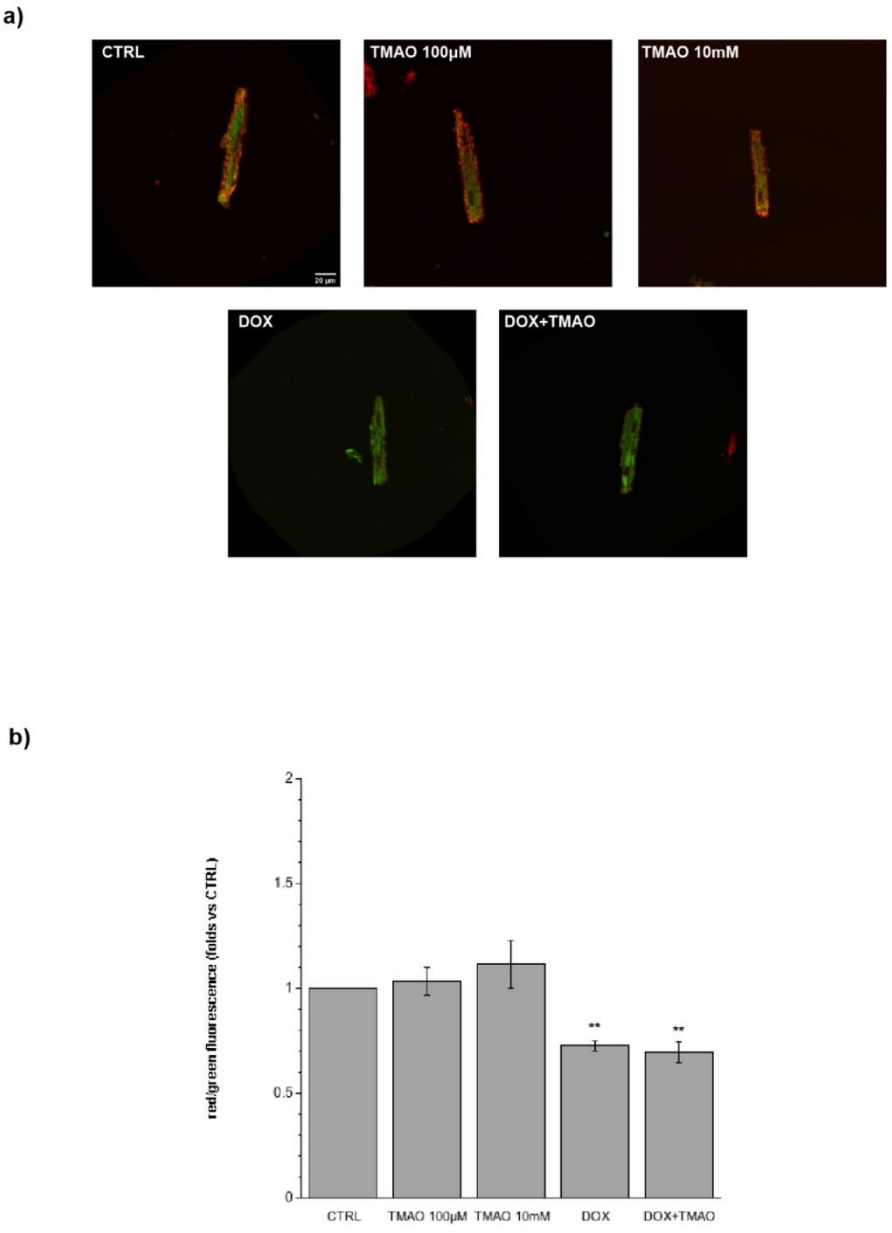

Figure 6. Mitochondrial membrane potential variation following 24 h treatment. (**a**) Confocal microscopy images of cells treated with TMAO 100 μM and TMAO 10 mM for 24 h and labeled with the JC-1 probe. In these experiments, doxorubicin (DOX) is used as a positive control (60× magnification). (**b**) Bar graph showing red/green fluorescence after 24 h of treatment, no variations of mitochondrial membrane potential are detected, a little but significant reduction of the ratio is visible after DOX treatment used here as a positive control, condition not changed in a simultaneous treatment with TMAO (refer to the main text for numerical values).

3. Discussion

This study provides novel insights into the physiological role of TMAO in isolated adult rat cardiomyocytes. Our findings do not show effects of TMAO on cell viability, sarcomere length, ROS production, and mitochondrial membrane potential within the range of concentration used. Moreover, we demonstrate that TMAO does not exacerbate or counteract the effect of known insults, such as H_2O_2 or doxorubicin, tested for up to 24 h of treatment. Taken together, these results suggest that

TMAO should not be considered a primary cause of acute cardiac damage and that the molecule could not revert or worsen existing risk factors of cardiac damage.

In the last few years, many studies suggest a strong relationship between diet, gut microbiota, and cardiovascular diseases [16]. In particular, some attention has been pointed to either TMAO directly coming from diet (fish), or produced from L-carnitine and choline conversion by gut microbiota into TMA and oxidized in the liver by FMO3 enzymes [14,17].

Experiments have mainly now focused on the role of TMAO in damaging endothelial cells. It has been described as upregulating cellular senescence, thereby reducing cell proliferation, increasing the expression of senescence markers, such as p53 and p21, and impairing cell migration [3]. TMAO also increases the oxidative stress of endothelial cells through a down-regulation of SIRT-1 and impairs NO production that causes endothelial dysfunction [4]. Hypertensive effects of TMAO have been evaluated by Ufnal and colleagues who demonstrated that TMAO has a role in stabilizing the action of Ang II and in prolonging its hypertensive effect, underlining the role of TMAO in stabilizing protein conformation and no direct role of the molecule in mediating hypertension [18]. Koeth and colleagues underlined the strong relationship between the high consumption of TMAO precursors, high TMAO plasma concentrations, and the development of atherosclerosis [19], while another study underlined the effect of the metabolite in enhancing platelet hyperreactivity and thrombosis risk in subjects with high TMAO plasma concentrations [5]. With respect to the cardiovascular effects of TMAO, Dambrova and collaborators showed that high plasma concentrations of the molecule are linked with increased body weight and insulin resistance and that it directly correlates with an augmented risk of diabetes [20].

Only a few studies are centered on the direct effect of the molecule on cardiac cells; in particular, they focus on the impairment of mitochondrial metabolism in the heart and underline TMAO as an agent that increases the severity of cardiovascular events or that enhances the progression of cardiovascular diseases [7]. Savi and colleagues showed a damaging effect of TMAO in cardiomyocytes because it worsens intracellular calcium handling with a reduced efficiency in the intracellular calcium removal and consequent loss in functionality of cardiac cells; furthermore, TMAO seems to alter energetic metabolism and to facilitate protein oxidative damage [8].

This scenario presents TMAO as either a marker or a direct agent involved in vascular and cardiac outcomes, but recent papers seem to oppose this point of view, highlighting uncertainty about the causative relation between TMAO and CVD [9]. The function of TMAO is still being debated, for example, the controversy surrounding fish-rich diets, because of the higher bioavailability of the compound in seafood products and their well-known role in lowering risk of CVD. Additionally, TMAO does not enhance atherosclerosis development because it seems not to be involved in foam cell formation even at higher concentrations than physiological ones [12], and there is no direct correlation between high plasma TMAO concentrations and coronary heart diseases [21,22]. Finally, findings by Huc et al. have also underlined a protective role of TMAO in reducing diastolic dysfunction and fibrosis in the pressure-overloaded heart [23].

The present study fits into this debate and the results presented agree with other works supporting TMAO as a non-damaging factor. In fact, it is well known that the loss of vital cardiac cells is a damaging condition that hampers primarily the functionality of the heart and has several aggravating responses also in peripheral tissues. Our first investigations underline no toxic effect in cardiomyocytes exposed to high concentrations of TMAO, highlighting the result that the molecule is not involved in inducing cardiac tissue cell loss, and no alterations of cardiac structure emerge from the evaluation of sarcomere length and cytoskeletal organization. Oxidative stress could be considered one of the causative factors of senescence in cells and one of the promoters of cardiometabolic reorganization in response to injury. With respect to TMAO as a possible inducer of ROS rising, both in a cytoplasmic and a mitochondrial environment, we show no variation in ROS production even after 24 h of treatment and we detect no depolarization of mitochondrial membrane potential, underlining the result of no direct influence by the molecule in inducing cardiac cell senescence.

4. Materials and Methods

4.1. Animal Care and Sacrifice

Experiments were performed on female adult rats which were allowed ad libitum access to tap water and standard rodent diet. The animals received human care in compliance with the Guide for the Care and Use of Laboratory Animals published by the US National Institutes of Health (NIH Publication No. 85-23, revised 1996), and in accordance with Italian law (DL-116, Jan. 27, 1992). The scientific project was supervised and approved by the Italian Ministry of Health, Rome, and by the ethical committee of the University of Torino (approval code 116/2017-PR, 3/2/2017). Rats were anaesthetized by i.p. injection of tiletamine (Zoletil 100, Virbac, Carros, France) and sacrificed by stunning and cervical dislocation.

4.2. Solutions and Drugs

Tyrode standard solution containing (in mM): 154 NaCl, 4 KCl, 1 $MgCl_2$, 5.5 D-glucose, 5 HEPES, 2 $CaCl_2$, pH adjusted to 7.34 with NaOH. Ca^{2+} free Tyrode solution containing (in mM): 154 NaCl, 4 KCl, 1 $MgCl_2$, 5.5 D-glucose, 5 HEPES, 10 2,3-Butanedione monoxime, 5 taurine, pH 7.34. All drug-containing solutions were prepared fresh before the experiments and the Tyrode solutions were oxygenated (O_2 100%) before each experiment. Unless otherwise specified, all reagents for cell isolation and experiments were purchased from Sigma-Aldrich (St. Louis, MO, USA).

4.3. Adult Rat Ventricular Cell Isolation

Isolated cardiomyocytes were obtained from the hearts of adult rats (200–300 g body weight) according to the previously described method [24]. Briefly, after sacrifice, rat heart was explanted, washed in Ca^{2+} free Tyrode solution, and cannulated via the aorta. All the following operations were carried on under a laminar flow hood. The heart was perfused at a constant flow rate of 10 mL/min with Ca^{2+} free Tyrode solution (37 °C) with a peristaltic pump for approximately 5 min to wash away the blood and then with 10 mL of Ca^{2+} free Tyrode supplemented with collagenase (0.3 mg/mL) and protease (0.02 mg/mL). Hearts were then perfused and enzymatically dissociated with 20 mL of Ca^{2+} free Tyrode containing 50 μM $CaCl_2$ and the same enzymatic concentration as before. Atria and ventricles were then separated and the ventricles were cut in small pieces and shaken for 10 min in 20 mL of Ca^{2+} free Tyrode solution in the presence of 50 μM $CaCl_2$, collagenase, and protease. Calcium ion concentration was slowly increased to 0.8 mM. Cardiomyocytes were then plated on glass cover slips or glass bottom dishes (Ibidi, Martinsried, Germany), both treated with laminin to allow cell adhesion.

4.4. Cell Viability

Cell viability was evaluated by propidium iodide (PI) staining on glass bottom dishes for adherent cells. At the end of the treatments, cells were incubated with PI (10 μg/mL, Invitrogen, Carlsbad, CA, USA) for 5 min in the dark. Nuclei of suffering cells were detected with confocal microscopy using an Olympus Fluoview 200 microscope (Shinjuku, Tokyo, Japan) at 568 nm (magnification 20×). Merged images were created with ImageJ (U.S. National Institutes of Health, Bethesda, MD, USA, https://imagej.nih.gov/ij/) and cell viability was calculated as percentage of (total cells-labeled cells)/total cells.

4.5. Evaluation of Sarcomere Length

Cardiomyocytes on glass coverslips were stimulated with TMAO and with H_2O_2 as a positive control. Cells were treated for 24 h with TMAO, at 100 μM and 10 mM, then the sarcomere protein α-actinin, localized in the Z lines, was detected using confocal microscopy. Subsequently, cells were fixed in 4% PFA for 40 min. After two washes with PBS, cells were incubated for 20 min with 0.3% Triton

and 1% bovine serum albumin (BSA) in PBS and stained for 24 h at +4 °C with a mouse monoclonal anti-α-actinin primary antibody (Sigma-Aldrich, 1:800). Cover slides were washed twice with PBS and incubated 1 h at room temperature with the secondary antibody (1:2000, anti-mouse Alexa Fluor 568, Thermo Fisher Scientific, Waltham, MA, USA). After two washes in PBS, coverslips were mounted on standard slides with DABCO and observed after 24 h under a confocal microscope. Confocal fluorimetric measurements were acquired using a Leica SP2 laser scanning confocal system (Wetzlar, Germany), equipped with a 40× water-immersion objective. Image processing and analysis were performed with ImageJ software. Sarcomere length was evaluated measuring the distance between Z lanes in $n = 10$ sarcomeres/cell.

4.6. Intracellular Reactive Oxygen Species (ROS) Measurement

Production of ROS was evaluated by fluorescence microscopy using a 2′-7′-dichlorofluorescein diacetate probe (DCF-DA). After adhesion on glass bottom dishes, DCF-DA solution (5 μg/mL) was added to each dish 30 min prior to the end of the treatment, then the cells were washed with standard Tyrode solution. Fluorescence images at 488 nm were acquired using an Olympus Fluoview 200 microscope (magnification 60×). Fluorescence variations were calculated with the definition and measurement of regions of interest (ROIs) using ImageJ software and expressed as relative Medium Fluorescence Index (MFI) compared to control, fixed at 1.

4.7. Mitochondrial Membrane Potential Measurement

Mitochondrial membrane potential was evaluated by staining cardiomyocytes with the dye 5,5′,6,6′-tetrachloro-1,1′,3,3′-tetraethyl-imidacarbocyanine iodide (JC-1). JC-1 solution (10 μM) was added to each dish 30 min prior to the end of the treatment, then the cells were washed with standard Tyrode solution. Fluorescence images at 488 nm and 568 nm were acquired using an Olympus Fluoview 200 microscope (magnification 60×). Amounts of the monomeric form of the dye were quantified using the red/green fluorescence ratio in the ROIs using ImageJ software and expressed as folds towards control, fixed at 1.

4.8. Statistical Analysis

All data are expressed as mean ± standard error of the mean. For differences between mean values, Bonferroni's multiple comparisons test was performed. Differences with $p < 0.05$ were regarded as statistically significant.

5. Conclusions

In summary, this study demonstrates that TMAO is not directly involved in causing or exacerbating cardiac damage in an acute stress model (Figure 7). However, this study has some limitations: a very wide range of plasmatic TMAO concentrations have been presented in literature, within different mammals, and also between different sexes of the same species; so, several orders of magnitude can be considered physiological [25,26]. Therefore, to test the direct effect of the molecule, high concentrations were used, even higher than human physiological ones. Another weakness of the study could be linked to the time of treatment, because the evaluations were no longer than 24 h and they only represented an acute exposure to TMAO. Moreover, in order to better evaluate the mechanism involved in TMAO-mediated responses, it may be necessary to treat cells for a longer period to assess a chronic stress compatible with the development of CVD. Furthermore, we only studied the TMAO effect on female ventricular cardiomyocytes and it may be interesting to extend the analysis also to male cardiomyocytes as gender differences have been observed in cardioprotective mechanisms [27] and TMAO-induced intracellular calcium imbalance has been described in male cardiomyocytes [8]. Finally, our findings provide new insights into the cardiac effect of TMAO, exploring the direct treatment of isolated cardiomyocytes.

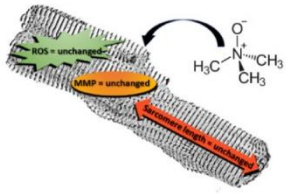

Figure 7. No effects of TMAO are detectable on isolated adult rat cardiomyocyte viability, sarcomere length, ROS production, and mitochondrial membrane potential.

Author Contributions: M.P.G. and R.L. conceived the study, assisted in its design, and revised the manuscript for important intellectual content. G.Q. and S.A. carried out all the experiments and statistical analysis, and all the authors interpreted the results. G.Q. wrote the manuscript. All authors read and approved the final manuscript.

Funding: This research received no external funding; it was supported by the local funding of the University of Turin (Maria Pia Gallo and Renzo Levi). The APC was funded by Maria Pia Gallo and Renzo Levi.

Acknowledgments: The authors acknowledge Nunzio Dibiase for his technical support.

Conflicts of Interest: The authors declare no conflict of interest.

Abbreviations

TMAO	Trimethylamine N-oxide
PI	Propidium iodide
ROS	Reactive oxygen species
DCF-DA	2′-7′-Dichlorofluorescein diacetate
JC-1	5,5′,6,6′-Tetrachloro-1,1′,3,3′-tetraethyl-imidacarbocyanine iodide

References

1. Ufnal, M.; Zadlo, A.; Ostaszewski, R. TMAO: A small molecule of great expectations. *Nutrition* **2015**, *31*, 1317–1323. [CrossRef] [PubMed]
2. Yancey, P.H. Organic osmolytes as compatible, metabolic and counteracting cytoprotectants in high osmolarity and other stresses. *J. Exp. Biol.* **2005**, *208*, 2819–2830. [CrossRef] [PubMed]
3. Ke, Y.; Li, D.; Zhao, M.; Liu, C.; Liu, J.; Zeng, A.; Shi, X.; Cheng, S.; Pan, B.; Zheng, L.; et al. Gut flora-dependent metabolite Trimethylamine-N-oxide accelerates endothelial cell senescence and vascular aging through oxidative stress. *Free Radic. Biol. Med.* **2018**, *116*, 88–100. [CrossRef] [PubMed]
4. Li, T.; Chen, Y.; Gua, C.; Li, X. Elevated Circulating Trimethylamine N-Oxide Levels Contribute to Endothelial Dysfunction in Aged Rats through Vascular Inflammation and Oxidative Stress. *Front. Physiol.* **2017**, *8*, 350. [CrossRef] [PubMed]
5. Zhu, W.; Gregory, J.C.; Org, E.; Buffa, J.A.; Gupta, N.; Wang, Z.; Li, L.; Fu, X.; Wu, Y.; Mehrabian, M.; et al. Gut Microbial Metabolite TMAO Enhances Platelet Hyperreactivity and Thrombosis Risk. *Cell* **2016**, *165*, 111–124. [CrossRef] [PubMed]
6. Shan, Z.; Sun, T.; Huang, H.; Chen, S.; Chen, L.; Luo, C.; Yang, W.; Yang, X.; Yoa, P.; Cheng, J.; et al. Association between microbiota-dependent metabolite trimethylamine-N-oxide and type 2 diabetes. *Am. J. Clin. Nutr.* **2017**, *106*, 888–894. [CrossRef] [PubMed]
7. Makrecka-Kuka, M.; Volska, K.; Antone, U.; Vilskersts, R.; Grinberga, S.; Bandere, D.; Liepinsh, E.; Dambrova, M. Trimethylamine N-oxide impairs pyruvate and fatty acid oxidation in cardiac mitochondria. *Toxicol. Lett.* **2017**, *267*, 32–38. [CrossRef] [PubMed]
8. Savi, M.; Bocchi, L.; Bresciani, L.; Falco, A.; Quaini, F.; Mena, P.; Brighenti, F.; Crozier, A.; Stilli, D.; Del Rio, D. Trimethylamine-N-Oxide (TMAO)-Induced Impairment of Cardiomyocyte Function and the Protective Role of Urolithin B-Glucuronide. *Molecules* **2018**, *23*, 549. [CrossRef]
9. Arduini, A.; Zammit, V.A.; Bonomini, M. Identification of trimethylamine N-oxide (TMAO)-producer phenotype is interesting, but is it helpful? *Gut* **2019**. [CrossRef]
10. Nowiński, A.; Ufnal, M. Trimethylamine N-oxide: A harmful, protective or diagnostic marker in lifestyle diseases? *Nutrition* **2018**, *46*, 7–12. [CrossRef]

11. Dumas, M.-E.; Maibaum, E.C.; Teague, C.; Ueshima, H.; Zhou, B.; Lindon, J.C.; Nicholson, J.K.; Stamler, J.; Elliott, P.; Chan, Q.; et al. Assessment of analytical reproducibility of 1H NMR spectroscopy based metabonomics for large-scale epidemiological research: The INTERMAP Study. *Anal. Chem.* **2006**, *78*, 2199–2208. [CrossRef] [PubMed]
12. Collins, H.L.; Drazul-Schrader, D.; Sulpizio, A.C.; Koster, P.D.; Williamson, Y.; Adelman, S.J.; Owen, K.; Sanli, T.; Bellamine, A. L-Carnitine intake and high trimethylamine N-oxide plasma levels correlate with low aortic lesions in ApoE−/− transgenic mice expressing CETP. *Atherosclerosis* **2016**, *244*, 9–37. [CrossRef] [PubMed]
13. Lupachyk, S.; Watcho, P.; Stavniichuk, R.; Shevalye, H.; Obrosova, I.G. Endoplasmic Reticulum Stress Plays a Key Role in the Pathogenesis of Diabetic Peripheral Neuropathy. *Diabetes* **2013**, *62*, 944–952. [CrossRef] [PubMed]
14. Zeisel, S.H.; Warrier, M. Trimethylamine N-Oxide, the Microbiome, and Heart and Kidney Disease. *Annu. Rev. Nutr.* **2017**, *37*, 157–181. [CrossRef] [PubMed]
15. Sarvazyan, N. Visualization of doxorubicin-induced oxidative stress in isolated cardiac myocytes. *Am. J. Physiol.* **1996**, *271*, H2079–H2085. [CrossRef]
16. Zununi Vahed, S.; Barzegari, A.; Zuluaga, M.; Letoumeur, D.; Pavon-Djavid, G. Myocardial infarction and gut microbiota: An incidental connection. *Pharmacol. Res.* **2018**, *129*, 308–317. [CrossRef]
17. Cho, C.E.; Taesuwan, S.; Malysheva, O.V.; Bender, E.; Tulchinsky, N.F.; Yan, J.; Sutter, J.L.; Caudill, M.A. Trimethylamine-N-oxide (TMAO) response to animal source foods varies among healthy young men and is influenced by their gut microbiota composition: A randomized controlled trial. *Mol. Nutr. Food Res.* **2017**, *61*, 1600324. [CrossRef]
18. Ufnal, M.; Jazwiec, R.; Dadlez, M.; Drapala, A.; Sikora, M.; Skrzypecki, J. Trimethylamine-N-oxide: A carnitine-derived metabolite that prolongs the hypertensive effect of angiotensin II in rats. *Can. J. Cardiol.* **2014**, *30*, 1700–1705. [CrossRef]
19. Koeth, R.A.; Wang, Z.; Levison, B.S.; Buffa, J.A.; Org, E.; Sheehy, B.T.; Britt, E.B.; Fu, X.; Wu, Y.; Li, L.; et al. Intestinal microbiota metabolism of L-carnitine, a nutrient in red meat, promotes atherosclerosis. *Nat. Med.* **2013**, *19*, 576–585. [CrossRef]
20. Dambrova, M.; Latkovskis, G.; Kuka, J.; Strele, I.; Konrade, I.; Grinberga, S.; Hartmane, D.; Pugovics, O.; Erglis, A.; Liepinsh, E. Diabetes is Associated with Higher Trimethylamine N-oxide Plasma Levels. *Exp. Clin. Endocrinol. Diabetes* **2016**, *124*, 251–256. [CrossRef]
21. Mueller, D.M.; Allenspach, M.; Othman, A.; Saely, C.H.; Muendlein, A.; Vonbank, A.; Drexel, H.; von Eckardstein, A. Plasma levels of trimethylamine-N-oxide are confounded by impaired kidney function and poor metabolic control. *Atherosclerosis* **2015**, *243*, 638–644. [CrossRef] [PubMed]
22. Yin, J.; Liao, S.-X.; He, Y.; Wang, S.; Xia, G.-H.; Liu, F.-T.; Zhu, J.-J.; You, C.; Chen, Q.; Zhou, L.; et al. Dysbiosis of Gut Microbiota with Reduced Trimethylamine-N-Oxide Level in Patients With Large-Artery Atherosclerotic Stroke or Transient Ischemic Attack. *J. Am. Heart Assoc.* **2015**, *4*, e002699. [CrossRef] [PubMed]
23. Huc, T.; Drapala, A.; Gawrys, M.; Konop, M.; Bielinska, K.; Zaorska, E.; Samborowska, E.; Wyczalkowska-Tomasik, A.; Paczek, L.; Dadlez, M.; et al. Chronic, low-dose TMAO treatment reduces diastolic dysfunction and heart fibrosis in hypertensive rats. *Am. J. Physiol. Heart Circ. Physiol.* **2018**, *315*, H1805–H1820. [CrossRef] [PubMed]
24. Gallo, M.P.; Femminò, S.; Antoniotti, S.; Querio, G.; Alloatti, G.; Levi, R. Catestatin induces glucose uptake and GLUT4 trafficking in adult rat cardiomyocytes. *Biomed. Res. Int.* **2018**. [CrossRef] [PubMed]
25. Lenky, C.C.; McEntyre, C.J.; Lever, M. Measurement of marine osmolytes in mammalian serum by liquid chromatography-tandem mass spectrometry. *Anal. Biochem.* **2012**, *420*, 7–12. [CrossRef] [PubMed]
26. Somero, G.N. From dogfish to dogs: Trimethylamines protect proteins from urea. *Am. J. Physiol.* **1986**, *1*, 9–12. [CrossRef]
27. Lagranha, C.L.; Deschamps, A.; Aponte, A.; Steenbergen, C.; Murphy, E. Sex differences in the phosphorylation of mitochondrial proteins result in reduced production of reactive oxygen species and cardioprotection on females. *Circ. Res.* **2010**, *106*, 1981–1991. [CrossRef] [PubMed]